San Acacia Reach
San Acacia Dam to Escondida Bridge
Hydraulic Modeling Analysis
1918-2006

Middle Rio Grande,
New Mexico
September 2011

Prepared For:
US Bureau of Reclamation
Albuquerque, New Mexico

Prepared By:
Seema C. Shah-Fairbank, PE
Jaehoon Kim
Dr. Pierre Julien
Colorado State University
Engineering Research Center
Department of Civil Engineering
Fort Collins, Colorado 80523

Abstract

Human influence on the Middle Rio Grande has resulted in major changes throughout the Middle Rio Grande region in central New Mexico. Many of these changes are associated with erosion and sedimentation. Therefore, hydraulic modeling analyses have been performed on the San Acacia reach to determine the changes in morphology and other important parameters.

This study is an extension of the previous reach report developed by Reclamation on the San Acacia reach. The 11.6 mile long reach extends from the San Acacia Diversion dam (River Mile 116.2) to the Escondida Bridge (104.6). Spatial and temporal trends in channel geometry, discharge and sediment have been analyzed. In addition, historical bedform data were analyzed and potential equilibrium conditions were predicted.

Aerial photographs, GIS active channel planforms, cross section surveys, hydraulic model analysis and channel classification methods were used to analyze spatial and temporal trends in channel geometry and morphology. Narrowing of the channel was observed from the GIS active channel planforms from 1918 to 2006. There is fluctuation in the channel properties (geometry) associated with complex channel response. There has been significant degradation in this reach due to channelization and the construction of the diversion dam. Due to the degradation, the particle diameter has coarsened from about 0.1 mm in 1972 to 0.36 mm in 2002.

Field observation of bedforms were compiled and compared to the bedforms predicted by the van Rijn and the Simons and Richardson methods. Both methods produced a large amount of scatter, which can be associated with the cross section variability and the variability in the bedform observations. However, the predicted dune formation was correct approximately 75% of the time. The methods were not as accurate for ripple and upper regime prediction.

A variety of approaches were used to predict future equilibrium width and slope conditions. The approaches used include hydraulic geometry equations, hyperbolic and exponential regressions, stable channel geometry, and sediment transport relationships. The equilibrium widths predicted ranged from 150 to 450 feet, and the predicted equilibrium slope ranged from 0.0003 to 0.00156. The equilibrium width seems to provide a reasonable estimate of the future trend because the tends are consistent with the current channel conditions which show a river, which is narrowing. ; However, the relocation of the LFCC, near RM 111 and 114, increases the potential meander length and channel width, which could change the prediction. In addition, there is a wide range of variability in the predicted equilibrium slopes.

Table of Contents

List of Figures

List of Tables

Middle Rio Grande Conservancy District (MRGCD)
U.S. Bureau of Reclamation (USBR or Reclamation)
U.S. Army Corps of Engineers (USACE)
Low Flow Conveyance Channel (LFCC)
U.S. Fish and Wildlife Service (USFWS)
National Oceanic and Atmospheric Administration (NOAA)
Rio Grande (RG)
San Acacia Range Lines (SA)
Socorro Range Lines (SO)

1. Introduction

The Rio Grande has been an important source of water for both humans and wildlife. Past and current trends are important to understand for better implementation of river maintenance and management practices. Historically, when considering the water in the Middle Rio Grande human needs have dominated the management decision. However, in July 1999, the U.S. Fish and Wildlife Service (USFWS) designated the Middle Rio Grande, New Mexico, from Cochiti Dam to the railroad bridge at San Marcial, as critical habitat for the Rio Grande silvery minnow (Hybognathus amarus), a federally listed endangered species. Alterations in the hydrologic regime, the hydraulic and sediment characteristics of the channel during the last century, through construction of dams and reservoirs, diversion dams and channelization, have reduced the quality and quantity of habitat for the minnow. The silvery minnow prefers shallow water with a sandy and silty substrate. Recent changes in the channel have resulted in a narrower, deeper and armored configuration (USFWS 1999). In addition, the deterioration of native plant and animal communities, associated with the riparian bosque habitat, has also occurred. In February 1995, the USFWS listed the southwestern willow flycatcher (Empidonax traillii extimus) as an endangered species. This species is a small, grayish-green migratory songbird found only in riparian habitats characterized by dense growths of willows, arrow weed and other species that provide foraging and nesting habitat. The loss of southwestern cottonwood-willow riparian habitat has been cited as the main reason for the decline of the population of the southwestern willow flycatcher (USFWS 1997). The challenge for decision makers today is to produce management plans that are beneficial to both human and wildlife. In order to make these decisions, they need to know how the Rio Grande has evolved and how it will continue with current management practices.

The Rio Grande from the San Acacia Diversion Dam to the Escondida Bridge defines the San Acacia study reach (Figure 1.1) and is located within the critical habitat designations region. To fully understand the river a thorough understanding of the past and present hydraulic, geomorphic and sediment conditions in this reach are necessary. In addition, prediction of future equilibrium conditions of the San Acacia reach will allow better planning for management of the reach.

This report is an update to a previous study conducted by Reclamation (USBR 2003), which documented and evaluated historical channel conditions of both the river and its floodplain, understand how and why the channel evolved from the historic conditions, and predict future channel morphology under the current management regime. The objective of this study is to extend the data analysis and to determine if previous predictions were accurate. In addition, a bedform analysis is performed on the reach based on observations made in the field.

Extensive data are available for the San Acacia reach, including the relocation of the LFCC and levee setback project(Appendix A), cross section surveys (Appendix B), aerial photos (Appendix C) water and sediment discharge data (Larsen et al. 2011),and bed and suspended sediment particle size data. The objectives of the study are met through the following analyses:

- Analysis of cross-section survey data to characterize spatial and temporal trends in channel geometry and longitudinal profile.

- Planform classification via analysis of aerial photos and channel geometry data.

- Analysis of temporal trends in water and sediment discharge, sediment concentration, and sediment continuity using USGS gauging station data.

- Assessment of the equilibrium state of the river via use of hydraulic geometry and minimum stream power methods, as well as determination of the equilibrium slope based on estimated incoming sediment load and channel sediment transport capacity.

- Comparison of bedform observation to predictions.

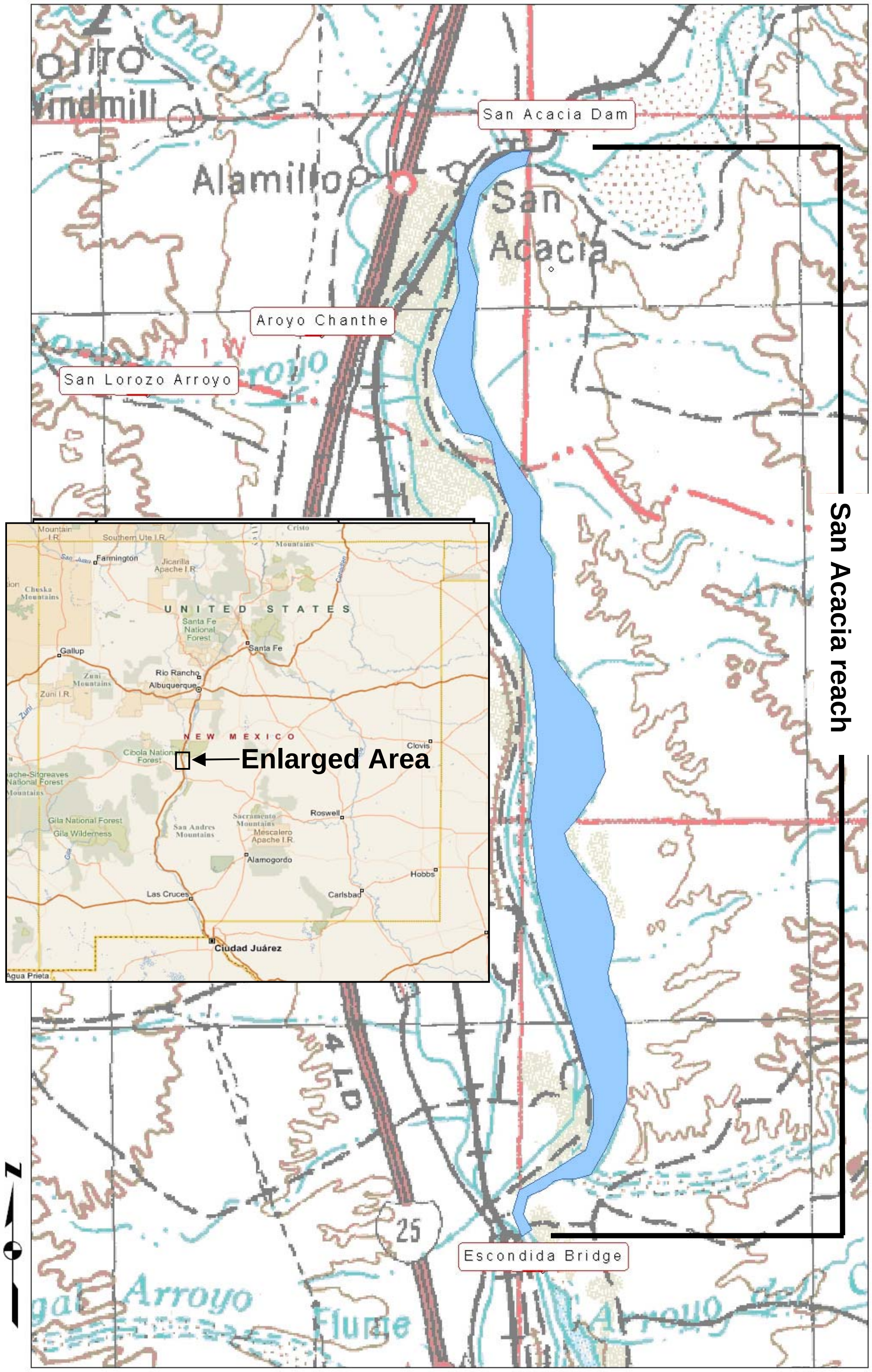

Figure 1.1 – San Acacia Location Map

2. Site Description and Background

The Middle Rio Grande covers about 170 miles of central New Mexico from Cochiti Dam to Elephant Butte Reservoir (TetraTech 2002). In recent years, the Middle Rio Grande Conservancy District (MRGCD), the U.S. Bureau of Reclamation (USBR) and the U.S. Army Corps of Engineers (USACE) have undertaken numerous projects along the Middle Rio Grande to combat floods and sedimentation problems (MRGCD 2006). The human influences on the river have caused significant habitat loss to native plant and animal species and have prompted detailed studies of the Middle Rio Grande.

The San Acacia study reach of the Middle Rio Grande spans 11.6 miles from the San Acacia Diversion Dam (River Mile 116.2) to the Escondida Bridge (River Mile 104.6). Prior to the construction of Cochiti Dam and the channelization along the Middle Rio Grande the San Acacia reach was a wide slightly braided reach, except for subreach 4 which was always relatively narrow (approximately 200 feet). This wide channel with slow turbid water was the ideal condition for the spawning of the silver minnow. However, due to channelization the reach currently is characterized as straight with a sinuosity close to one and a valley slope of 0.00085. The reach is characterized primarily by a sand-bed channel with median bed material size of about 0.36 mm.

Figures 2.1 to 2.3 show aerial photographs from 2006 of the study reach. There are a few arroyos entering the reach. The river runs nearly parallel to the Low Flow Conveyance Channel (LFCC). The LFCC is located on the west bank of the river and is protected by a levee, which is influencing the path of the river. Reclamation has completed the relocation of portions of the LFCC at RM 111 and RM 113/114. The relocation is intended to increase the available area for the river, thus reducing the need for levee protection while, hoping to restore a portion of the river to a wider more braided planform, which would promote habitat for the silvery minnow. Refer to Appendix A for a map of the relocation and Appendix C for site photographs.

Due to severe flooding in the late 1800's and early 1900's, congress developed legislation known as the Flood Control Acts. The Middle Rio Grande was classified as a wide, shallow channel that extended from levee to levee by the 1950's. In addition, the channel bottom was higher in elevation than existing floodplain (Massong 2005a). Due to the floodplain elevations in reference to the channel banks and the continued flooding, Congress authorized river modifications to control sedimentation and flooding along the Middle Rio Grande. The following improvements were authorized: additional channelization, Kellner jetty jacks and several large dams (USBR 2007). Cochiti Dam, which is one of the larger flood control dams along the Middle Rio Grande was authorized for construction under the 1960 Flood Control Act.

The anthropogenic alterations of the river and surrounding land created a number of environmental concerns. Extensive grazing and logging has increased overland erosion, which amplified river aggradation. As the river widened, flow velocities decreased thus sufficient flow was not available for irrigation. Additionally, considerably less water was reaching central New Mexico because of upstream uses.

By the late 1800's, environmental concerns were so severe that the government began making policy to alleviate the strain on the river (Scurlock 1998). Several projects were initiated in the early to mid 20th century. The U.S. Army Corps of Engineers (USACE) constructed six dams and the Middle Rio Grande Conservancy District (MRGDC) constructed five dams, over a thousand miles of irrigation channels (MRGCD 2006) and levees along the river. Two notable dams include the Elephant Butte Dam (1916) and the Cochiti Dam (1973). Elephant Butte Dam created a reservoir in southern New Mexico to ensure water for agriculture and urban development in southern New Mexico, Texas and Mexico. North of Albuquerque, Cochiti Dam was built to control flooding and sediment deposition and to improve overall water supply.

In the 1950's, through the 1970's, extensive channelization occurred to control the river. These engineering feats succeeded in controlling the Rio Grande, but they brought new environmental problems to the region. By the 1990's, two species that depend on the Rio Grande were placed on the endangered species list: the southwestern willow flycatcher and the Rio Grande silvery minnow. Both depend upon periodic flooding of the river to maintain their natural habitats. In addition, the silvery minnow requires low flow velocities and high sediment for eggs to hatch. In order to preserve the habitat of these threatened species, policy makers have strictly managed river flows. These policy reforms are often detrimental to farmers, who depend on the Rio Grande for their livelihood. Understanding dynamic properties of the river, especially changes induced by human engineering, is necessary in order to maintain the river for future users and to meet ecological needs.

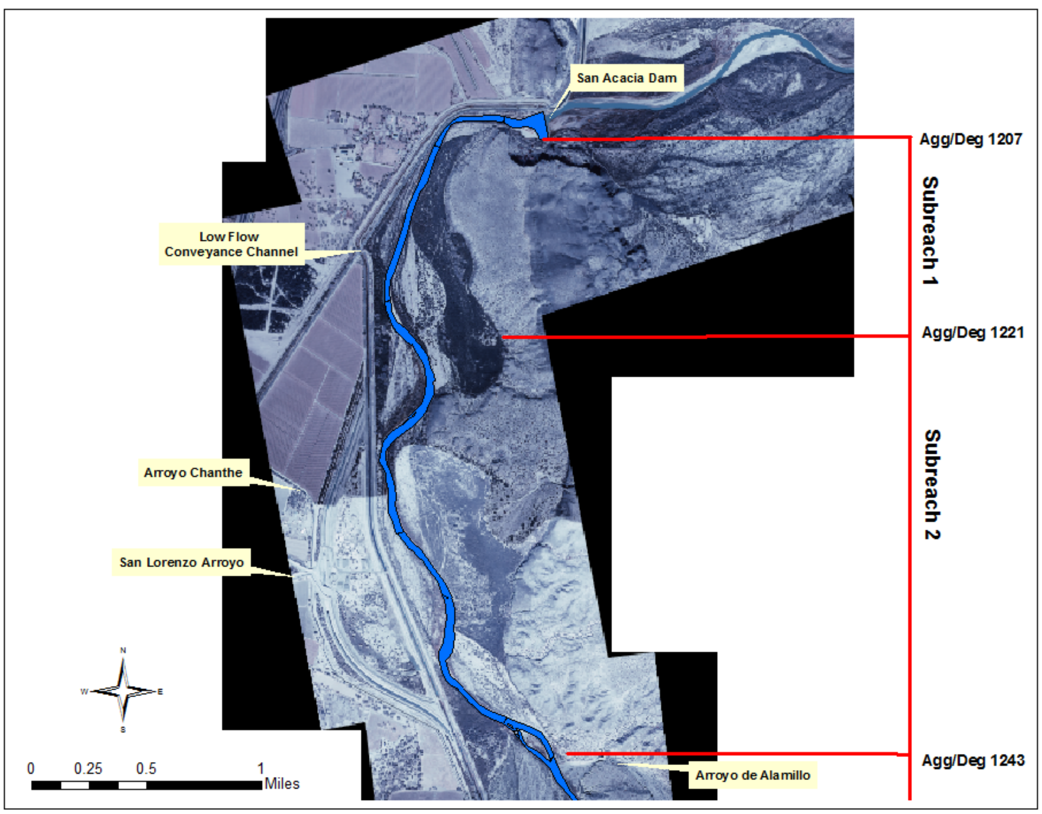

Figure 2.1 – 2006 Aerial Photo of Subreach 1 and 2

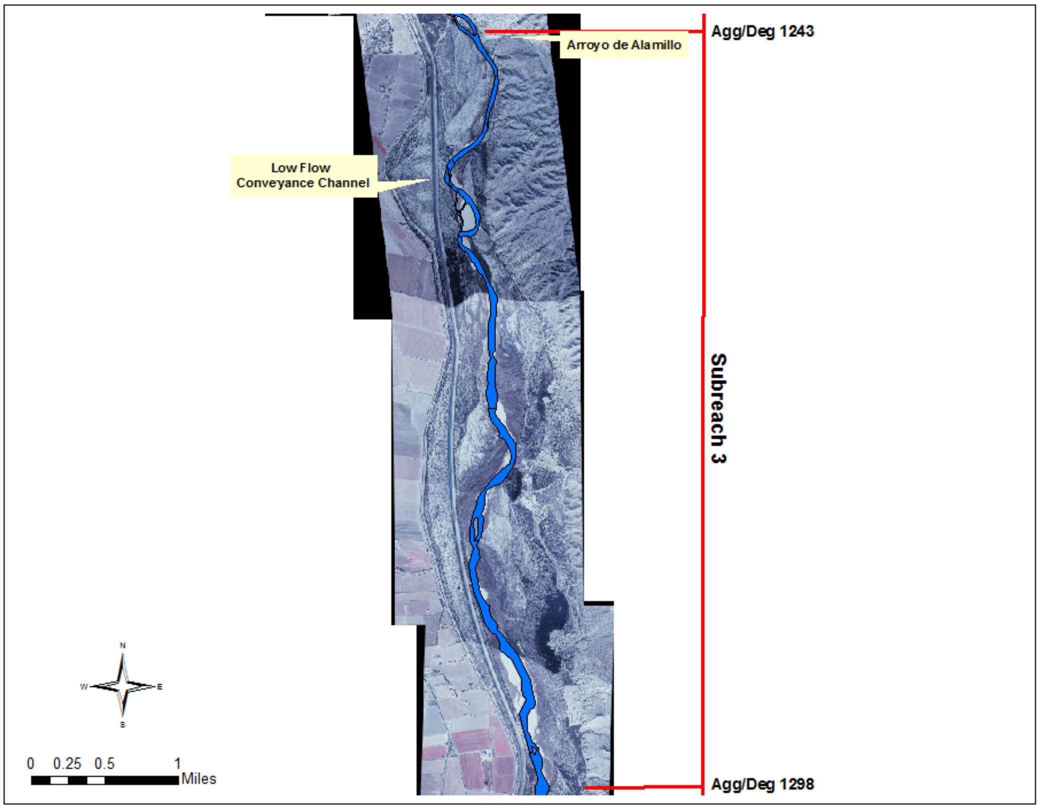

Figure 2.2 – 2006 Aerial Photo of Subreach 3

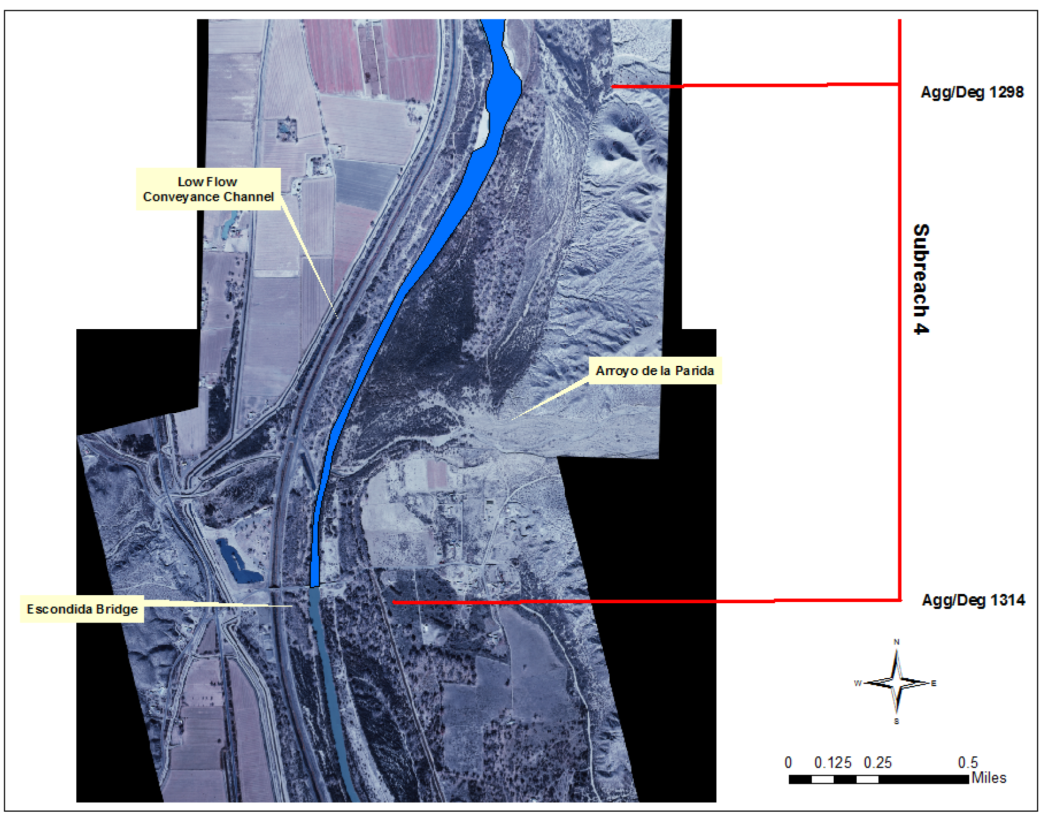

Figure 2.3 – 2006 Aerial Photo of Subreach 4

2.1. Subreach definition

To aid in the historic changes and characterization of the San Acacia reach, as well as to make better predictions of possible future conditions, the reach was divided into four subreaches by Reclamation (USBR 2003). The location of the subreach delineations can be seen in Figure 2.4.

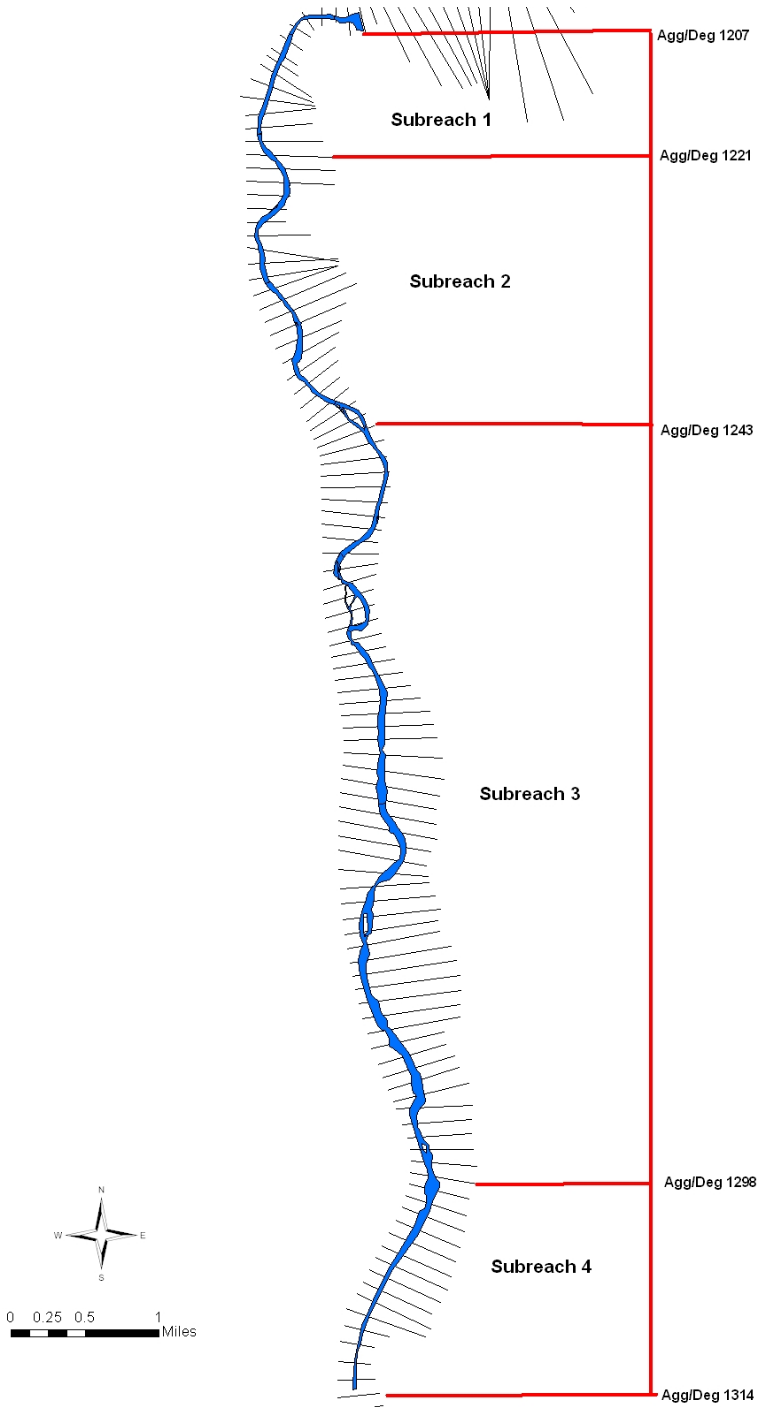

Figure 2.4 – Subreach Delineation

Subreach 1 stretches from the San Acacia Diversion Dam (River Mile 116.1) to Agg/Deg line 1221 (River Mile 114.66). Subreach 2 stretches from Agg/Deg line 1221 to Agg/Deg 1243 (River Mile 112.3). Subreach 3 stretches from Agg/Deg line 1243 to Agg/Deg line 1298 (River Mile 106.3). Finally, Subreach 4 stretches from Agg/Deg 1298 to the Escondida Bridge (River Mile 104.44).

2.2. Available Data

This study is an extension to the previous study performed by Reclamation (2003). To complete this study, data was retrieved from a number of different agencies including Reclamation, the United States Geological Survey (USGS), the National Oceanic and Atmospheric Administration (NOAA), and the Middle Rio Grande database compiled at Colorado State University for Reclamation.

2.2.1. Water and Suspended Sediment Data

Historical mean daily discharge data was obtained from two USGS gages; the Rio Grande Floodway at San Acacia (08354900), located at the upstream study limits and, and the Rio Grande Floodway at San Marcial (08358400), located approximately 36 miles downstream of the study reach. The dates of available discharge data from the USGS website are shown in Table 2.1.

Table 2.1 – Available Daily Discharge Data

USGS Gauging Station	Dates
RG Floodway at San Acacia	1958-current
RG Floodway at San Marcial	1949-current

An additional gage is located at the Escondida Bridge; however it only records real-time discharge data, not the historical data necessary for this study. Figure 2.5 provides a hydrograph from a typical year for the San Acacia and San Marcial gages. This hydrograph has a peak discharge of 5000 cfs, which is defined as the bankfull discharge and will be described in Section 2.3. There are two peaks in the hydrograph. The first peak is longer and occurs between April and June and is the result of snowmelt in the Rio Grande headwaters. The second peak seen in August is the result of an intense summer thunderstorm characteristic of the Middle Rio Grande watershed. In addition, Figure 2.6 shows the peak year discharge for each gage.

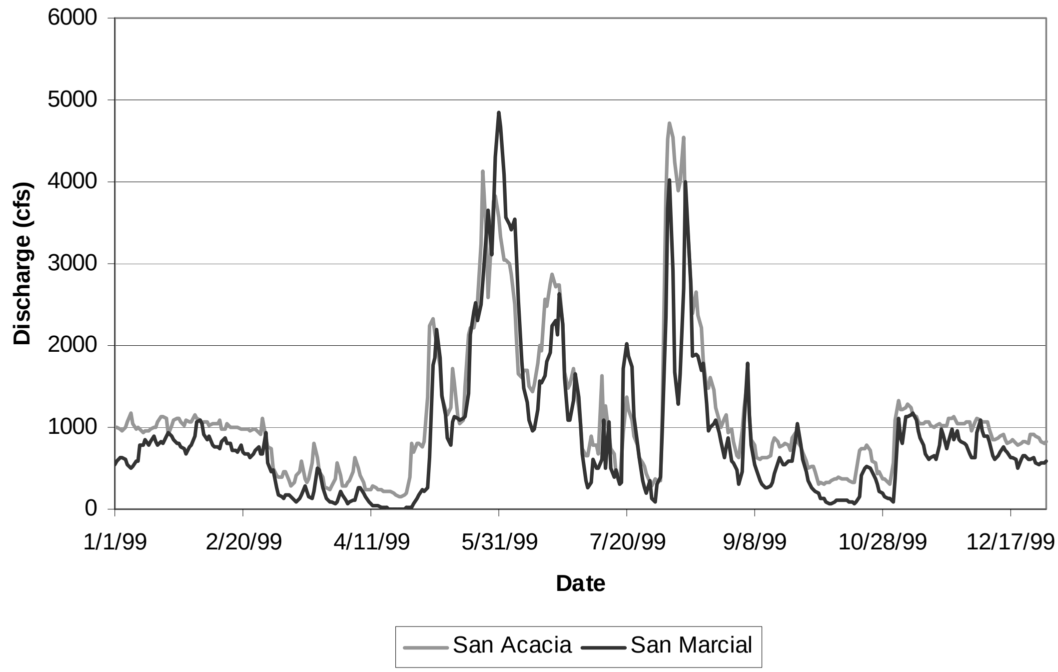

Figure 2.5 – Hydrograph for San Acacia and San Marcial Gages

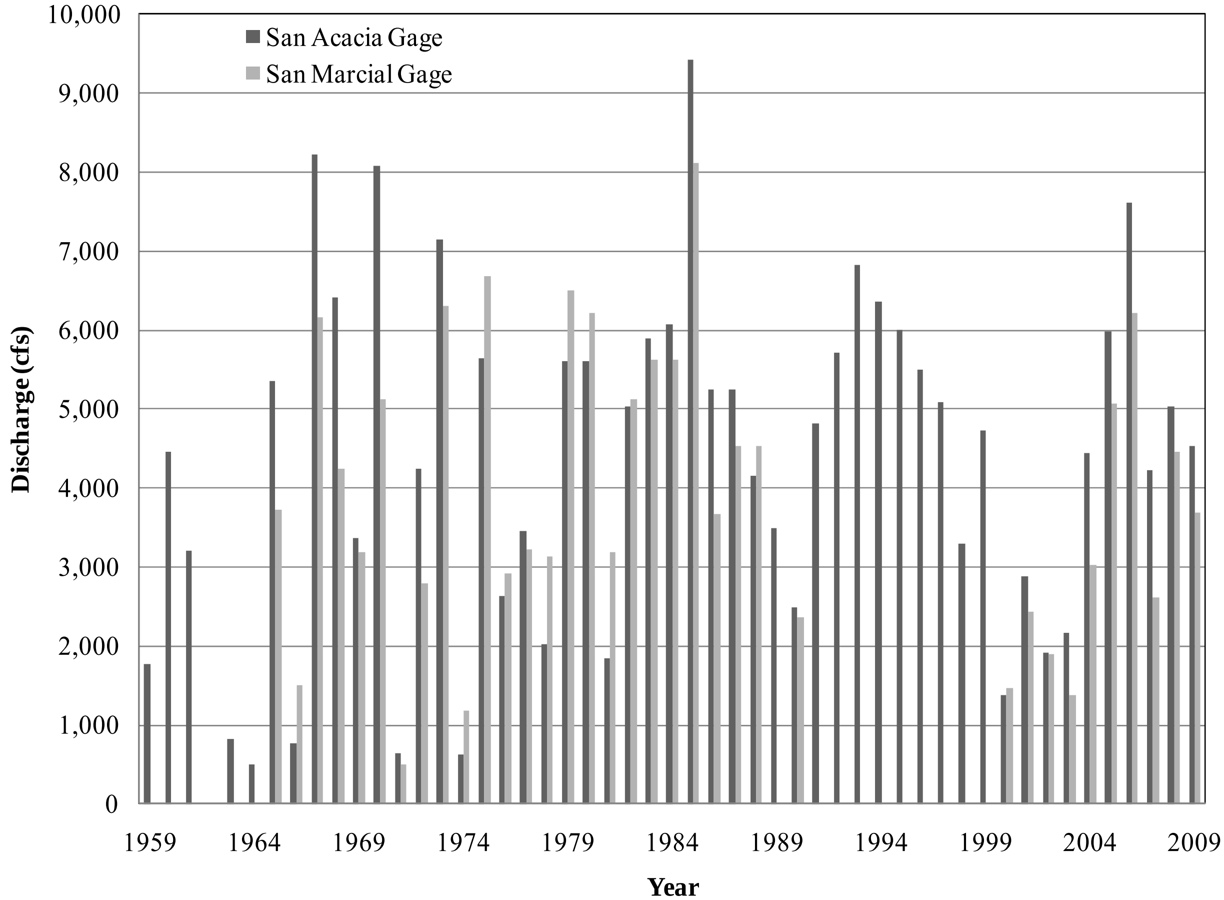

Figure 2.6 – Annual Peak Discharge at San Acacia and San Marcial Gages

In addition, daily suspended sediment data was also available at the at San Acacia and San Marcial gages. Figure 2.7 shows the annual suspended sediment load at each gage. A blank year indicates that complete sediment data was not available for that year.

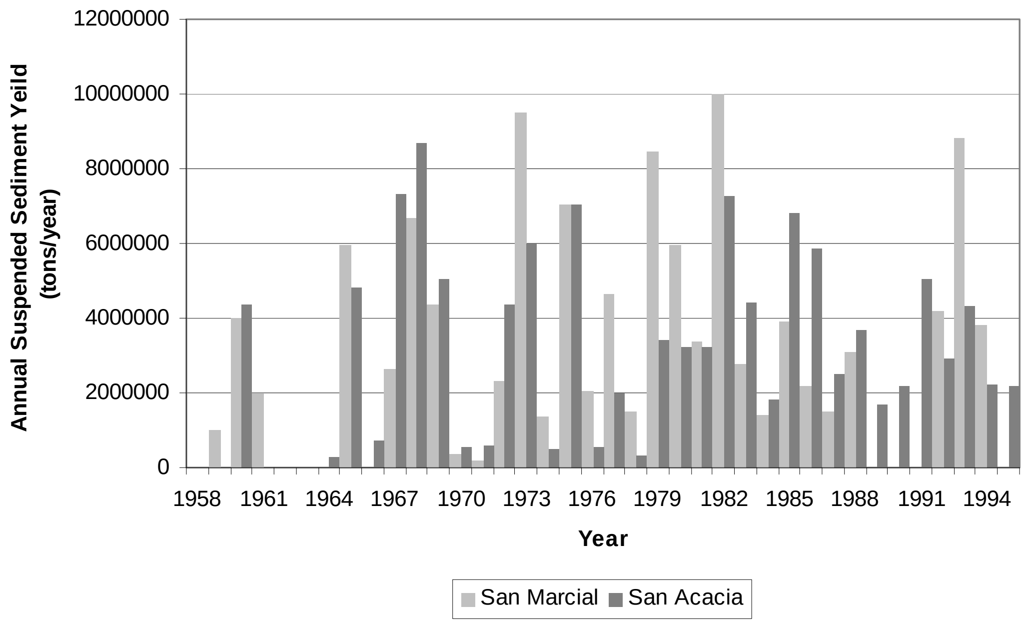

Figure 2.7 – Annual Suspended Sediment Yield

The graph shows that the suspended sediment load measured at the San Acaica gage is not equal to the load measured at the San Marcial gage. This indicates that the tributaries and arroyos, in addition to the channel itself may have a tendency to transport sediment downstream and that there is an inbalance in the channels supply and capacity.

Suspended sediment data was only available for certain time periods. Table 2.2 provides a summary of the available data. Additional sediment data from 1955 to 2005 was provided by Reclamation (2011). This data set contained yearly suspended sediment totals, while Table 2.2 provides daily suspended sediment load that were obtained from the USGS sediment website (http://co.water.usgs.gov/sediment/).

Table 2.2 – Available Suspended Sediment Data

USGS Gauging Station	Dates
RG at San Marcial	Oct. 1956 - July 1962 Sep. 1962 - Aug. 1966 Oct. 1966 - Sep. 1989 Oct. 1991 - Sep. 1995
RG at San Acacia	Jan 1959 - Sep. 1959 Jan 1960 - Sep. 1961 July 1961 April 1962 - July 1962

	Aug 1962 - Sep. 1962 March 1963 - Sep. 1996

2.2.2. Bed Material

Bed material data was collected at San Acacia (SA) and Socorro (SO) range lines by Reclamation from 1990-2005, refer to Figure 2.8 for location of range lines. The surveys include grain-size distributions for each sample. The dates and locations of the material collected are displayed in Table 2.3.

Table 2.3 – Available Bed Material Data

Years	SA Line Number																						SO Line Number					
	1207	1210	1215	1218	1221	1223	1224	1225	1228	1229	1230	1231	1232	1236	1243	1246	1256	1262	1268	1280	1283	1292	1298	1306	1308	1311	1313	1316
1995		x	x		x									x	x	x		x						x		x		x
1996								x						x		x		x						x				x
1997		x	x		x	x		x	x		x		x	x	x	x		x				x	x	x				x
1998					x	x		x	x		x		x	x														
1999																							x	x	x		x	
2000	x			x	x	x	x		x	x		x			x	x	x		x	x			x					
2005			x											x		x		x			x			x				

Additional bed material data was also obtained from the USGS gaging stations located on the Rio Grande at San Acacia and San Marcial floodways. Data were sporadically available from 1966-2004 at the San Acacia gage and from 1968-2004 at the San Marcial gage. The information from the gaging stations was only used in analysis when appropriate bed material data were not available from the range lines.

2.2.3. Tributary and Arroyo Information

There are four arroyos that enter the Middle Rio Grande in the San Acacia reach. The arroyos entering the river include the Arroyo Chanthe, San Lorenzo Arroyo, Arroyo de Alamillo and Arroyo de la Parida. In addition, the intake for the LFCC and the Socorro Main Canal are both located at the San Acacia Diversion Dam.

The arroyos supply large quantities of sediment into the Middle Rio Grande. From previous studies the arroyos contribute sand and gravel particles into the Rio Grande. During spring runoff the sediment supply is low, however during the intensity summer thundershowers large quantities of sediment are carried into the river from the arroyos (USBR 2003).

2.2.4. Survey Lines and Dates

Cross-section surveys were collected by Reclamation using two methods. All Agg/Deg lines were surveyed using aerial photography. These surveys cannot differentiate the difference between ground and water; however, they do provide information about the floodplain topography. Agg/Deg lines 1207-1315 were used in the hydraulic analysis. This includes one cross-section upstream of the study reach and one cross-section downstream of the study reach. Because the extent of the Agg/Deg lines used does not exactly match the limits of study, the length of the reach used for hydraulic analysis is slightly longer than the actual study reach. Agg/Deg lines are spaced about 500 feet apart and were surveyed in 1962, 1972, 1992, and 2002.

SA and SO range lines were surveyed by Reclamation beginning in 1987. These surveys provide detailed information about the channel cross-section that are not available from the aerial photographs. Figure 2.8 shows the location of the SA and SO lines and Table 2.4 provides a list of the available survey data for a given year. The SA and SO numbers correspond to the Agg/Deg line numbers. In addition, Appendix B contains figures that show the cross section variability over time.

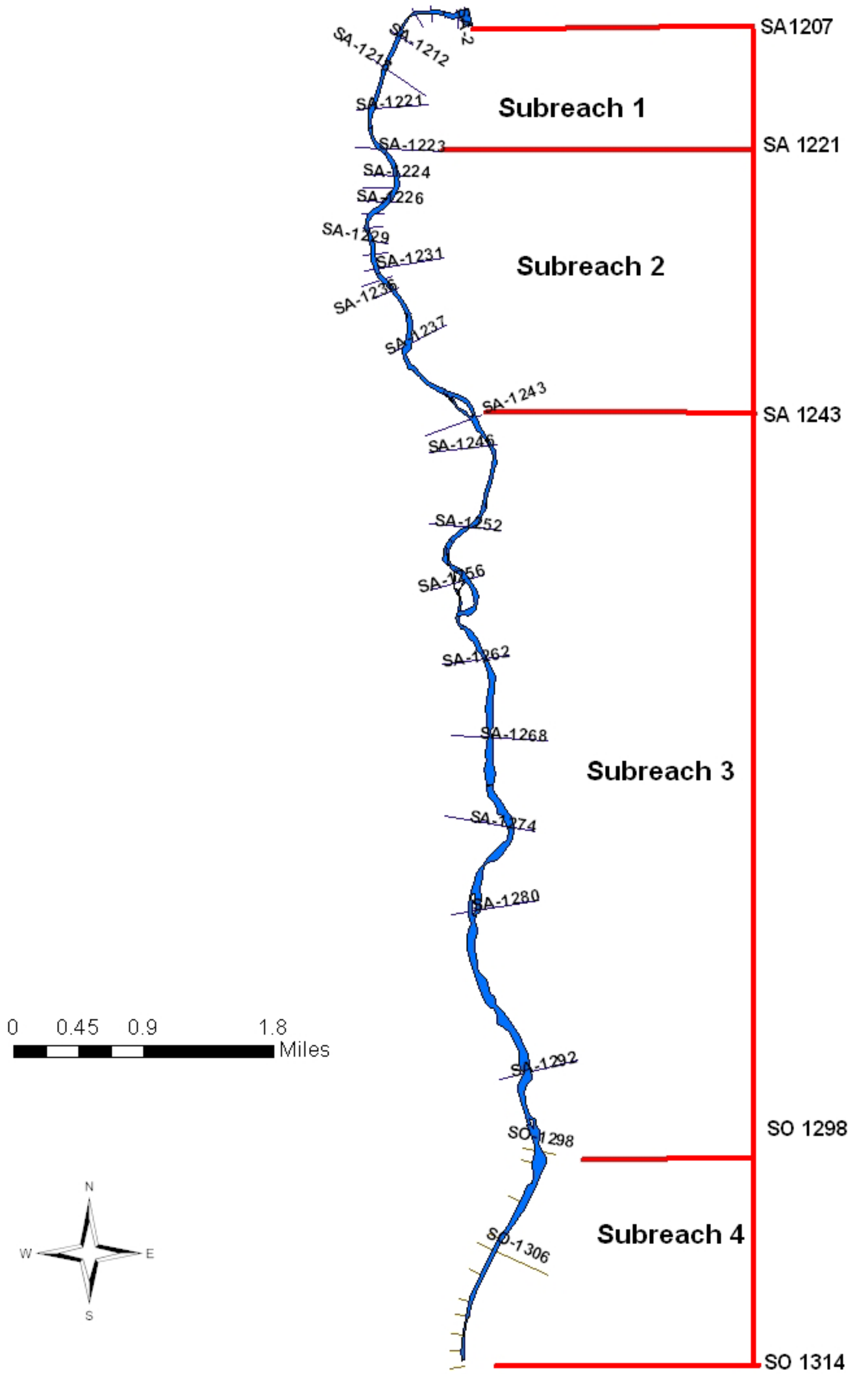

Figure 2.8 – San Acacia and Socorro Range Line Locations

Table 2.4 – San Acacia and Socorro Range Line Survey Dates

Cross Section	Survey Year												
	1988	1989	1990	1991	1992	1995	1996	1997	1998	1999	2002	2003	2005
SA 1207	x	x	x	x	x	x	x	x		x	x		x
SA 1208	x	x	x	x	x	x	x	x		x	x		x
SA 1290	x	x	x			x	x	x		x	x		x
SA 1210	x	x	x	x	x	x	x			x	x		x
SA 1212	x	x	x	x	x	x	x	x		x	x		x
SA 1215	x	x	x	x	x	x	x	x		x	x		x
SA 1218	x	x	x	x	x	x	x	x		x	x		x
SA 1220													x
SA 1221	x	x	x	x	x	x	x	x	x	x	x		x
SA 1223								x	x	x			x
SA 1224								x	x	x			
SA 1225	x	x	x	x	x	x	x	x	x	x	x		x
SA 1226								x	x	x			x
SA 1227								x	x	x			x
SA 1228								x	x	x			x
SA 1229								x	x	x			x
SA 1230								x	x	x			
SA 1231.6	x	x	x	x	x	x	x	x	x	x	x	x	x
SA 1232.4								x	x	x		x	
SA 1235												x	
SA 1936	x	x	x		x	x	x	x	x	x	x	x	x
SA 1237												x	x
SA 1238												x	x
SA 1239												x	
SA 1240												x	
SA 1241												x	
SA 1242												x	x
SA 1243	x	x	x	x	x	x	x	x		x	x		x
SA 1246		x	x	x	x	x	x	x		x	x		x
SA 1252		x	x	x	x	x	x	x		x	x	x	x
SA 1253												x	x
SA 1254												x	x
SA 1255												x	x
SA 1256		x	x	x	x	x	x	x		x	x	x	x
SA 1257												x	x
SA 1258												x	x
SA 1259										x	x		
SA 1262		x	x		x	x	x	x		x	x		x
SA 1268		x	x	x	x	x	x	x		x	x		
SA 1268.8											x		x
SA 1274		x	x		x	x	x	x		x	x		x
SA 1280		x	x		x	x	x	x		x	x	x	x
SA 1280.9												x	x
SA 1283													x
SA 1292		x	x		x		x	x		x	x		x
SO 1298			x			x		x		x	x		x
SO 1299										x		x	x
SO 1299.6												x	
SO 1302								x		x			
SO 1305										x			
SO 1306		x	x	x	x	x		x		x	x		x
SO 1308						x		x		x			x
SO 1310						x		x		x			x
SO 1311						x		x		x			x
SO 1312						x		x		x			x
SO 1313						x		x		x			
SO 1314						x		x		x			x

2.3. Channel Forming Discharge

Different methods are used to determine channel forming discharge. An analysis on effective, dominant and bankfull discharge was performed on the Escondida reach (Larsen et al. 2011) and are applicable for the use on the San Acacia reach. Effective discharge was determined using Geo Tool (Raff et al. 2003). Recurrence interval or dominant discharge was calculated using the annual peak flow at the San Acacia gage and performing a Weibull distribution on the available data. Finally, bankfull was observed by Reclamation in August, 1999 on the Middle Rio Grande. Table 2.5 provides a summary of the channel forming discharge analysis. For more detail refer to the Escondida Reach Report (Larsen et al. 2007).

Table 2.5 – Channel Forming Discharge Analysis at San Acacia
(Larsen et al. 2007)

Analysis		**Discharge (cfs)**
Effective		4,600
Recurrence Interval	2yr	4,587
	5yr	5,984
Bankfull		5,000

The data suggest that all three methods result in similar flow rates. A 5,000 cfs bankfull discharge determined by Reclamation will be used in the hydraulic analysis of the San Acacia reach.

3. Channel Classification

3.1. Channel Planform Methods

Numerous quantitative channel classification methods were investigated to determine the methods most applicable to the San Acacia reach. The channel was classified based on slope-discharge relationships, channel morphology methods and the stream power relationships. In addition, a qualitative classification of the channel was also made based on GIS evaluation of aerial photographs.

In the previous San Acacia reach report the following classification methods were used: Leopold and Wolman (1957), Lane (from Richards 2001), Henderson (1966), Schumm and Khan (1972), Parker (1976), Ackers and Charlton (1982) and van den Berg (1995). However based on a detailed literature review, some methods were determined to not apply to this reach and additional methods were investigated. The Ackers and Charlton (1982) method was developed for gravel-bed rivers and van den Berg (1995) was developed for channels with a sinuosity greater than 1.3, both of which are not applicable for the San Acacia reach. In addition, the Rosgen (1996) classification method which is based on channel morphology and the Nanson and Croke (1992) and Chang (1979) classification methods which are based on stream power have been included in the analysis.

3.1.1. Slope-Discharge Methods

Leopold and Wolman (1957) determined a critical slope value, based on discharge, which separates braided from meandering planforms. The following equation shows the slope-discharge relationship developed based on Figure 3.1:

$$S = 0.6Q^{-0.44}$$

Where S is the critical slope and Q is the channel discharge (cfs). Channels with slopes greater than the critical slope will have a braided planform, while channels with slopes less than the critical slope will have a meandering planform. Straight channels may fall on either side of the critical slope. Leopold and Wolman identified channels with a sinuosity greater than 1.5 as meandering and channels with a sinuosity less than 1.5 as straight. Using the slope-discharge relationship and the critical sinuosity value, channels can be divided into straight, meandering, braided, or straight/braided channels.

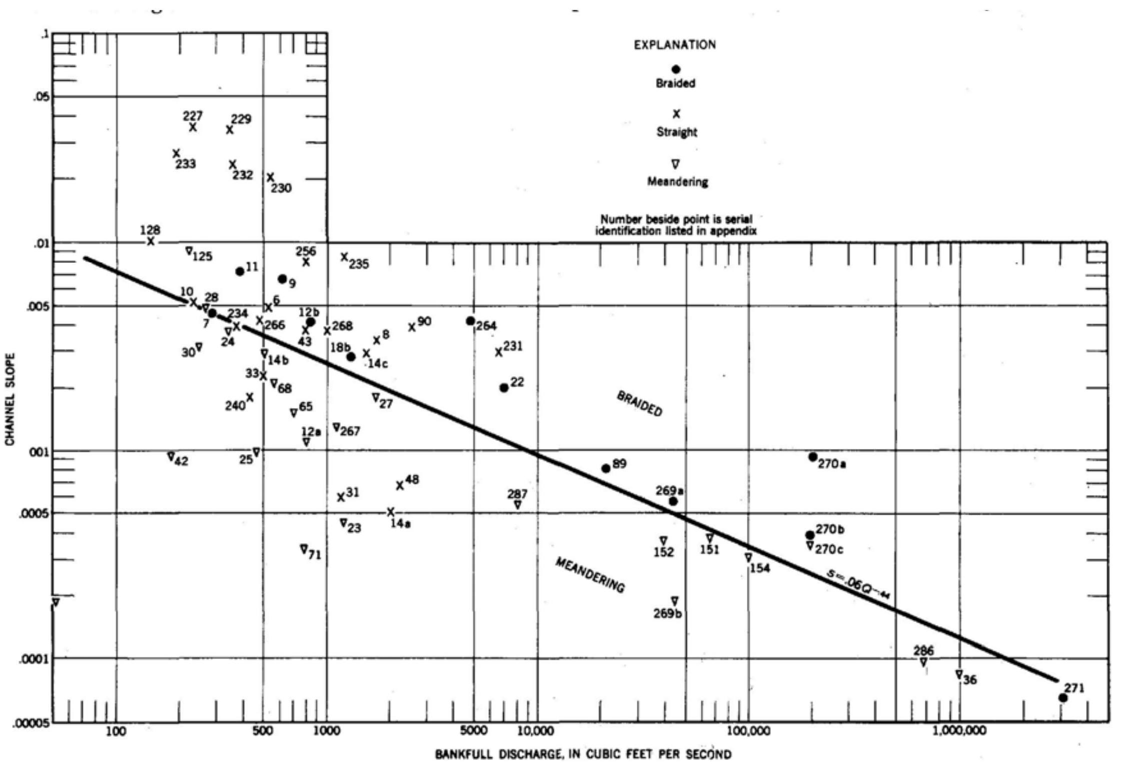

Figure 3.1 – Classification for braided and meandering planform
(Leopold and Wolman 1957)

Lane (from Richards 2001) developed a slope-discharge threshold value (κ) calculated by this equation:

$$\kappa = SQ^{0.25}$$

Where S is the channel slope and Q is the channel discharge (cfs). The classification of the stream is based on the value of κ as shown below:

Meandering:	$\kappa \leq 0.0017$
Intermediate:	$00010 > \kappa > 0.0017$
Braided:	$\kappa \geq 0.010$

These threshold values assume the use of English units. Values of κ are also available for SI units.

Henderson (1966) developed a slope-discharge method, which accounts for the median bed size by plotting the critical slope as defined by Leopold and Wolman against the median bed size. The following equation shows the relationship of the slope as a function of both median particle size and discharge based on Figure 3.2:

$$S = 0.64 d_s^{\,1.14} Q^{-0.44}$$

Where S is the critical slope, d_s is the median grain size (ft), and Q is the discharge (cfs). For slope values that plot close to this line have a straight or meandering planform. Braided channels plot well above and below this line.

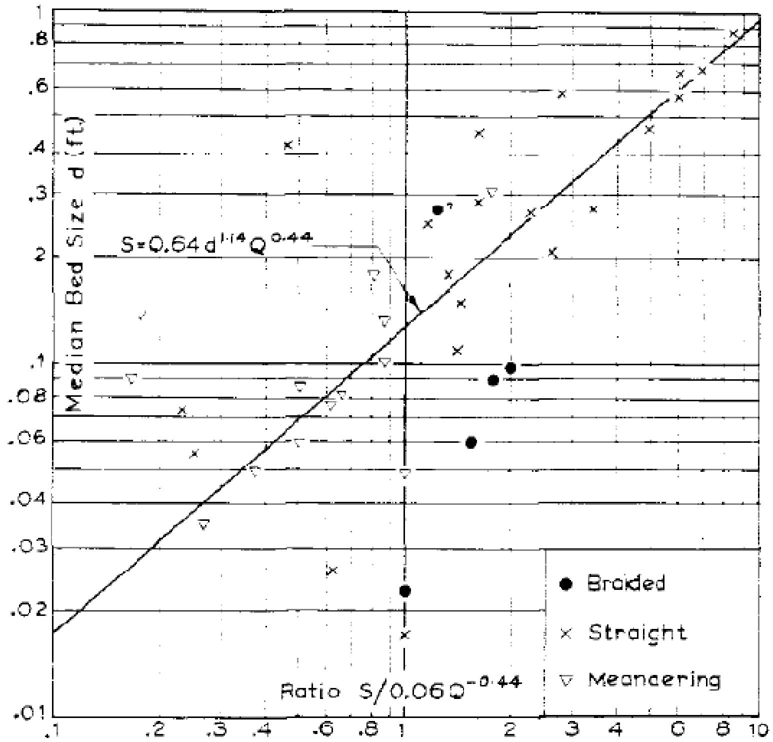

Figure 3.2 – S-d-Q Relationship for Natural Rivers (Henderson 1966)

Schumm and Khan (1972) developed empirical relationships between valley slope (S_v) and channel planform based on flume experiments. Thresholds were determined for each channel classification as follows:

Straight:	$S_v < 0.0026$
Meandering:	$0.0026 < S_v < 0.016$
Braided:	$S_v > 0.016$

3.1.2. Channel Morphology Methods

Rosgen (1996) developed a channel classification method based on entrenchment ratio, width/depth ratio, sinuosity, slope, and bed material. Using these channel characteristics, Rosgen developed eight major classifications and a number of sub-classifications. Figure 3.3, shows Rosgen's method for stream classification.

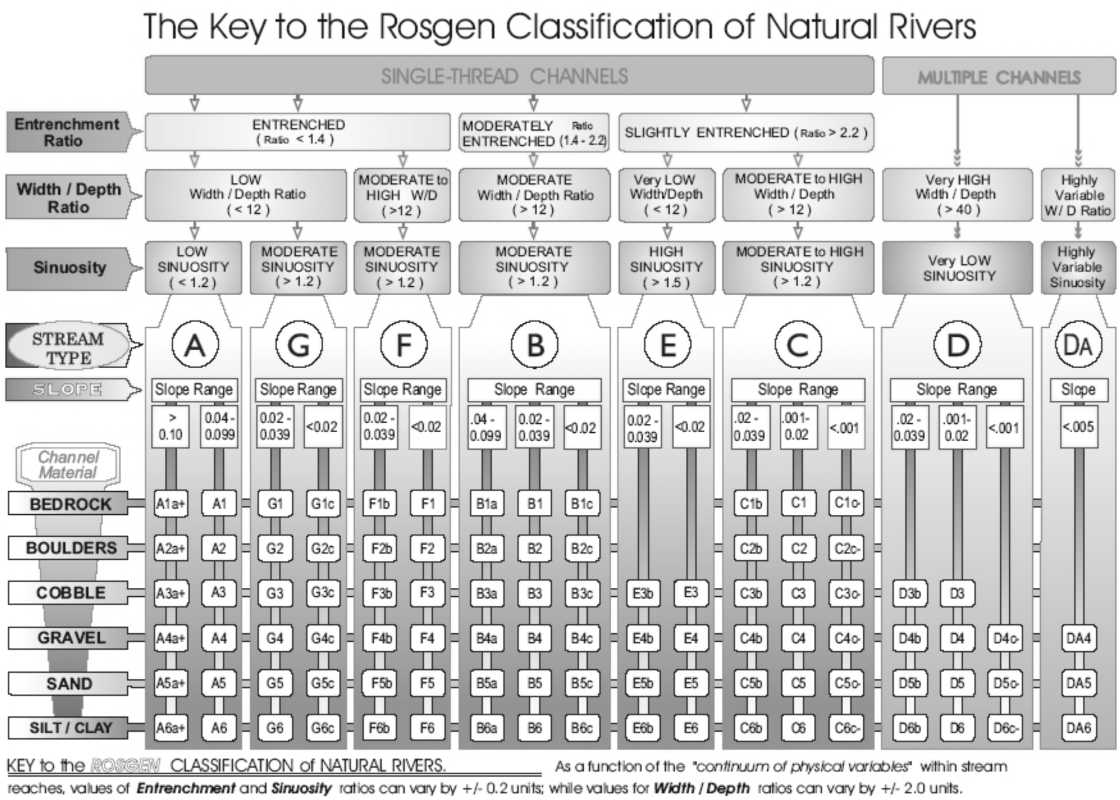

Figure 3.3 – Rosgen Channel Classification Key (Rosgen 1996)

Parker (1976) considered the relationship between slope, Froude number, and width to depth ratio. Experiments in laboratory flumes and observations of natural channels lead to the Figure 3.4 and the following channel planform classifications:

Meandering: $\frac{S}{Fr} << \frac{W}{h}$

Transitional: $\frac{S}{Fr} \sim \frac{W}{h}$

Braided: $\frac{S}{Fr} >> \frac{W}{h}$

Where S is the channel slope, Fr is the Froude number, and W/h represents the width to depth ratio.

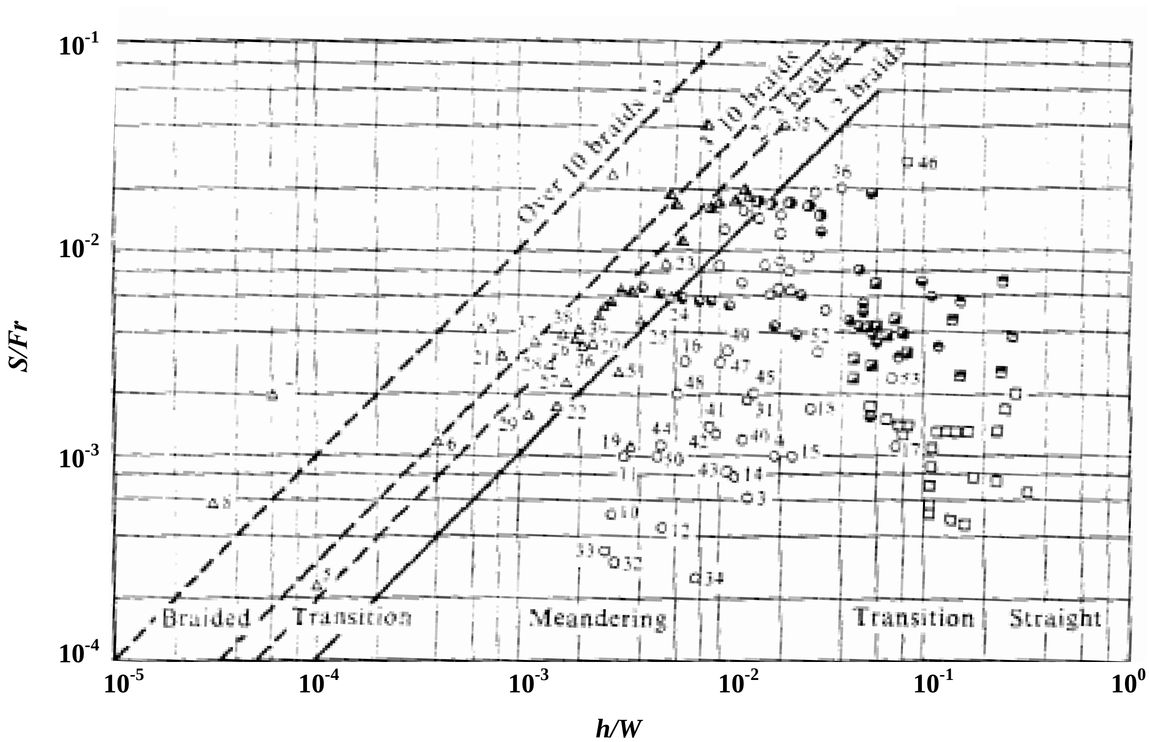

Figure 3.4 – Parker's Channel Planform Classification (Parker 1976)

3.1.3. Stream Power Methods

Nanson and Croke (1992) used specific stream power and sediment characteristics to differentiate between types of channel planforms. The equation used to determine specific stream power is as follows:

$$\omega = \gamma QS / W$$

Where ω is specific stream power (W/m^2), γ is the specific weight of water (N/m^3), S is channel slope, and W is channel width (m). Three main classes and twelve sub-classes where developed by Nanson and Croke. Three classifications of interest in this reach, along with the corresponding specific stream power and expected sediment type, are shown in Table 3.1.

Table 3.1 – Nanson and Croke (1992)Planform Classification

Planform	**Description**	**Specific Stream Power (W/m^2),**	**Sediment Type**
Braided	Braided-river floodplains	ω = 50-300	gravels, sand, and occasional silt
Meandering	Meandering river, lateral migration floodplains	ω = 10-60	gravels, sands, and silts
Straight	Laterally stable, single-channel floodplains	ω <10	silts and clays

Chang (1979) used data from numerous rivers and canals to develop channel classifications based on stream power. The classifications are presented in terms of valley slope and discharge. Figure 3.5, below, shows the four classification regions (1, 2a, 2b and 2) defined by Chang for sand streams.

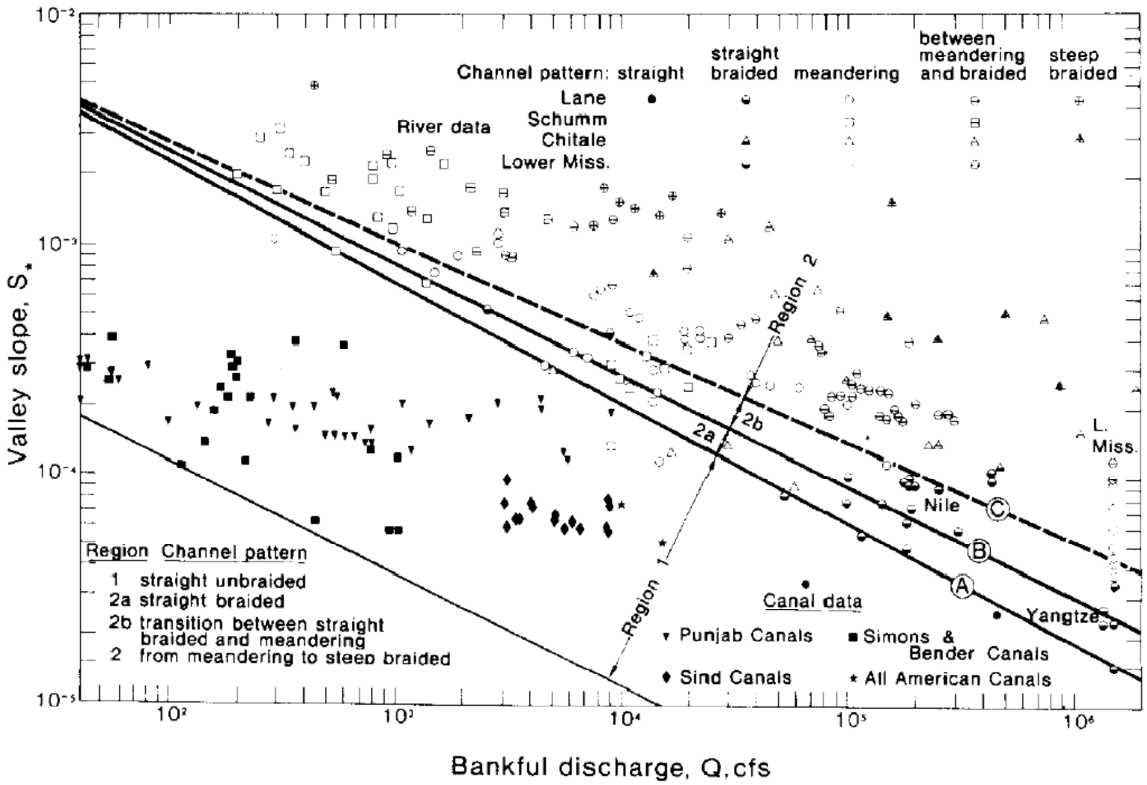

Figure 3.5 – Chang's Stream Classification Method Diagram (Chang 1979)

Chang found that at low valley slopes, rivers will have a straight planform. With constant discharge, an increase in valley slope will cause the channel to transform to a braided or meandering planform.

3.2. Channel Planform Results

Visual, qualitative characterization of the channel was performed using channel planforms delineated from aerial photographs using GIS. Figure 3.6 shows the historical planform has changed from 1918 to 2006.

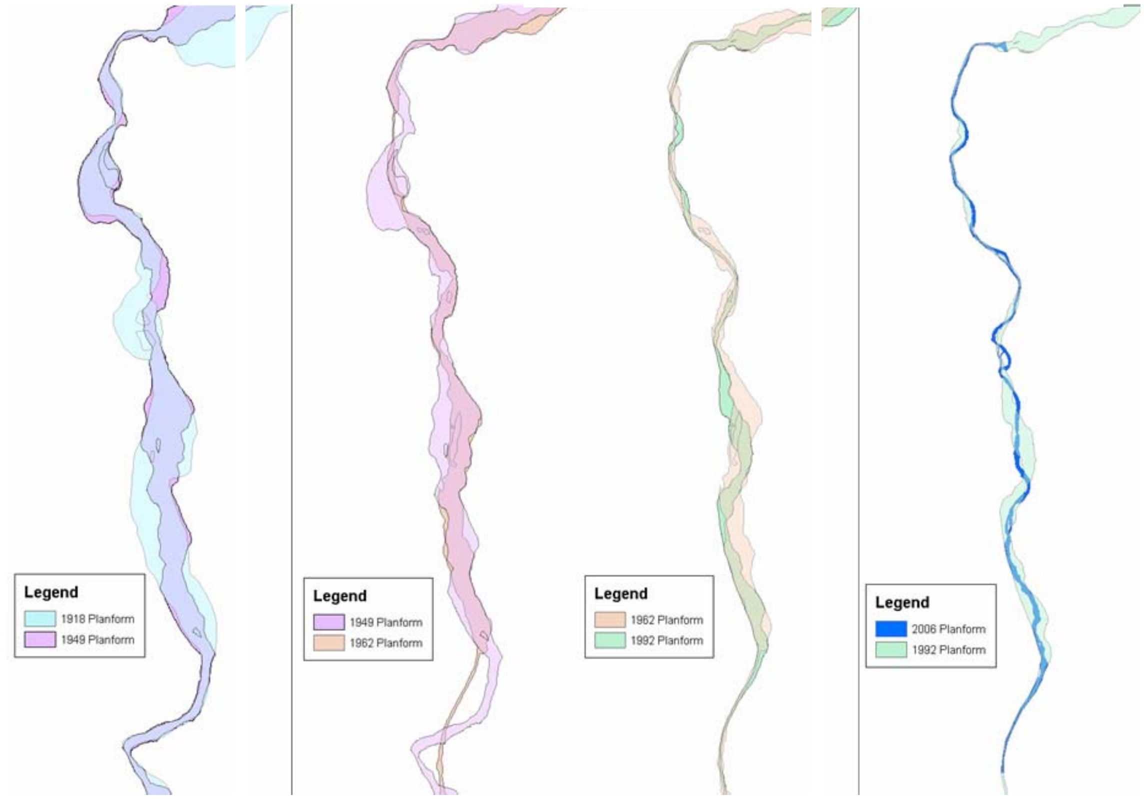

Figure 3.6 – Historical Planforms

The previous study (USBR 2003) stated that the river consisted of two morphologies which were determined based on aerial photography from 1918, 1935, 1949, 1962, 1972, 1985, 1992 and 2001. The following were the morphologies identified:

1) A mostly straight, narrow, single channel along 51% of the overall length
2) A wide, mostly straight, active channel that alternates single threaded channel and a braided morphology.

In 2002, 2005 and 2006 addition aerial photograph were flown. Figure 3.7 shows the more recent change from 2001 to 2006.

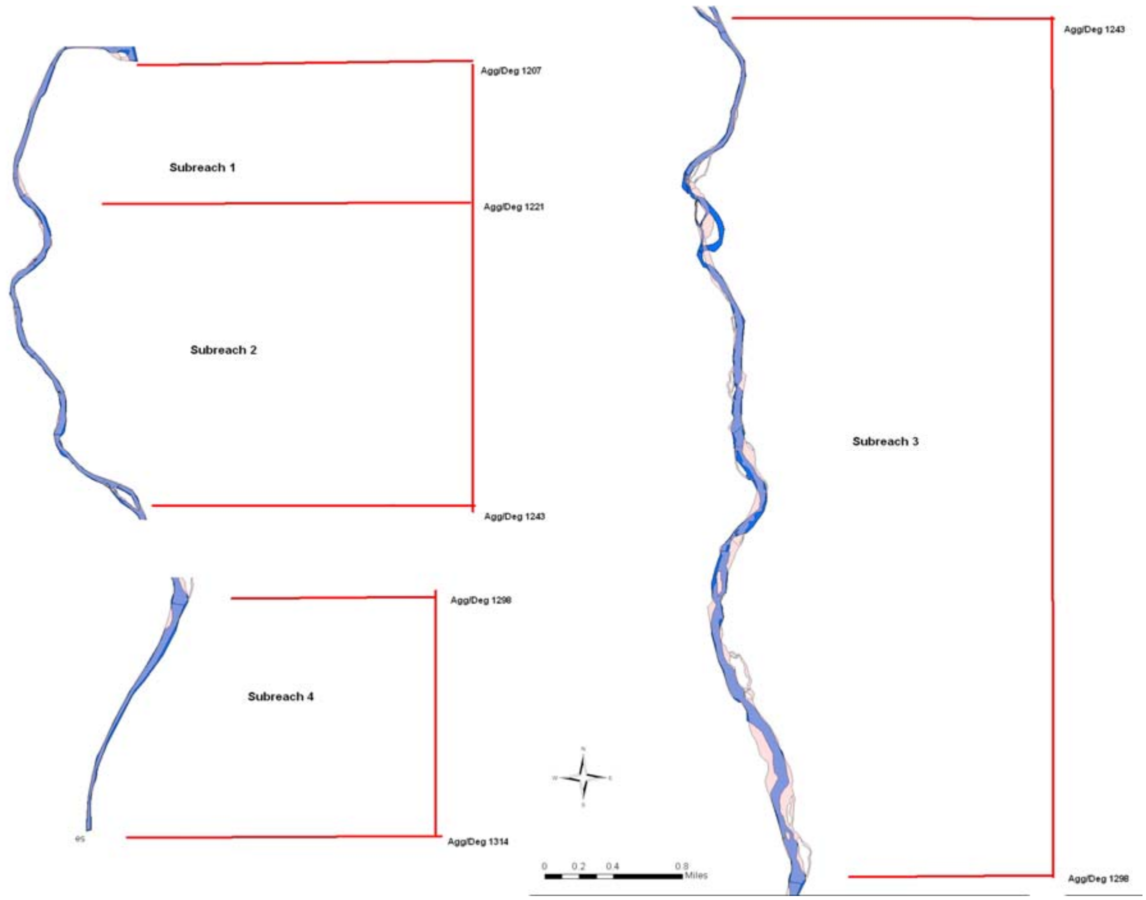

Figure 3.7 – Planform Comparison between 2001 to 2006

Based on the figure, subreaches 1, 2 and 4 show little to no change from 2001 to 2006. However, subreach 3 has shown recent changes in planform width. In addition, the meanders are becoming more pronounced in certain areas. There also seems to be a tendency in subreach 3 for the channel to want to meander, however a levee is located on the west bank, which are preventing further migration. Reclamation has set back the levee in certain locations (Appendix A); this will allow portions of the reach to widen and the channel to have a more meandering planform or return to a more natural braided state, which could benefit silver minnow habitat.

Currently, it can be stated that the channel is still considered to be a straight, single threaded narrow channel, which has a tendency to braid in certain areas during low flows. However, over time the relocation of the levee will allow the river to meander during high flows and potentially braid during low flows.

HEC-RAS was used to determine the necessary values to input into the quantitative channel classification model. The model was run using data from the Agg/Deg survey information. Measurements of the channel and valley lengths were obtained from aerial photos in GIS.

The channel classification from the previous study is compared with the classification based on the 2002 data. It is not stated what data was used to determine the classification in the previous study by Reclamation (2003). Table 3.2 shows a comparison table of the previous study and current study results.

Table 3.2 – Channel Classification Results and Comparison

Subreach	Study	Slope-discharge				Channel Morphology		Stream Power	
		Leopold and Wolman	Lane	Henderson	Schumm & Khan	Rosgen	Parker	Nanson & Croke	Chang
1	Previous	Straight	Transition	Meandering	Straight	F4/F5	Straight/ Meandering	NA	NA
	Current (2002 data)	Straight	Transition	Braided	Straight	F5c	Meandering	Meandering	Meandering to Steep Braided
2	Previous	braided	Transition	Meandering	Straight	F4/F5	Meandering	NA	NA
	Current (2002 data)	Straight	Transition	Braided	Straight	B5c	Meandering / Transitional	Meandering	Meandering to Steep Braided
3	Previous	braided	Braided	Meandering	Meandering	F5/D5	Braided	NA	NA
	Current (2002 data)	Straight	Transition	Braided	Straight	B5c	Meandering / Transitional	Straight	Meandering to Steep Braided
4	Previous	Straight	Transition	Braided	Straight	F5	Straight	NA	NA
	Current (2002 data)	Straight	Transition	Braided	Straight	C5c	Meandering	Meandering	Meandering to Steep Braided
Total	Previous	Braided	Transition	Meandering	Meandering	NA	Meandering	NA	NA
	Current (2002 data)	Straight	Transition	Braided	Straight	C5c	Meandering / Transitional	Straight	Meandering to Steep Braided

The comparison table above shows that there is some variability between the two studies. The Leopold and Wolman, Lane, and Schumm and Khan methods show similar results from the previous study. Both the Leopold and Wolman and Schumm and Khan methods indicate a straight planform. However the Lane methods indicates a transition planform between meandering and braiding.

When compared with the observations from the aerial photographs, the methods that indicate a straight or braided channel classification provide the best representation of the actual channel characteristics. Because braiding is only seen in large sections of the channel at low flows, the straight classification given by Leopold and Wolman (1957) and Schumm and Khan (1972) is the most accurate for the bankfull discharge of 5000 cfs.

The other methods suggest that the reach might be in a transitional zone shifting its planform but there are no direct observations that can prove a change to a meandering trend since the sinuosity is still less than 1.5 (Section 3.3).

3.3. Sinuosity

3.3.1. Methods

The sinuosity was measured in GIS from aerial photographs of the reach. The valley length was measured for the entire reach and for each subreach as the straight-line distance between the upstream and downstream extents of the reach. The channel length was measured by estimating the location of the river thalweg based on the aerial photographs and planform delineations. The channel length was divided by the valley length to calculate the sinuosity.

It was uncertain how sinuosity was calculated in the previous study by Reclamation, so it was recalculated in the report.

3.3.2. Results

Table 3.3, summarizes the overall sinuosity from 1918 to 2006. Although the trend was toward a decreasing sinuosity, there this is a slight increase from 1992 to 2002 in Subreach 1. Since 2002 there has been no change to the sinuosity in the San Acacia reach, this could be attributed to the significant narrowing observed throughout the reach.

Table 3.3 – Sinuosity Changes

San Acacia	Sinuosity									
Reach	1918	1935	1949	1962	1972	1985	1992	2002	2005	2006
Reach 1	1.41	1.27	1.26	1.23	1.24	1.25	1.25	1.26	1.26	1.26
Reach 2	1.18	1.21	1.19	1.06	1.06	1.06	1.1	1.04	1.04	1.04
Reach 3	1.04	1.04	1.02	1.06	1.04	1.04	1.07	1.01	1.01	1.01
Reach 4	1.27	1.27	1.24	1.02	1.03	1.03	1.03	1.02	1.02	1.02
Total	1.19	1.2	1.18	1.11	1.11	1.11	1.14	1.09	1.09	1.09

From aerial photographs subreach 3 suggested a tendency towards a meandering planform; however, the sinuosity analysis does not show a meandering planform. This is because it looked at the overall channel and not at the few locations where the meandering planform occurred. In addition, between 1949 and 1962 levees were constructed, which reduced the area available for river migration and reduced sinuosity. Figure 3.8 provides a graphical representation of how the sinuosity has changed in each subreach and in the entire reach over time.

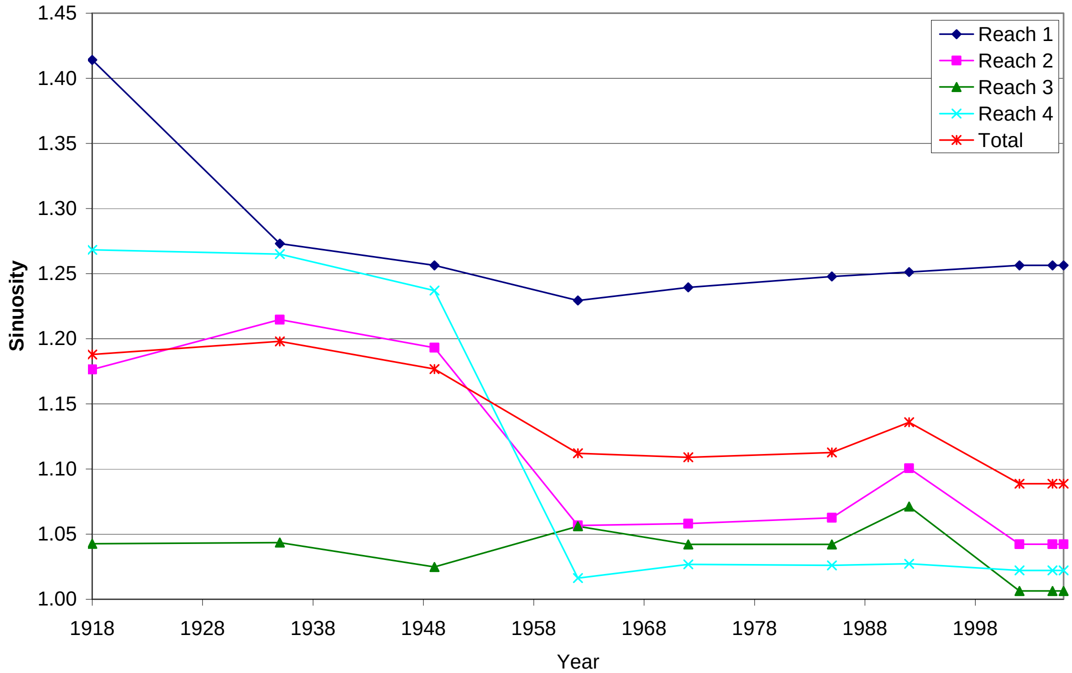

Figure 3.8 – Sinuosity

The figure shows an overall decrease in the sinuosity from 1918 to 2006. The decrease is due to major channelization efforts that have occurred along the Rio Grande. The set back levee and LFCC will give the channel more space for lateral migration potentially increasing local sinuosity and follow a more historical course.

3.4. Longitudinal Profile

The data used for the longitudinal profiles are obtained from the range lines. The range lines were surveyed by the USBR at various dates. A vertical datum shift occurred from 2002 to 2005. The 2005 data is on NAVD 88, while all the other data is on NGVD 29. Thus near the San Acacia reach in New Mexico the NAVD 88 data is 2.4 feet higher than the NGVD 29 data. Thus adjustments were made to the data for comparison purposes.

3.4.1. Methods

Thalweg Elevation

The thalweg elevation was calculated as the lowest point in the channel based on the SA and SO-line survey. This was used because the detailed cross section surveys provided more detail of the thalweg location verses the Agg/Deg surveys which are based on aerial photography, which cannot differentiate the difference between the channel bed and water surface. SA and SO-line data were only available from 1988-2005.

Mean Bed Elevation

Trends in mean bed elevation were evaluated using the Agg/Deg survey data based on aerial photographs. Agg/Deg surveys were generally conducted during low flows to assure a relatively accurate mean bed elevation. This elevation was used to show the changes in mean bed elevation through time. Because the SA and SO-lines usually fall at the same location as the Agg/Deg lines, only the Agg/Deg lines were used to analyze the mean bed elevation. The change in mean bed elevation at each cross-section was evaluated, along with the changes in the average mean bed elevation by subreach.

3.4.2. Results

Thalweg Elevation

Figure 3.9 shows a temporal and spatial change of the thalweg elevation at various SA and SO-line for the San Acacia reach. A total of 11 cross sections were selected.

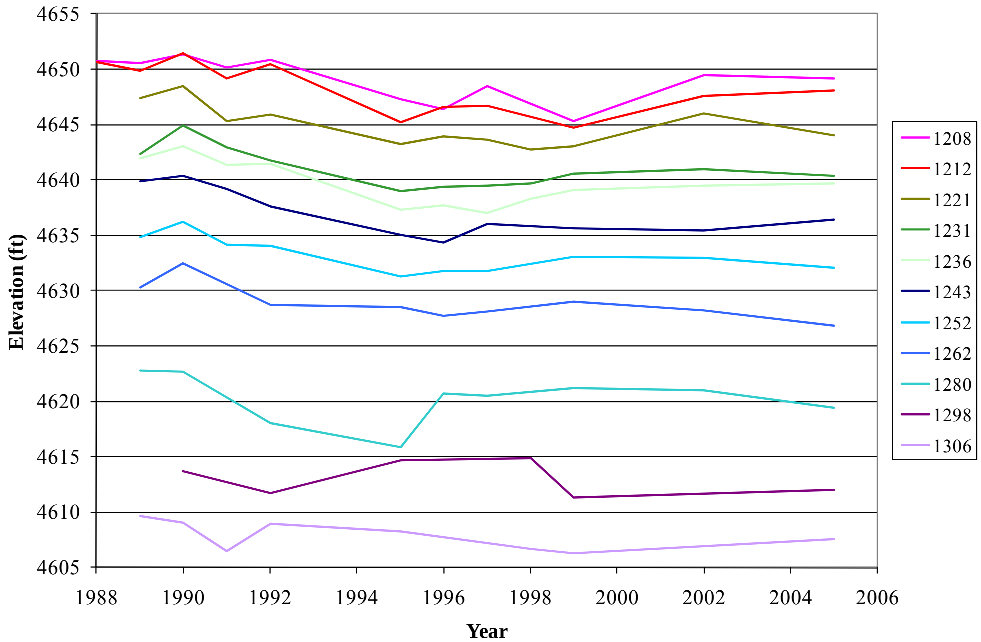

Figure 3.9 – Change in thalweg elevation by SO-line

The figure shows that there is change in the thalweg elevation for year to year and from cross section to cross section. This change is due to the channel adjusting to the discharge and sediment supply entering the reach. The variation in elevation can be explained based on the river responding to the reach until a dynamic equilibrium can be reached.

Figure 3.10 shows the thalweg elevation profile of the entire reach.

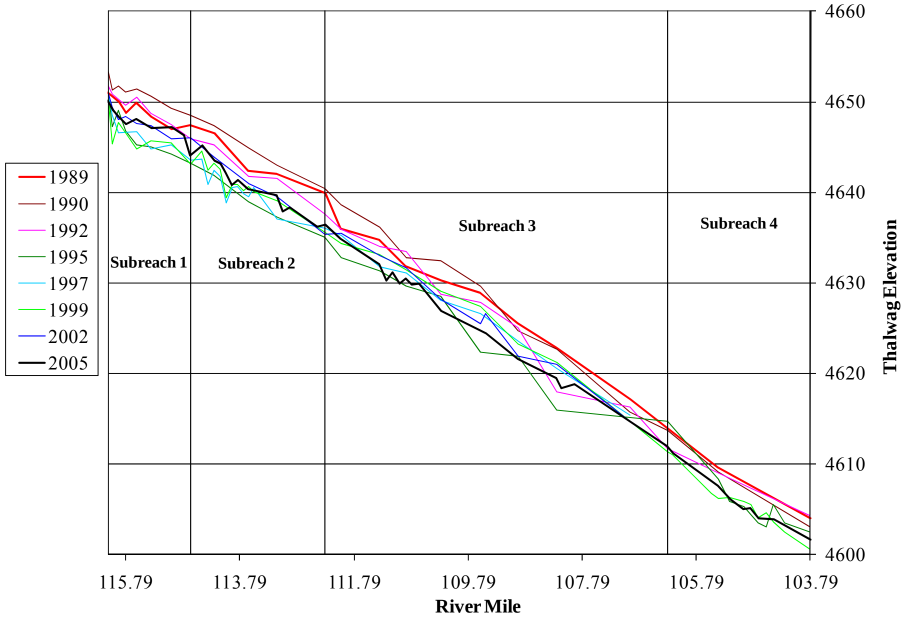

Figure 3.10 – Thalweg elevation profile

Figure 3.11a shows the comparison of the thalweg from 1989 to each subsequent year. A positive result suggest degradation, while a negative result suggest aggradation.

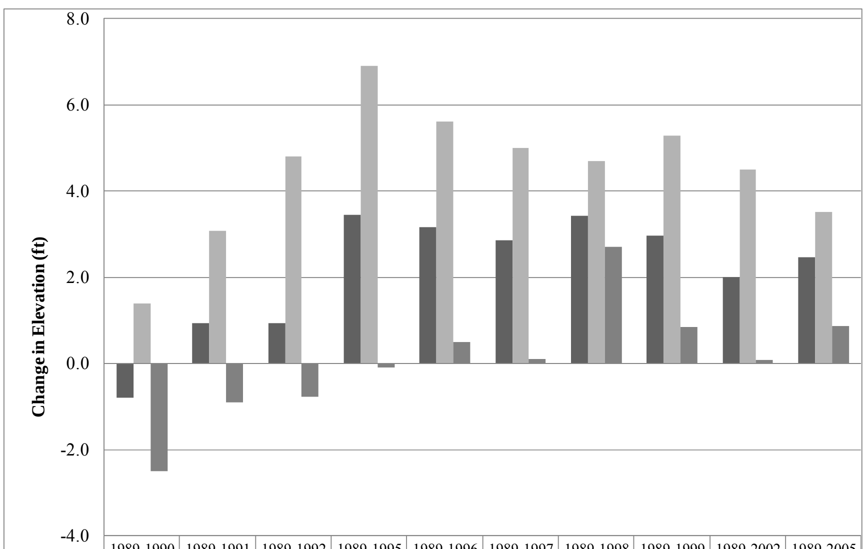

	1989-1990	1989-1991	1989-1992	1989-1995	1989-1996	1989-1997	1989-1998	1989-1999	1989-2002	1989-2005
Average	-0.8	0.9	0.9	3.4	3.2	2.9	3.4	3.0	2.0	2.5
Maximum	1.4	3.1	4.8	6.9	5.6	5.0	4.7	5.3	4.5	3.5
Minimum	-2.5	-0.9	-0.8	-0.1	0.5	0.1	2.7	0.8	0.1	0.9

Figure 3.11a – Difference in Thalweg elevation profile compared to 1989

When comparing the thalweg profile from 1989 to 2005 the overall elevation change on average in 2.5 feet, which is degradation. In general, the river has shown a trend toward degradation. However, when you compare the change in elevation from year to year as shown in Figure 3.11b, the river changes from aggradation to degradation at so own. The overall change in elevation is becoming less variable from year to year. The channel seems to be moving back and forth, trying to reach a dynamic equilibrium.

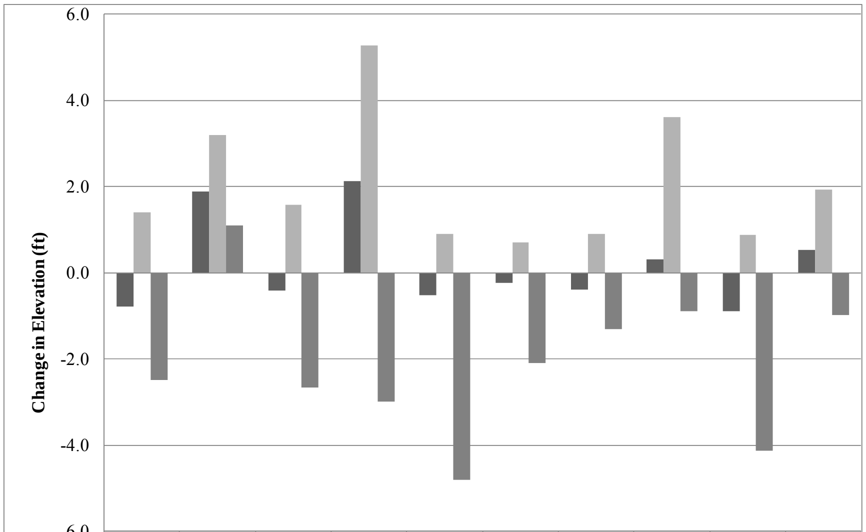

	1989-1990	1990-1991	1991-1992	1992-1995	1995-1996	1996-1997	1997-1998	1998-1999	1999-2002	2002-2005
Average	-0.8	1.9	-0.4	2.1	-0.5	-0.2	-0.4	0.3	-0.9	0.5
Maximum	1.4	3.2	1.6	5.3	0.9	0.7	0.9	3.6	0.9	1.9
Minimum	-2.5	1.1	-2.7	-3.0	-4.8	-2.1	-1.3	-0.9	-4.1	-1.0

Figure 3.11b – Difference in Thalweg elevation from year to year

In addition, cross section surveys are plotted and provided in Appendix B.

<u>*Mean Bed Elevation*</u>

Changes in mean bed elevation over time are shown in Figure 3.12 for each subreach and for the entire reach. This is based on the HEC-RAS data obtains for Reclamation TSC in Denver whom modified the in stream channel portion of the cross sections by lowering the bed elevation iteratively, to minimize the error difference between the observed wetted width from the aerial photography and the HEC-RAS model results for wetted width.

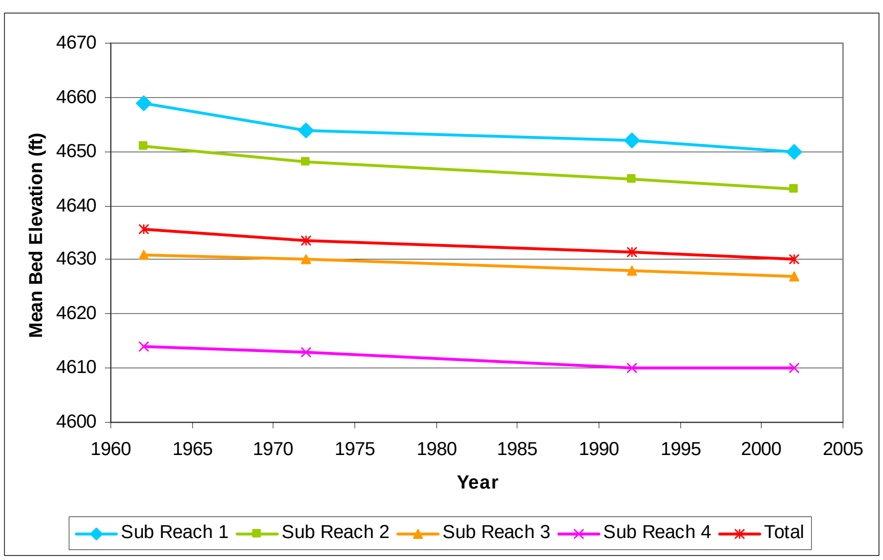

Figure 3.12 – Reach averaged mean bed elevation

The mean bed elevation from 1962 to 2002 has decreased. Table 3.4 provides a summary of the average overall bed degradation for each subreach based on the Agg/Deg lines.

Table 3.4 – San Acacia reach Degradation Summary

Subreach	Degradation (ft)
1	9
2	8
3	4
4	4
Total	6

The possible causes of the degradation are associated with the reduction in upstream sediment supply.   Thus the river has a tendency to degrade due to in channel erosion. The reduced sediment supply is attributed to both reservoir construction and reduced sediment flow from the Rio Puerco.

To assist with flood control, water supply and water diversion reservoirs and dams were construct, which have reduced the sediment supply within the river. This has casued erosion and degradation within the Middle Rio Grande. In addition, there has been a reduction in sediment supply from the Rio Pureco located 10 miles upstream of the San Acacia Diversion Dam (Gillis 2006). The following are suggested reason for sediment reduction: arroyo evolution (Gillis 1992), successful land-management treatments which reduced erosion(SCS 1977; Burkham 1966) and a decrease in the annual peak flows and introduction of the tamarisk (Love 1997).

The change in mean bed elevation at each Agg/Deg line can be seen in Figure 3.13. The entire reach has been experiencing degradation, with subreaches 1 and 2 experiencing the most degradation overall due to the proximity to the San Acacia Diversion Dam and the Rio Puerco. The diversion dam also provides a river grade control. The degradation trends are similar to those observed by Bauer (2000). This suggests that the channel which is not stable.

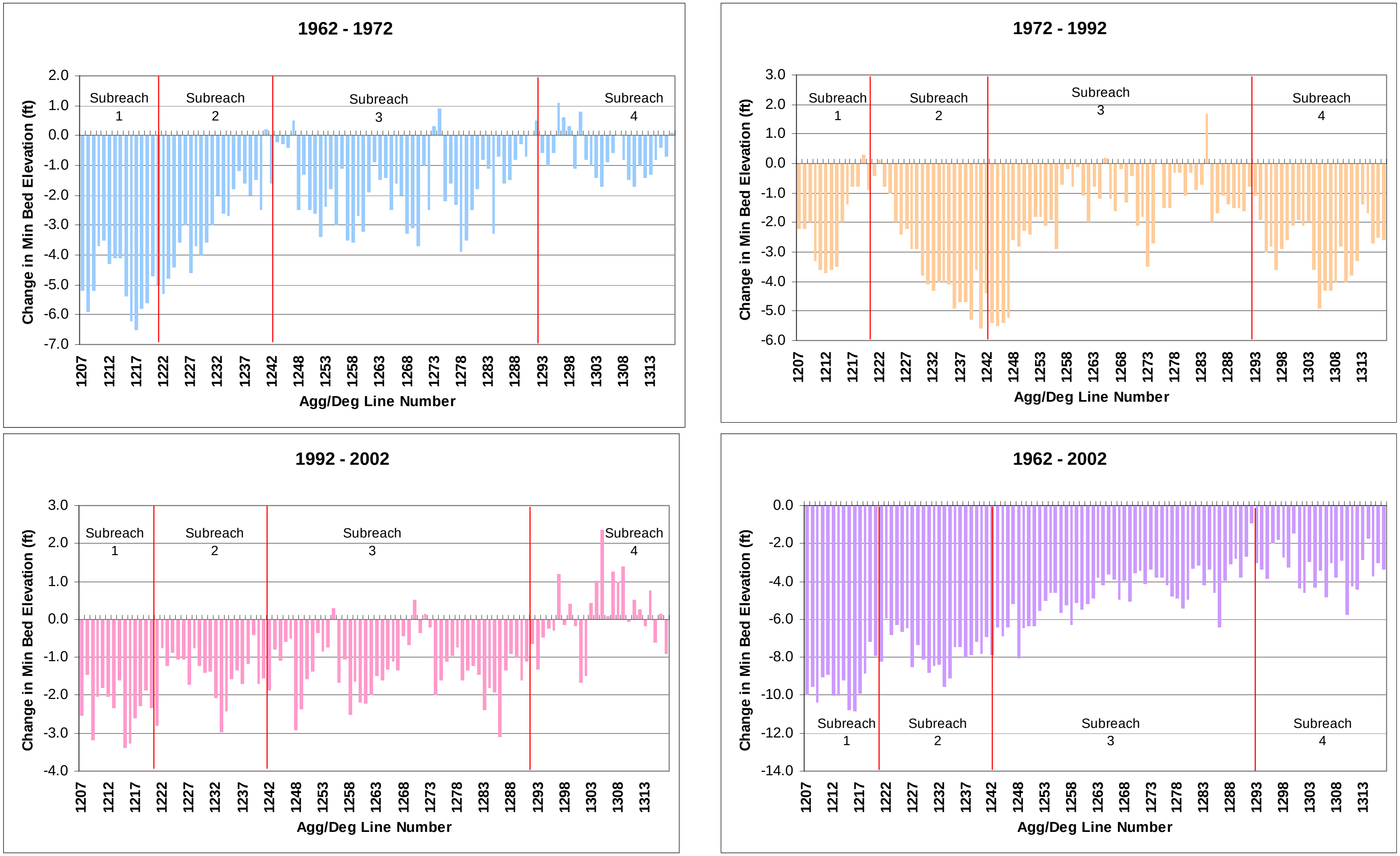

Figure 3.13 – Change in mean bed elevation between 1962 to 2002

3.5. Channel Geometry

3.5.1. Methods

Trends in geometric properties where analyzed from HEC-RAS model run using the bankfull discharge of 5,000 cfs. Reclamation used HEC-RAS to determine channel geometry using 1962, 1972 and 1992 Agg/Deg line survey data, and 1997 and 1999 detailed SA and SO-line cross section survey. They determined the overall trend for different hydraulic parameters.

This study added data from 2002 Agg/Deg and 2005 SA and SO-line surveys. A Manning's "n" value of 0.02-0.024 was used for the main channel and a Manning's value of 0.1 was used for the overbank area. Manning's "n" values, bank station and levee locations, and downstream reach lengths where originally determined by Reclamation. Each geometry file was evaluated and compared to GIS aerial photography for the corresponding year. Adjustments to the bank stations, levee locations, and reach lengths where made based on engineering judgment to best represent the actual channel conditions.

Channel geometry parameters calculated at each cross section by HEC-RAS include:

Cross-Sectional Area	A
Top Width	W
Wetted Perimeter	P_w
Hydraulic Depth	D
Velocity	V
Froude Number	Fr

The numerical results from the HEC-RAS are located in Appendix D. The above geometric parameters and other properties available from HEC-RAS were used to calculate two additional channel geometry properties. These properties include:

Max Depth	D_{max} = Water Surface Elevation – Min Channel Elevation
Width/Depth Ratio	W/D = Top Width / Hydraulic Depth

3.5.2. Results

Figure 3.14 shows the trends in the average cross-sectional area, top width, wetted perimeter, hydraulic depth, maximum depth, channel velocity, Froude number, and width/depth ratio in each subreach and in the overall reach.

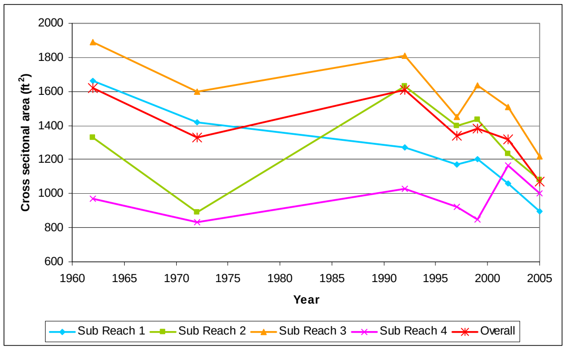

a.) Cross Sectional Area

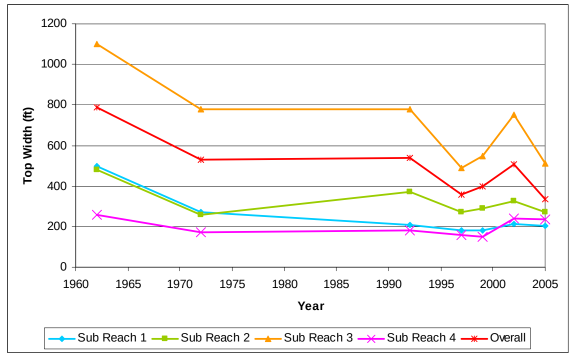

b.) Top Width

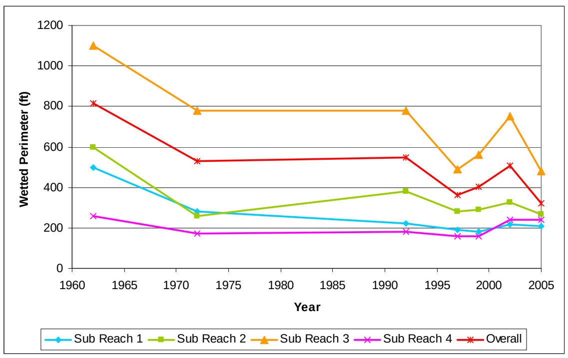

c.) Wetted Perimeter

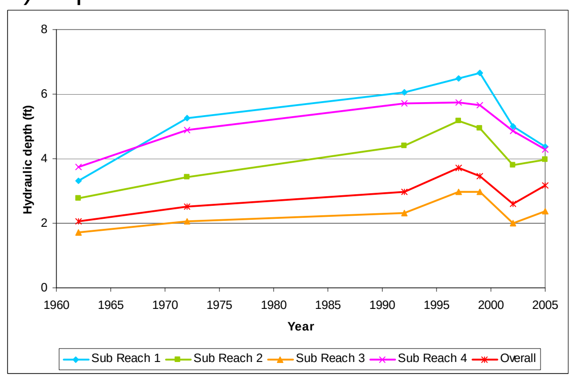

d.) Hydraulic Depth

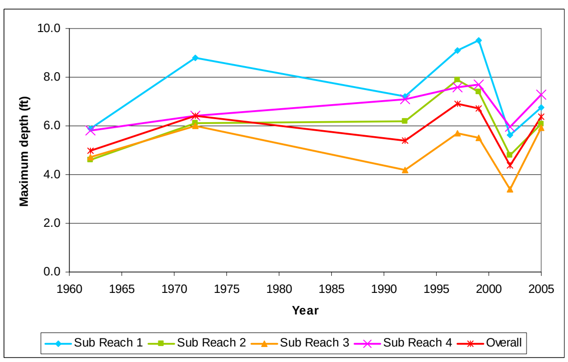

e.) Maximum Depth

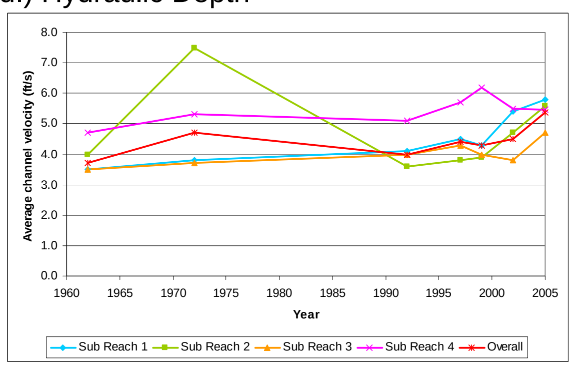

f.) Channel Velocity

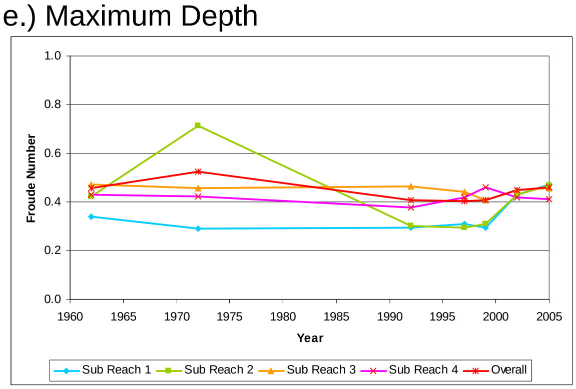

g.) Froude Number

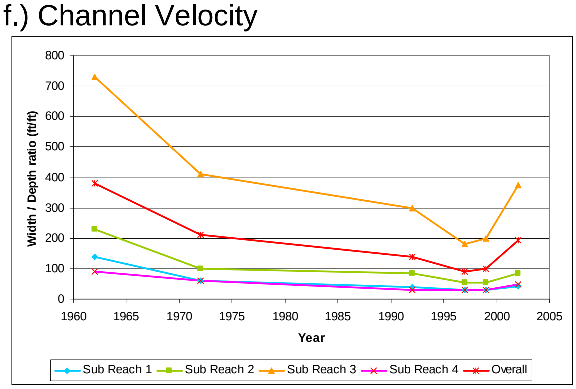

h.) Width to Depth Ratio

Figure 3.14 – Channel Geometry Properties

Tables 3.5 to 3.9 provide a summary showing how the different hydraulic parameters have changed over time for the overall reach and each subsequent reach.

Table 3.5 – Summary of reach average values for San Acacia reach

HEC-RAS Results	1962	1972	1992	1997	1999	2002	2005	Rate of Change from 1962 to	
Total Wetted Width (ft) - Includes overbank width	1,170	900	560	460	460	503	336	-19.40	ft/yr
Width of Channel (ft)	790	530	540	360	440	453	319	-10.95	ft/yr
Maximum Depth (ft)	5.0	6.4	5.4	6.9	6.7	4.4	6.4	0.39	inch/yr
Average Depth (ft)	2.1	2.5	3.8	4.1	4.1	2.6	3.9	0.50	inch/yr
Width/Depth Ratio (ft/ft)	380	210	140	90	100	192	86	-6.84	1/year
Channel Area (ft^2)	1,620	1,330	1,610	340	1,380	1,330	1,069	-12.81	ft^2/yr
Wetted Perimeter (ft)	814	532	550	364	404	460	323	-11.42	dt/yr
Average Velocity (ft/sec)	3.7	4.7	4.0	4.4	4.3	4.5	5.4	0.04	ft/sec-yr
Mean Bed Elevation (ft)	4,639.5	4,639.0	4,633.9	4,631.2	4,630.4	4,630.2	4,633.3	-0.14	ft/yr
Energy Grade Line (ft/ft)	0.00091	0.00085	0.00086	0.00081	0.00080	0.00094	0.00085	`$-1.4*10^{-6}$	1/yr

Table 3.5 provides the overall reach average hydraulic characteristics, which indicate that the channel seems to be narrowing and incising. The San Acacia reach has narrowed at a rate of approximately 20 feet per year and the channel has been incising causing the mean bed elevation to continue to drop 6.2 feet over 33 years. In addition, the maximum and average flow depth has decreased, which has caused the velocity to increase slightly, which is adding to the degradation of the reach due to high flow velocities within the reach.

Table 3.6 summarizes the hydraulic characteristics for subreach 1.

Table 3.6 – Summary of subreach 1 average values for San Acacia reach

HEC-RAS Results	1962	1972	1992	1997	1999	2002	2005	Rate of Change from 1962 to	
Total Wetted Width (ft) - Incldes overbank width	570	350	220	190	190	212	205	-8.49	ft/yr
Width of Channel (ft)	500	270	210	180	180	210	203	-6.91	ft/yr
Maximum Depth (ft)	5.9	8.8	7.2	9.1	9.5	5.6	6.8	0.25	inch/yr
Average Depth (ft)	3.7	4.5	5.8	6.3	6.6	5.0	4.4	0.20	inch/yr
Width/Depth Ratio (ft/ft)	1,400	600	40	30	30	43	47	-31.47	1/year
Channel Area (ft^2)	1,660	1,420	1,270	1,170	1,200	936	898	-17.72	ft^2/yr
Wetted Perimeter (ft)	500	280	220	190	180	214	206	-6.84	dt/yr
Average Velocity (ft/sec)	3.5	3.8	4.1	4.5	4.3	5.4	5.8	0.05	ft/sec-yr
Mean Bed Elevation (ft)	4,661.3	4,658.2	4,653.3	4,648.8	4,648.0	4,649.7	4,649.9	-0.27	ft/yr
Energy Grade Line (ft/ft)	0.00072	0.00053	0.00065	0.00077	0.00084	0.00076	0.00086	`$3.26*10^{-6}$	1/yr

Table 3.6 provides the characteristics of subreach 1. Compared to other reaches, subreach 1 has been relatively narrow. Over the past 40 years the channel has continued to narrow and the channel has incised. However, from 1999 to 2005 the channel width has had a tendency to increase and the maximum depth and average depth have decreased. The overall bed elevation has constantly been decreasing since 1962 at a rate of 0.26 feet per year. These trends can be explained by the fact that the

cross sectional area has been on a steady decrease from 1962 to 2005 resulting in an increased channel velocity (Figure 3.14). In addition, based on the HEC-RAS model the bankfull flow of 5000 cfs is primarily contained within the channel banks.

Table 3.7 summarizes the hydraulic characteristics for subreach 2.

Table 3.7 – Summary of subreach 2 average values for San Acacia reach

HEC-RAS Results	1962	1972	1992	1997	1999	2002	2005	Rate of Change from 1962 to	
Total Wetted Width (ft) - Incldes overbank width	910	530	400	290	290	319	272	-14.84	ft/yr
Width of Channel (ft)	480	260	370	270	290	308	235	-5.70	ft/yr
Maximum Depth (ft)	4.6	6.1	6.2	7.9	7.4	4.8	6.1	0.42	inch/yr
Average Depth (ft)	2.1	2.5	4.4	4.8	5.1	3.8	4.0	0.53	inch/yr
Width/Depth Ratio (ft/ft)	230	100	85	55	55	85	69	-3.74	1/year
Channel Area (ft^2)	1,330	890	1,630	1,397	1,436	1,233	1,082	-5.77	ft^2/yr
Wetted Perimeter (ft)	600	260	380	280	290	316	480	-2.79	dt/yr
Average Velocity (ft/sec)	4.0	7.5	3.6	3.8	3.9	4.7	5.6	0.04	ft/sec-yr
Mean Bed Elevation (ft)	4,653.3	4,652.1	4,646.4	4,643.8	4,641.8	4,643.5	4,643.1	-0.24	ft/yr
Energy Grade Line (ft/ft)	0.00066	0.00050	0.00091	0.00076	0.00070	0.00085	0.00092	`$6.05*10^{-6}$	1/yr

Table 3.7 proved a summary of subreach 2. As in the previous study (USBR 2003) subreach 2 seemed to follow similar trends as subreach one, however the cross sectional area slightly increased in the late 1990's. In the current trend analysis the cross sectional area has continued to decrease, however the wetted perimeter has slightly increased from 1997. This subreach continues to degrade at a rate of 0.24 feet per year.

Table 3.8 summarizes the hydraulic characteristics for subreach 3.

Table 3.8 – Summary of subreach 3 average values for San Acacia reach

HEC-RAS Results	1962	1972	1992	1997	1999	2002	2005	Rate of Change from 1962 to	
Total Wetted Width (ft) - Incldes overbank width	1,470	1,120	800	670	650	758	513	-22.25	ft/yr
Width of Channel (ft)	1,100	780	780	490	550	666	565	-12.45	ft/yr
Maximum Depth (ft)	4.7	6.0	4.2	5.7	5.5	3.4	5.9	0.33	inch/yr
Average Depth (ft)	1.5	1.9	2.6	2.8	2.8	2.0	2.4	0.25	inch/yr
Width/Depth Ratio (ft/ft)	730	410	300	180	200	373	216	-11.95	1/year
Channel Area (ft^2)	1,890	1,600	1,810	1,450	1,510	1,507	1,219	-15.60	ft^2/yr
Wetted Perimeter (ft)	1,100	780	780	490	560	659	480	-14.42	dt/yr
Average Velocity (ft/sec)	3.5	3.7	4.0	4.3	4.0	3.8	4.7	0.03	ft/sec-yr
Mean Bed Elevation (ft)	4,635.1	4,635.1	4,630.2	4,628.1	4,627.6	4,626.8	4,628.4	-0.16	ft/yr
Energy Grade Line (ft/ft)	0.00093	0.00095	0.00082	0.00071	0.00073	0.00104	0.00086	`$-1.63*10^{-6}$	1/yr

Table 3.8 provides a summary of subreach 3. Even thought subreach 3 has been the widest reach historically, there has been a similar trend towards channel narrowing and incising. There is a lower rate of degradation in subreach 3 compared to the previous reaches due to the tendency towards a wider channel geometry. In addition, the cross sectional area and wetted perimeter have decreased significantly primarily due to the width decreasing at a rate of approximately 20 feet per year.

Table 3.9 summarizes the hydraulic characteristics for subreach 4.

Table 3.9 – Summary of subreach 4 average values for San Acacia reach

HEC-RAS Results	1962	1972	1992	1997	1999	2002	2005	Rate of Change from 1962 to	
Total Wetted Width (ft) - Incldes overbank width	950	1,050	180	160	150	163	234	-16.65	ft/yr
Width of Channel (ft)	360	170	180	160	150	163	271	-2.07	ft/yr
Maximum Depth (ft)	5.8	6.4	7.1	7.6	7.7	6.0	7.3	0.42	inch/yr
Average Depth (ft)	3.0	2.8	5.8	5.9	5.5	5.0	4.3	0.36	inch/yr
Width/Depth Ratio (ft/ft)	90	60	30	30	30	5	55	-0.81	1/year
Channel Area (ft^2)	970	830	1,030	920	850	1,225	1,001	0.72	ft^2/yr
Wetted Perimeter (ft)	260	170	180	160	160	251	238	-0.51	dt/yr
Average Velocity (ft/sec)	4.7	5.4	5.1	5.7	6.2	5.5	5.5	0.02	ft/sec-yr
Mean Bed Elevation (ft)	4,615.7	4,614.4	4,610.7	4,607.7	4,607.8	4,610.1	4,609.3	-0.15	ft/yr
Energy Grade Line (ft/ft)	0.00110	0.00087	0.00110	0.00180	0.00140	0.00080	0.00059	-1.19E-05	1/yr

Finally, Table 3.9 summarized subreach 4. Subreach 4 is relatively narrow and incised. The data shows that even thought the change in the maximum depth has increased significantly, the bed has only decreased at a rate of 0.15 feet per year. This can be due to the fact that this channel had always been relatively narrow, which can be observed when comparing the 1962 channel width for each subreach.
A graphical representation of the time varying hydraulic characterization was shown in Figure 3.14.

3.6. Bed Material Analysis

3.6.1. Methods

The bed material surveys taken at the SA and SO-lines were used to determine the median bed grain size for each subreach. When appropriate data was not available at the SA and SO-lines, bed material from the San Acacia gage was used. Grain size classification was determined using Figure 3.15 from Julien (1998).

	Size range	
Class name	mm	in.
Boulder		
Very large	4,096–2,048	160–80
Large	2,048–1,024	80–40
Medium	1,024–512	40–20
Small	512–256	20 10
Cobble		
Large	256–128	10–5
Small	128–64	5–2.5
Gravel		
Very coarse	64–32	2.5–1.3
Coarse	32–16	1.3–0.6
Medium	16–8	0.6–0.3
Fine	8–4	0.3–0.16
Very fine	4–2	0.16–0.08
Sand		
Very coarse	2.000–1.000	
Coarse	1.000–0.500	
Medium	0.500–0.250	
Fine	0.250–0.125	
Very fine	0.125–0.062	
Silt		
Coarse	0.062–0.031	
Medium	0.031–0.016	
Fine	0.016–0.008	
Very fine	0.008–0.004	
Clay		
Coarse	0.004–0.0020	
Medium	0.0020–0.0010	
Fine	0.0010–0.0005	
Very fine	0.0005–0.00024	

Figure 3.15 – Grain size classification (Julien 1998)

3.6.2. Results

Figure 3.16 shows the change in grain size in each subreach from the SA and SO-line survey. The figures show that there is variation in the particle size from year to year. In most cases the reach has had a tendency to coarsen over the years. However, bed material samples are not taken at the same location from year to year and this can cause some discrepancy in the data.

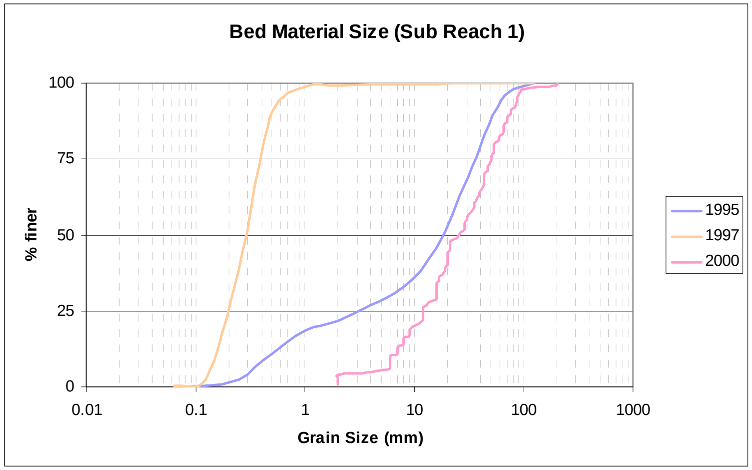

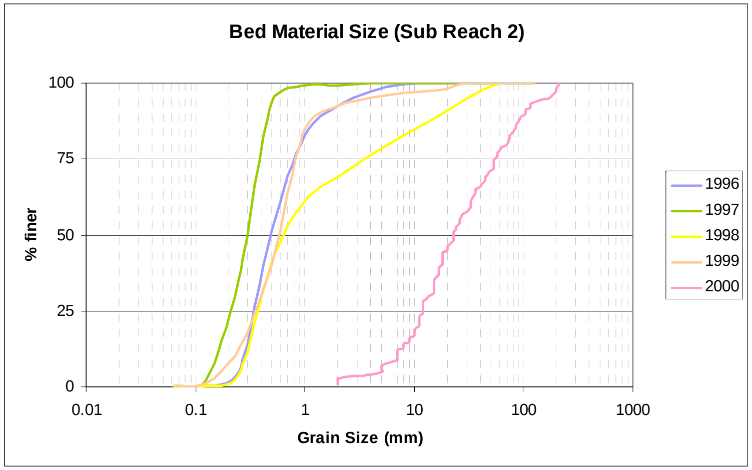

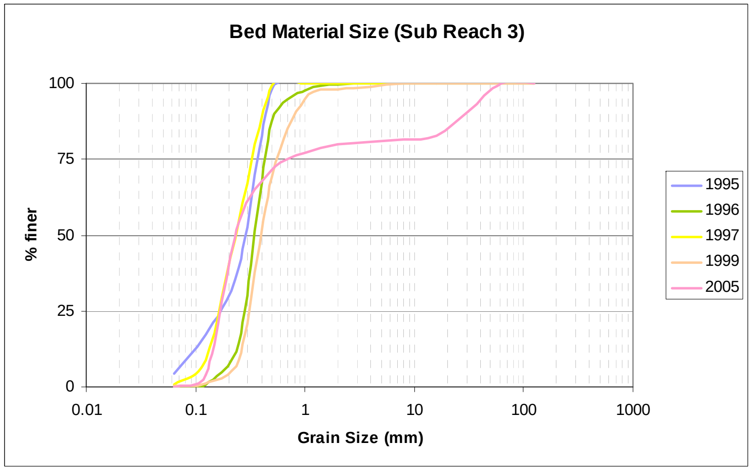

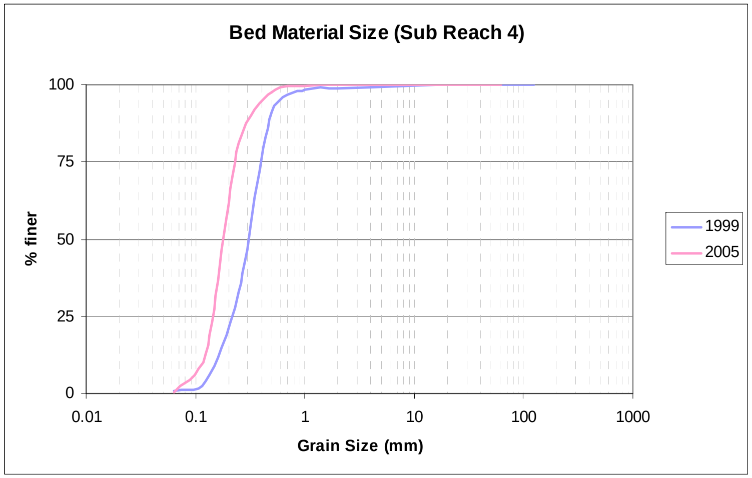

Figure 3.16 – Bed material mean grain size

Data from the San Acacia gage is used to check and evaluate how bed material samples varied with time. Figure 3.17 provides the particle size distribution from 1962 to 2002 for samples taken at the San Acacia gaging station.

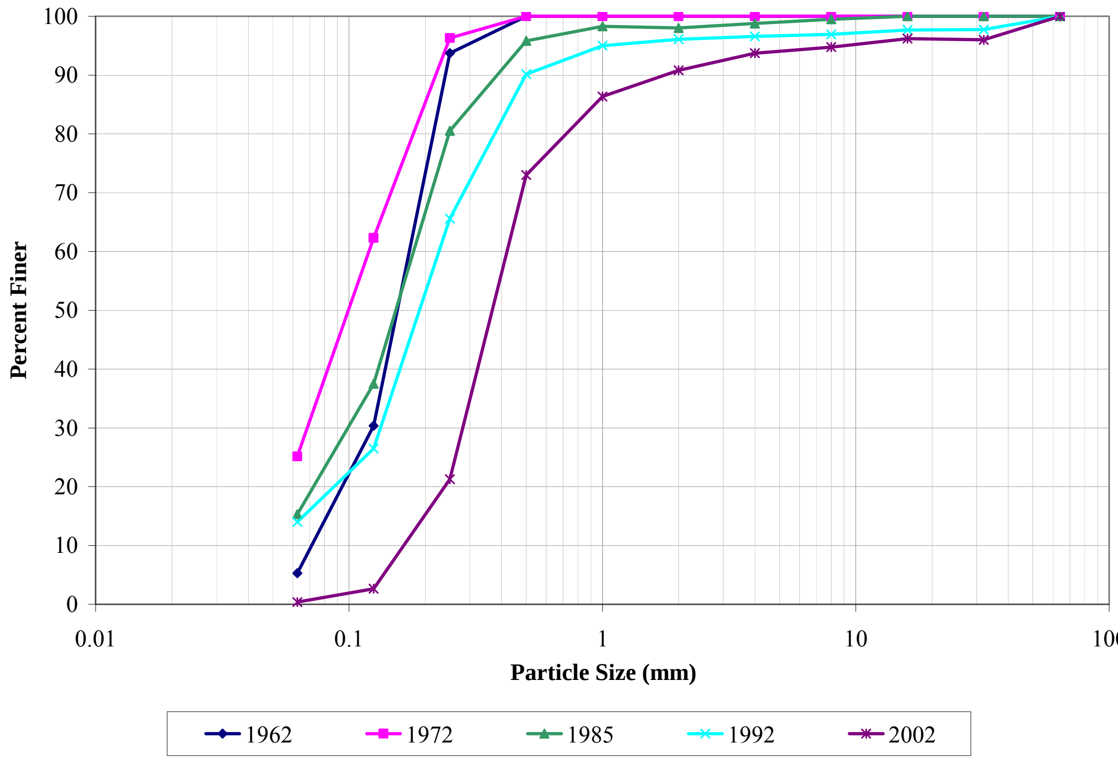

Figure 3.17 – Bed material particle size distributions

The data shows that from 1962 to 1972 there was a slight fining of particles from a d_{50} of 0.16 mm to 0.1 mm. However the overall trend has been a coarsening for of the bed material from 1972 to 2002, with the d_{50} ranging from 0.1 mm to 0.36 mm. Even thought there is a coarsening taking place the particles are still in the sand range and this reach is a sand dominated channel. The primary causes are associated with sediment reduction from dam closure (Cochiti), arroyo evolution (Gillis 1992), land-management (SCS 1977; Burkham 1966) and reduction in peak flows associated with tamarisk (Love 1997).

4. Bedforms

4.1. Methods

Two methods for predicting bedforms were selected for use in this analysis. The methods were developed by Simons and Richardson (from Julien 1998) and van Rijn (1984).

Simons and Richardson (from Julien 1998) performed laboratory experiments to develop a bedform prediction method based on stream power and median grain size diameter.

Stream power: $\tau_o V = \gamma q S$

Where τ_o (lb/ft^2) is shear stress, V (ft/s) is velocity, γ (lb/ft^2) is the specific weight of water, q (ft^2/s) is unit discharge and S is channel slope. Figure 4.1 shows the region where each bedform is expected based on the observations from Simons and Richardson's experiments.

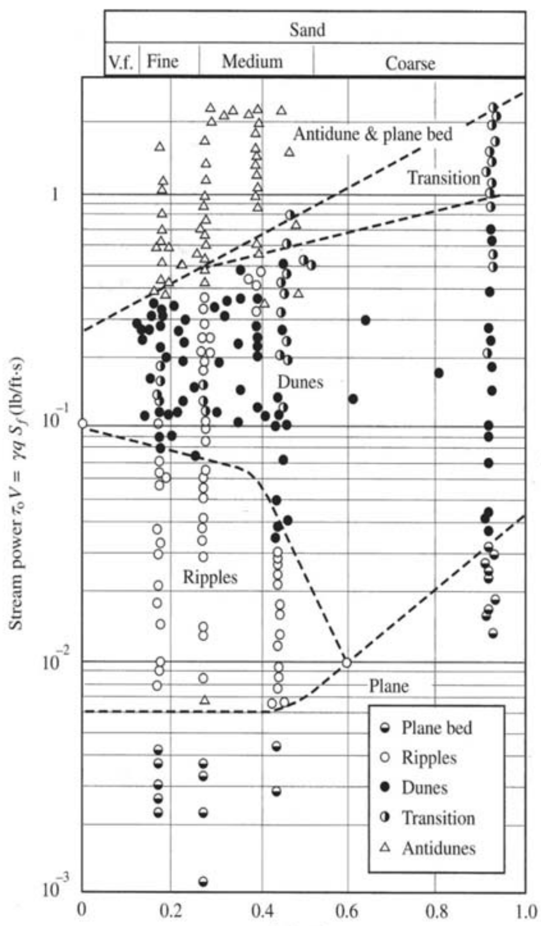

Figure 4.1 – Bedform classification by Simons and Richardson (from Julien 2010)

van Rijn (1984)developed a bedform prediction method based on the dimensionless grain diameter and transport-stage parameter.

Dimensionless grain diameter: $$d_* = d_{50}\left[\frac{(G-1)g}{v_m^2}\right]^{1/3}$$

Where d_* is the dimensionless grain diameter, d_{50} (ft) is the median grain diameter, G is the specific gravity of the sediment and v (lb*s/ft^2) is the kinematic viscosity of water.

Transport-stage parameter: $$T = \frac{\tau_*^{'} - \tau_{*c}}{\tau_{*c}}$$

Where T is the transport-stage parameter, τ'_* is the grain Shield's parameter, and τ_{*c} is the critical Shield's parameter. Figure 5.2 shows the bedforms expected based on van Rijn's method.

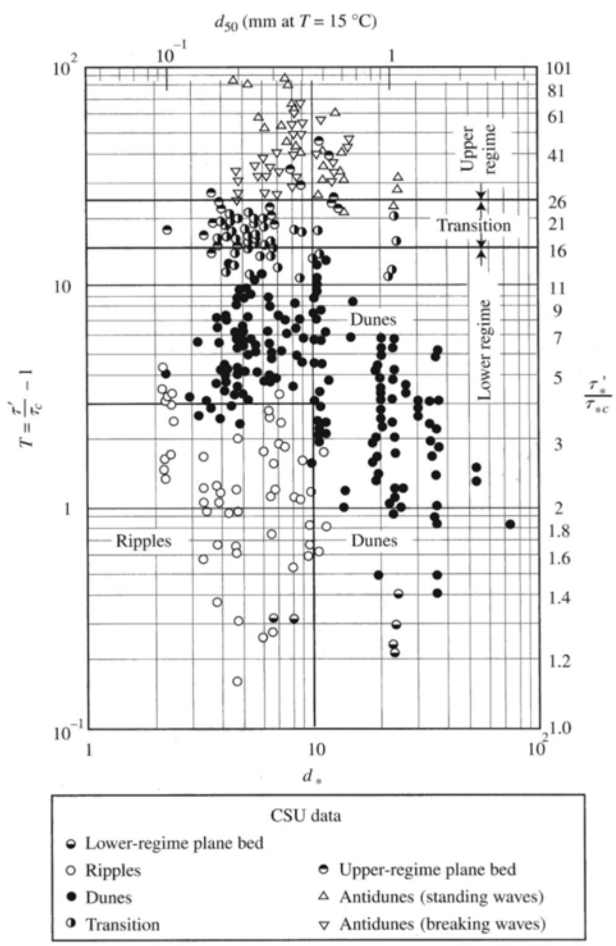

Figure 4.2 – Bedform classification by van Rijn (from Julien 2010; 1984)

Bedform data were collected by Reclamation at a number of SA and SO-lines between 1990 and 1995 within the San Acacia reach. The data is based on observations made during surveying. The dominant bedform was selected from the actual field notes as the bedform that covered the largest portion of the main flow area based on cross sectional area (i.e. a combination of both discharge and width). This is assumed to be the observed bedform. The discharge recorded at the San Acacia gage on the dates the bedform data were collected was used in HEC-RAS to determine the necessary parameters used in the Simons and Richardson and van Rijn methods. In addition, the methods require information on the bed materials. When possible, bed material samples taken at the same time as the bedform observations (SA and SO-lines) were used in the calculations. When this information was not available, bed material samples from the nearest SA and SO-line were used. The predicted bedforms were then compared with the dominant bedform at each cross-section to determine the ability of the methods to correctly predict bedforms on the Middle Rio Grande.

4.2. Results

The bedform type observed at each location was plotted on the charts developed by Simons and Richardson and van Rijn based on the calculations performed for each method. Figures 4.3 – 4.5 show each of the three bedform types plotted on both graphs. Figure 4.3 shows observed ripples and the predicted bedform.

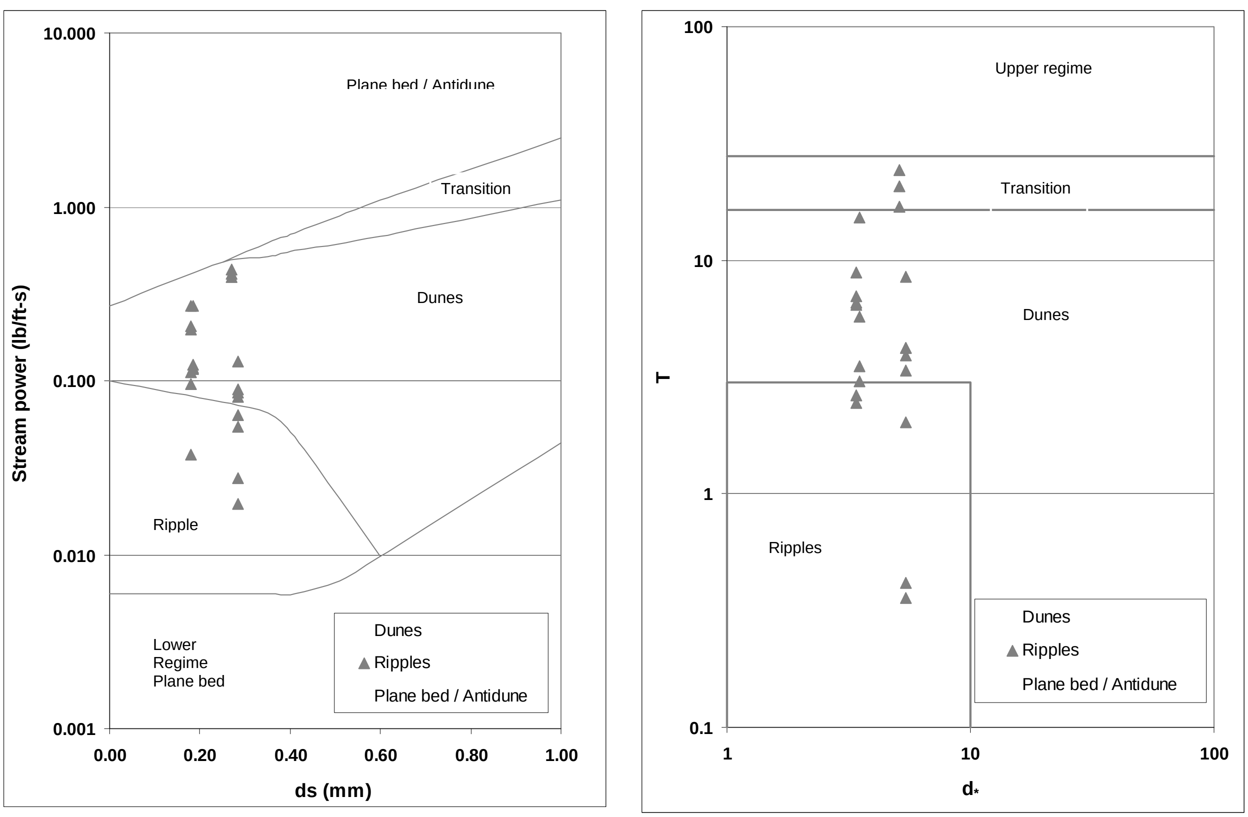

Simons and Richardson *b) van Rijn*

Figure 4.3 – Observed ripples plotted on bedform graphs

Figure 4.3, above shows significant scatter in the data where ripples are observed. The Simons and Richardson seems to contain less scatter than the van Rijn. In both predictions there are a total of twenty one points observed to be ripples, however only five points were predicted to be ripples. The reason for the discrepancy is due to the fact that multiple bedforms are observed and occasionally bed material data was not available at the cross section the observations were made at, thus data from an adjacent range line was used. Figure 4.4 shows observed dunes and the predicted bedform.

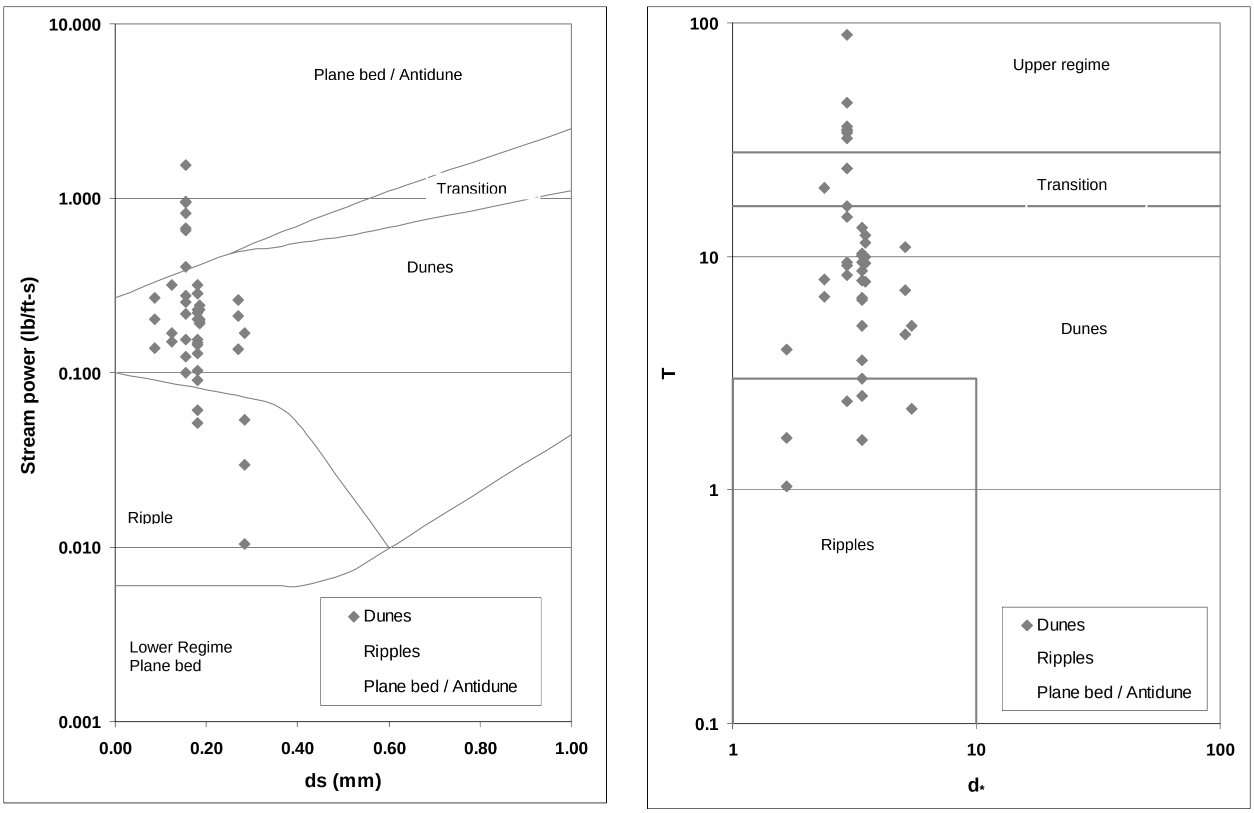

a) Simons and Richardson *b) van Rijn*

Figure 4.4 – Observed dunes plotted on bedform graphs

Figure 4.4 provides data at 45 cross sections where dune formation were the dominate bedform. The above figures show that approximately 75% of the observations are predicated to be dunes. The reason for 25% of the data not to be predicted as dunes is because multiple bedforms are observed at certain cross sections.

Figure 4.5 provides observed data for upper regime plane bed and antidues. The figure shows significant scatter in the data. The Simons and Richardson seems to contain less scatter than the van Rijn. In both predictions there are a total of fifteen points observed to be plane bed. Only 50% of the data is predicted to be upper regime (plane bed) or transition. Due to the nature of the irregularity of cross sections some of the calculations show ripples and dunes when plane bed/antidunes should have been predicated.

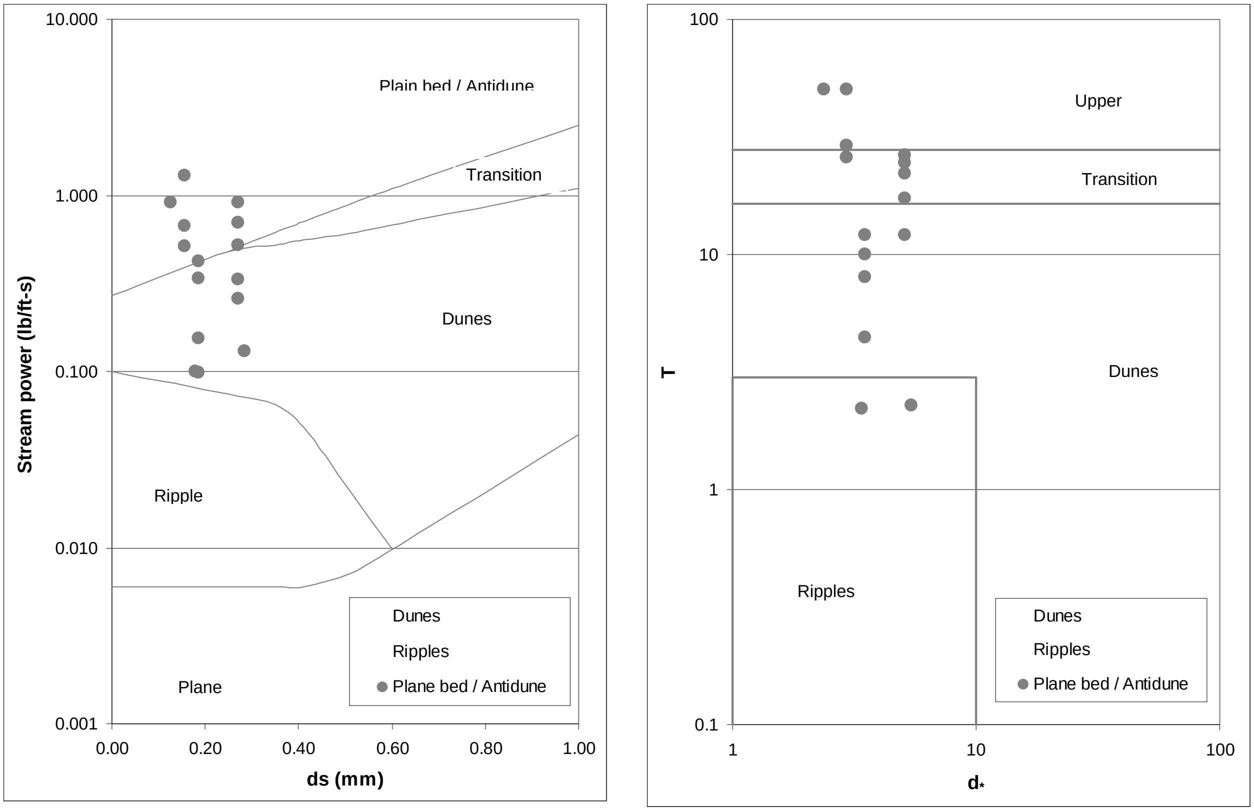

a) Simons and Richardson *b) van Rijn*

Figure 4.5 – Observed upper regime plane bed/antidunes plotted on bedform graphs

Figures 4.3 – 4.5 show that the predicted bedforms have significant scatter when compared to the observed bedforms. However, for this reach dunes were the most reliably predicted bedforms, followed by plane bed. Lower regime bedforms such as ripples were difficult to predict correctly due to the difficulty in determining whether ripples or dunes were actually observed.

A likely explanation for the discrepancy between the predicted and observed bedforms is the high variability in important parameters such as flow depth, slope and velocity across a cross-section. This variability results in the observation of several different bedforms in a single cross-section. The prediction methods are unable to account for the variability within the cross-section because they are based on cross-section average properties. In addition, all current prediction methods have been developed based on laboratory data. Therefore, there may be a discrepancy when using these methods in the field. Hence, more research is needed to truly predict bedforms in the field.

5. Equilibrium State Predictors

5.1. Hydraulic Geometry

5.1.1. Methods

Several hydraulic geometry equations were used to determine the equilibrium channel width. These methods use channel characteristics such as channel width and slope, sediment concentration, and discharge. All of the equilibrium width equations were developed in simplified conditions such as man-made channels.

Julien and Wargadalam (1995) used the concepts of resistance, sediment transport, continuity, and secondary flow to develop semi-theoretical hydraulic geometry equations.

$$h = 0.2Q^{2/(5+6m)} d_s^{6m/(5+6m)} S^{-1/(5+6m)} \quad \text{Eq 5.1}$$

$$W = 1.33Q^{(2+4m)/(5+6m)} d_s^{-4m/(5+6m)} S^{-(1+2m)/(5+6m)} \quad \text{Eq 5.2}$$

$$V = 3.76Q^{(1+2m)/(5+6m)} d_s^{-2m(5+6m)} S^{(2+2m)/(5+6m)} \quad \text{Eq 5.3}$$

$$\tau^* = 0.121Q^{2/(5+6m)} d_s^{-5/(5+6m)} S^{(4+6m)/(5+6m)} \quad \text{Eq 5.4}$$

$$m = \frac{1}{\ln(\frac{12.2h}{d_{50}})} \quad \text{Eq 5.5}$$

Where h (m) is the average depth, W (m) is the average width, V (m/s) is the average one-dimensional velocity, and τ_* is the Shield's parameter, and d_{50} (m) is the median grain size diameter.

Simons and Alberston (1963) used five sets of data from canals in India and America to develop equations to determine equilibrium channel width. Simons and Bender collected data from irrigation canals in Wyoming, Colorado and Nebraska. These canals had both cohesive and non cohesive bank material. Data were collected on the Punjab and Sind canals in India. The average bed material diameter found in the Indian canals varied from 0.43 mm in the Punjab canals to between 0.0346 mm and 0.1642 mm in the Sind canals. The USBR data was collected in the San Luis Valley in Colorado and consisted of coarse non-cohesive material. The final data set was collected in the Imperial Valley canal system, which have conditions similar to those seen in the Indian canals and the Simons and Bender canals (Simons and Albertson 1963).

Two figures were developed by Simons and Albertson to obtain the equilibrium width: Figure 5.1 represents the relationship between wetted perimeter and discharge and Figure 5.2 represents the relationship between average width and wetted perimeter.

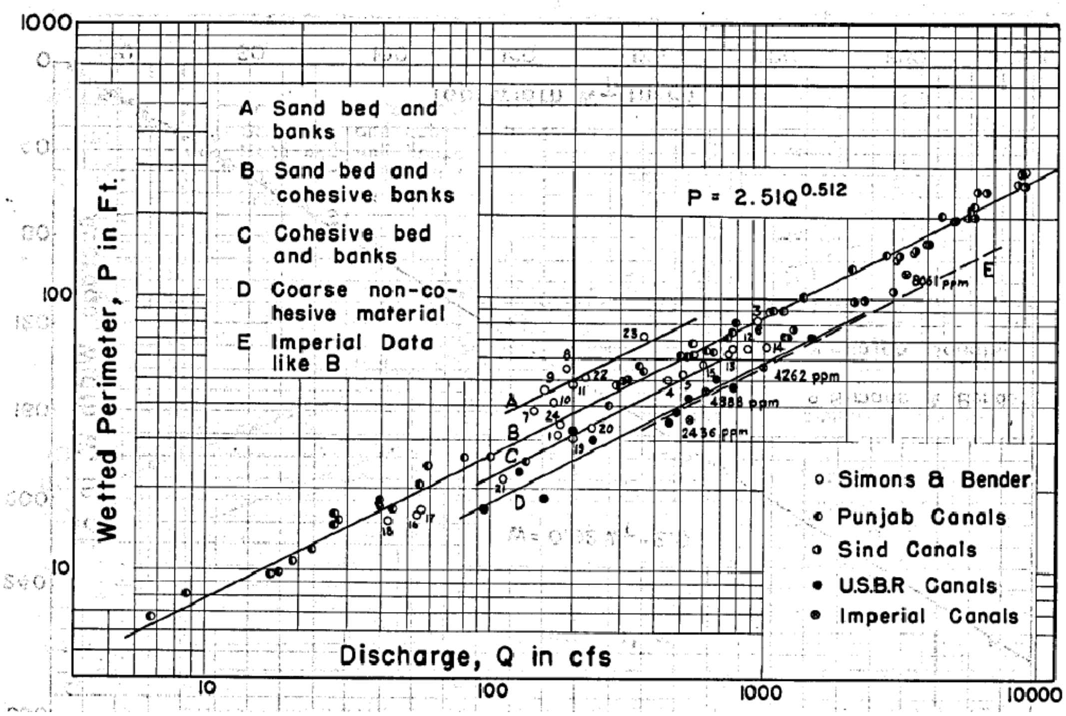

Figure 5.1 – Variation of wetted perimeter vs. discharge and channel type
(after Simons and Albertson 1963)

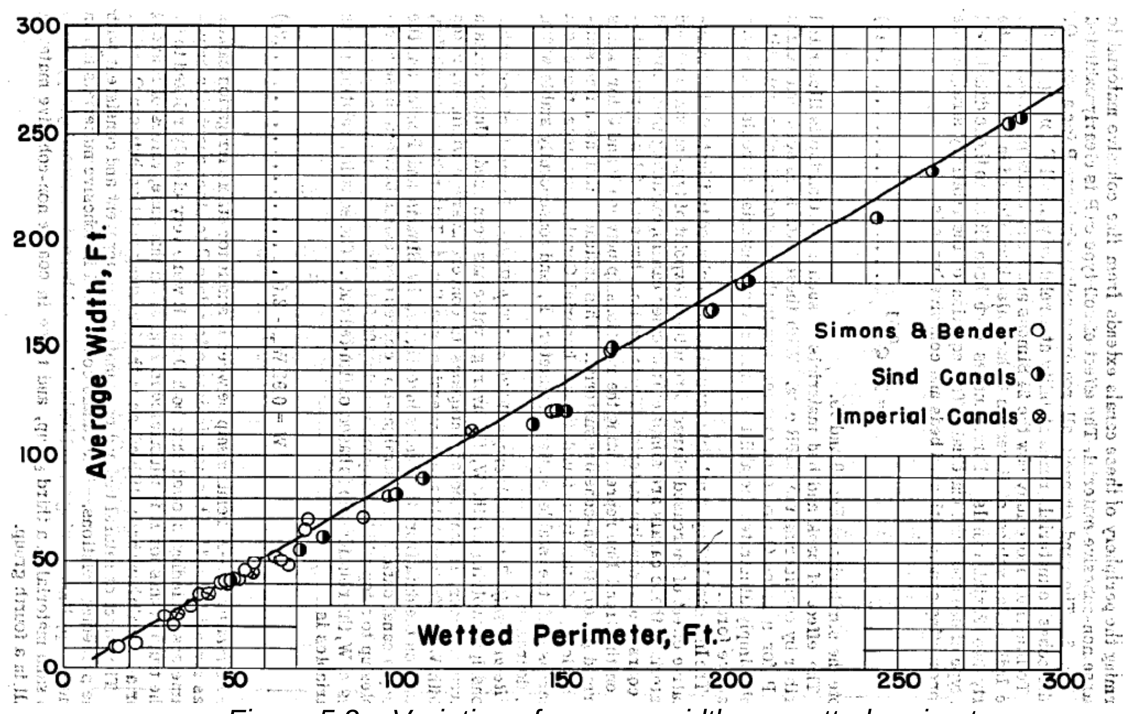

Figure 5.2 – Variation of average width vs. wetted perimeter
(after Simons and Albertson 1963)

Blench (1957) used flume data to develop regime equations. A bed and a side factor (F_s) were developed to account for differences in bed and bank material.

$$W = \left(\frac{9.6(1 + 0.012C)}{F_s} \right)^{1/2} d^{1/4} Q^{1/2} \qquad \text{Eq 5.6}$$

Where W (ft) is channel width, C (ppm) is the sediment load concentration, d (mm) is the median grain diameter, and Q (ft^3/s) is the discharge. The side factor, F_s = 0.1 for slight bank cohesiveness.

Lacey (from Wargadalam 1993) developed a power relationship for determining wetted perimeter based on discharge.

$$P = 2.667Q^{0.5} \qquad \text{Eq 5.7}$$

Where P (ft) is wetted perimeter and Q (ft^3/s) is discharge. For wide, shallow channels, the wetted perimeter is approximately equal to the width.

Klaassen-Vermeer (1988) used data from the Jamuna River in Bangladesh to develop a width relationship for braided rivers.

$$W = 16.1Q^{0.53} \qquad \text{Eq 5.8}$$

Where W (m) is width, and Q (m^3/s) is discharge.

Nouh (1988) developed regime equations based on data collected in extremely arid regions of south and southwest Saudi Arabia.

$$W = 2.83\left(\frac{Q_{50}}{Q} \right)^{0.83} + 0.018(1 + d)^{0.93} c^{1.25} \qquad \text{Eq 5.8}$$

Where W (m) is channel width, Q_{50} (m^3/s) is the peak discharge for a 50 year return period, Q (m^3/s) is annual mean discharge, d (mm) is mean grain diameter, and c (kg/m^3) is mean suspended sediment concentration.

Table 5.1 shows the input values used to estimate channel width from the hydraulic geometry equations. The peak discharges for a 50-year return period were taken from Bullard and Lane (1993). The average sediment concentrations were obtained from the double mass curves analyzed by Larsen et al. (2007) for the San Acacia gage. Suspended sediment data was only available until 1995, so all suspended sediment concentrations after 1995 were extrapolated from the double mass curves.

Table 5.1 – Hydraulic geometry calculation inputs

	Q (cfs)	Q_{50} (cfs)	d_{50} (mm)	Channel Slope (ft/ft)	Sediment Concentration Avg C (ppm)
1962					
1	5000	28050	0.15	0.0010	13058
2	5000	28050	0.15	0.0008	13058
3	5000	28050	0.15	0.0011	13058
4	5000	28050	0.15	0.0006	13058
Total	5000	28050	0.15	0.0009	13058
1972					
1	5000	19800	0.10	0.0010	13058
2	5000	19800	0.10	0.0004	13058
3	5000	19800	0.10	0.0010	13058
4	5000	19800	0.10	0.0007	13058
Total	5000	19800	0.10	0.0008	13058
1992					
1	5000	19800	0.19	0.0007	2629
2	5000	19800	0.19	0.0008	2629
3	5000	19800	0.19	0.0009	2629
4	5000	19800	0.19	0.0006	2629
Total	5000	19800	0.19	0.0008	2629
2002					
1	5000	19800	0.37	0.0007	2629
2	5000	19800	0.37	0.0007	2629
3	5000	19800	0.37	0.0010	2629
4	5000	19800	0.37	0.0006	2629
Total	5000	19800	0.37	0.0003	2629

An empirical width relationship was developed for the San Acacia reach based on active channel widths determined from GIS channel planforms and peak flows for the 5 years prior to the survey date (Knighton 1998). Knighton (1998) suggests that it is the high magnitude, low frequency floods that may control the channel form in arid-zone rivers where the flow regime is very variable. For the hydraulic geometry equations, the peak discharge from the 5 years prior to the survey was used. Peak flows for the relationship were obtained from the gage located at San Acacia Diversion Dam. The resulting power relationship takes the following form:

$$W = aQ^b \qquad \text{Eq 5.9}$$

Where W (ft) is channel width and Q (cfs) is peak discharge. Table 5.2 shows the input values used to develop the empirical width relationship for the San Acacia reach.

Table 5.2 – San Acacia empirical width-discharge inputs

Year	Average 5-year peak discharge (cfs)	GIS widths (ft)				
		Subreach 1	Subreach 2	Subreach 3	Subreach 4	Overall
1962	3,840	380	550	1,160	200	790
1972	3,510	230	230	1,070	160	650
1985	6,736	200	320	870	190	580
1992	4,433	190	270	680	170	460
2001	3,053	186	273	472	181	345
2002	2,535	181	236	481	189	343
2005	3,722	189	244	477	190	344

5.1.2. Results

The equilibrium channel widths predicted by the hydraulic geometry equations are shown in Table 5.3. The methods outlined by Simons-Albertson, Klaassen-Vermeer and Lacey result in constant equilibrium widths regardless of year because the width is only a function of discharge which is held constant. This might not be the best indicator since concentration and particle sizes are variable. The Blench method has a tendency to over predict the channel widths because it is based on flume data. However, based on the 2002 HEC-RAS results the following three methods have a tendency to provide a good prediction of the equilibrium width: Simons and Albertson, Nouh, and Julien-Wargadalam because their results are similar. All three methods suggest that the equilibrium width range is between 250 feet to about 350 feet. Based on this analysis the GIS measure widths and HEC-RAS calculated top widths are comparable to the predicted widths as shown in Table 5.3. However, some reach have a tendency to narrow while other have a tendency to widen. The overall channel will narrow and the river has not reached equilibrium.

Table 5.3 – Predicted equilibrium widths from hydraulic geometry at 5000 cfs

	GIS Active Channel Width (feet)	Reach-Averaged HEC-RAS Main Channel Width (feet)	Predicted Width (feet)					
			Simons & Albertson	Klassen & Vermeer	Nouh	Blench	Lacey	Julien-Wargadalam
1962								
1	380	570	274	729	390	2437	189	264
2	550	910	274	729	390	2437	189	273
3	1160	1470	274	729	390	2437	189	261
4	200	950	274	729	390	2437	189	294
Total	790	1170	274	729	390	2437	189	268
1972								
1	230	350	274	729	293	2169	189	266
2	230	530	274	729	293	2169	189	317
3	1070	1120	274	729	293	2169	189	264
4	160	1050	274	729	293	2169	189	282
Total	650	1170	274	729	293	2169	189	274
1992								
1	190	220	274	729	291	1164	189	283
2	270	400	274	729	291	1164	189	274
3	680	800	274	729	291	1164	189	268
4	170	180	274	729	291	1164	189	288
Total	460	560	274	729	291	1164	189	273
2002								
1	181	212	274	729	291	1374	189	283
2	236	319	274	729	291	1374	189	283
3	481	758	274	729	291	1374	189	265
4	189	163	274	729	291	1374	189	289
Total	343	503	274	729	291	1374	189	345

The Julien-Wargadalam method was also used to predict the equilibrium slope of the channel. Table 5.4 shows the predicted equilibrium slope and the observed channel slope for each subreach and the total reach between 1962 and 2002.

Table 5.4 – Equilibrium slope predictions with Q = 5000 cfs

	Reach	1962	1972	1992	2002
Observed Slope	1	0.00100	0.00097	0.00069	0.00084
	2	0.00085	0.00041	0.00069	0.00069
	3	0.00105	0.00102	0.00097	0.00099
	4	0.00059	0.00073	0.00062	0.00065
	Total	0.00093	0.00084	0.00026	0.00072
Equilibrium Slope	1	0.00059	0.00025	0.00053	0.00122
	2	0.00051	0.00024	0.00053	0.00131
	3	0.00068	0.00031	0.00062	0.00156
	4	0.00048	0.00026	0.00051	0.00133
	Total	0.00066	0.00029	0.00060	0.00138

The results of the equilibrium slope calculations indicate that the channel had a steeper slope than the predicted slope in 1962 and 1972. In 1992, the observed channel slope is approximately 20% greater than the equilibrium slope however the value is off for the overall reach. In 2002, the observed slope tends to be shallower then the predicted slope. Thus in order for the river to reduce its slope it will need to meander. The levee setback projects should aid in the slope reduction.

Figure 5.3 shows the plot and regressions used to find the empirical equations for the reach based on data from Table 5.2. The non-vegetated active channel width obtained from GIS planforms was plotted versus the 5-year average peak flow. Regressions were then developed for each subreach and the total reach. 1962 was the first year used in the regression because prior to 1962 there were no dams on the river, which would be an incorrect regression, based on current conditions.

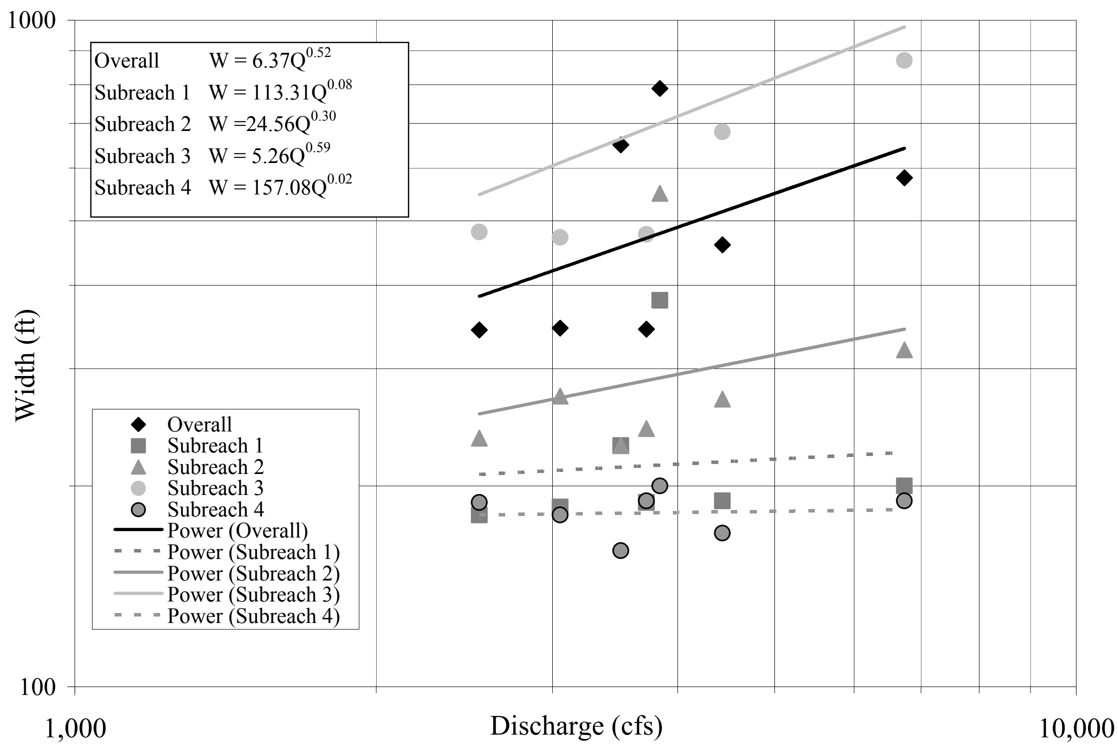

Figure 5.3 – San Acacia reach empirical width-discharge relationships

The results of the equilibrium width calculations performed using the empirical equation developed for the San Acacia reach are shown in Table 5.5 along with the non-vegetated active channel widths.

Tables 5.5 – San Acacia reach empirical width-discharge results

	Year	1962	1972	1985	1992	2001	2002	2005
	Average 5-year peak discharge (cfs)	3840	3510	6736	4433	3053	2535	3722
GIS Width (ft)	1	380	230	200	190	186	181	189
	2	550	230	320	270	273	236	244
	3	1160	1070	870	680	472	481	477
	4	200	160	190	170	181	189	190
	Total	790	650	580	460	345	343	344
Predicted Width (ft)	1	219	218	229	222	215	212	219
	2	292	284	346	305	273	258	289
	3	685	650	954	746	598	536	673
	4	185	185	187	186	184	184	185
	Total	466	444	624	502	413	375	458

In general in 1962 and 1972 the measured widths had a tendency to be higher than the predicated widths. However after 1985 the predicted widths closely match the measured widths in all subreaches and in all years except subreach 3. This is most likely due to the fact that this reach has narrowed significantly in the past 40 years. The empirical equations may be a good indicators of the actual expected width at a given discharge because they are based on the historical conditions rather than an ideal, equilibrium state. These equations, however, may not be reliable in predicting the equilibrium width over time.

5.2. Width Regression Model

5.2.1. Methods

Hyperbolic Model

The downstream effects of dams on alluvial rivers were studied by Williams and Wolman (1984). They found a hyperbolic equation to describe the changes in channel width with time.

$$\frac{1}{Y} = C_1 + C_2 \frac{1}{t} \qquad \text{Eq 5.10}$$

Where C_1 and C_2 are empirical coefficients, t is the time in years after the initial change in the channel, and Y is the relative change in channel width and is equal to the ratio of the initial width (Williams and Wolman) to the width at time t (W_t). The coefficients are be a function of channel characteristics such as discharge and boundary material.

A hyperbolic equation was fit to data from the each subreach. The initial time (t = 0) was assumed to be the first year a narrowing trend was observed in the channel. The initial year was different in each subreach and in the total reach. To adjust the equations to an origin of 0, 1.0 was subtracted from the relative width ratio (W_t/W_i)

before the regression was fit to the data. The constants C_1 and C_2 were determined by setting the R^2 of the regression as close to one as possible.

Exponential Model

Richard et al (2005) developed prediction equations for active channel width, total channel width, migration rate and lateral mobility based on data collected in the Cochiti reach of the Middle Rio Grande and verified by data from four rivers including the Jemez River, the Arkansas River, Wolf Creek and the North Canadian River. An exponential regression equation was developed to describe channel width as a function of time.

$$W(t) = W_e + (W_i - W_e)e^{-kt} \qquad \text{Eq 5.11}$$

Where W_e is the equilibrium width, W_i is the channel width at the initial time, k is the rate of decay, and t is time after the initial time.

The exponential equation was fit to the GIS active channel width beginning in the first year showing a trend toward decreasing width. The decay constant and the equilibrium width were determined by setting the R^2 of the exponential regression equation as close to one as possible.

Table 5.6 shows the input information for the hyperbolic and exponential regression equations.

Table 5.6 – Hyperbolic and exponential regression input

Subreach 1		
Year	t (yr)	Wt (ft)
1949	0	650
1962	13	380
1972	23	230
1985	36	200
1992	43	190
2001	52	186
2002	53	181
2005	56	189
2006	57	176

Subreach 2		
Year	t (yr)	Wt (ft)
1949	0	1420
1962	13	550
1972	23	230
1985	36	320
1992	43	270
2001	52	273
2002	53	236
2005	56	244
2006	57	225

Subreach 3		
Year	t (yr)	Wt (ft)
1949	0	1650
1962	13	1160
1972	23	1070
1985	36	870
1992	43	680
2001	52	472
2002	53	481
2005	56	477
2006	57	464

Subreach 4		
Year	t (yr)	Wt (ft)
1949	0	650
1962	13	200
1972	23	160
1985	36	190
1992	43	170
2001	52	181
2002	53	189
2005	56	190
2006	57	176

Overall		
Year	t (yr)	Wt (ft)
1949	0	1320
1962	13	790
1972	23	650
1985	36	580
1992	43	460
2001	52	345
2002	53	343
2005	56	344
2006	57	329

5.2.2. Results

Five hyperbolic and five exponential equations were developed for the San Acacia reach. Figures 5.4 to 5.8 show the regression curves for each of the four subreaches and the overall reach. All of the graphs start in the initial year and continue through 2020.

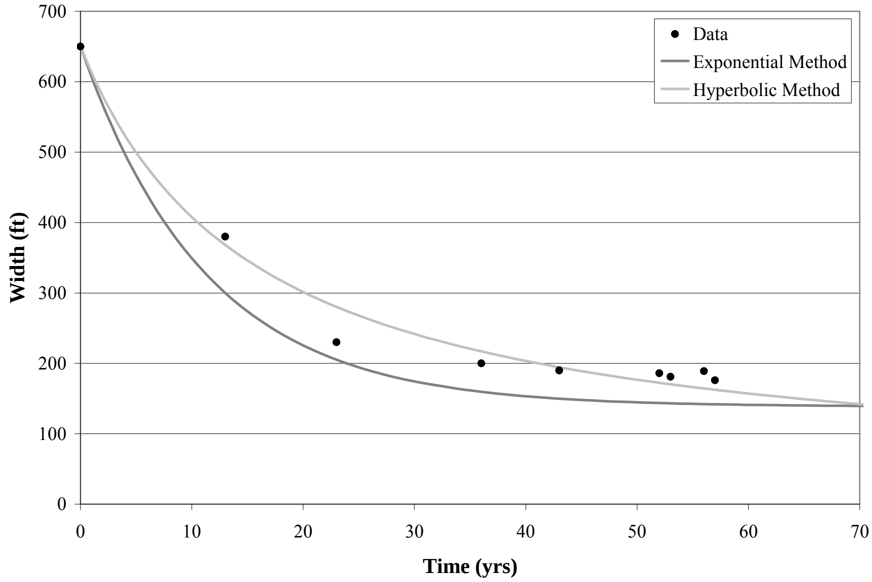

Figure 5.4 – Hyperbolic and exponential regressions – subreach 1

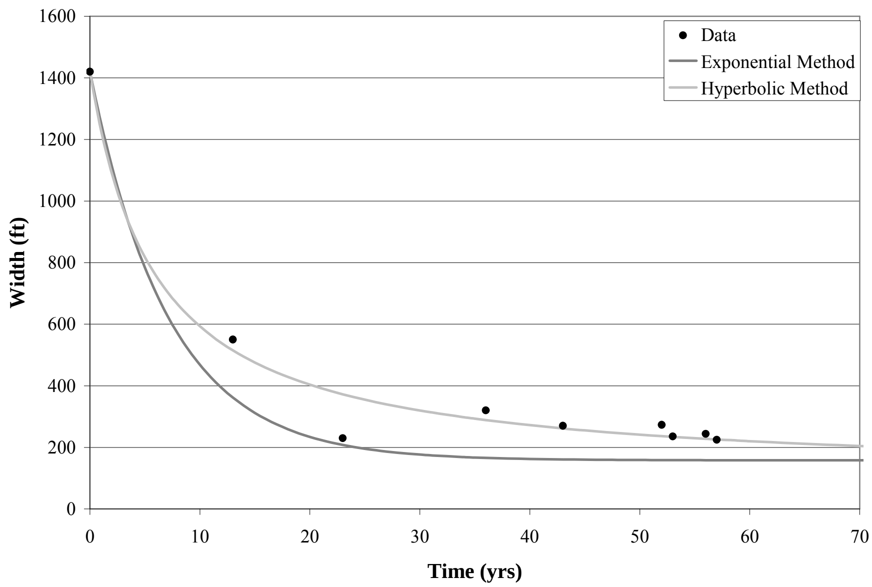

Figure 5.5 – Hyperbolic and exponential regressions – subreach 2

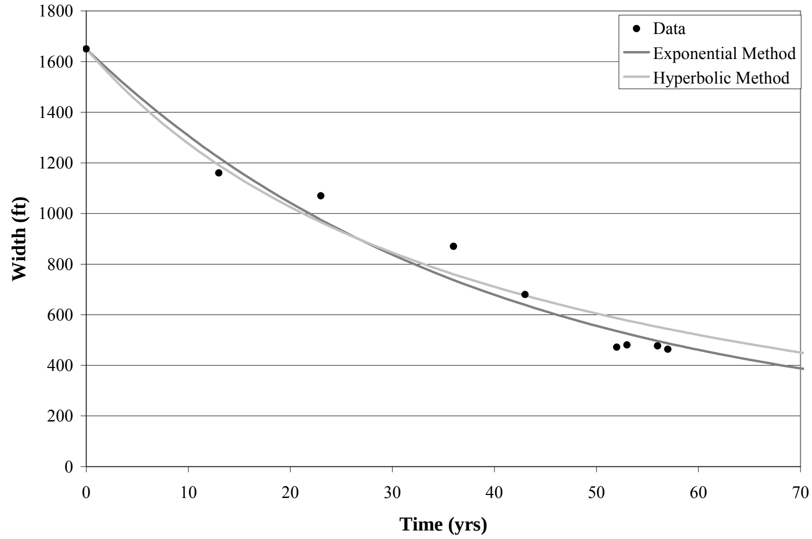

Figure 5.6 – Hyperbolic and exponential regressions – subreach 3

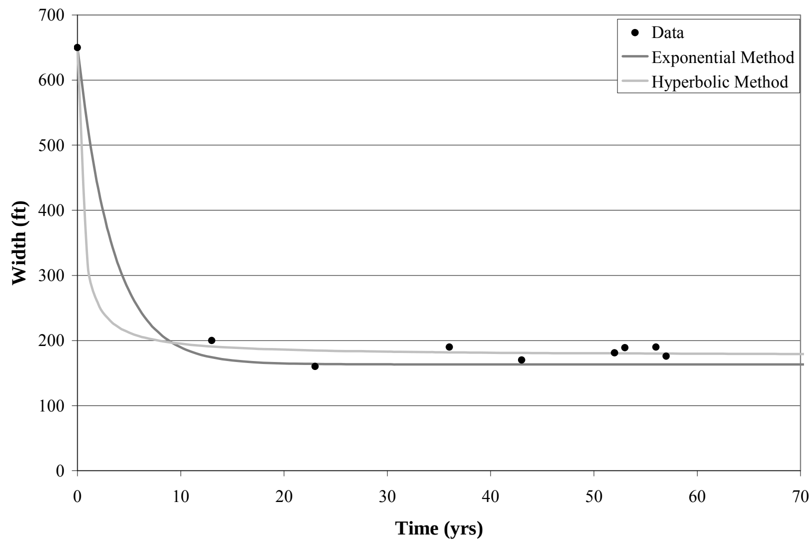

Figure 5.7 – Hyperbolic and exponential regressions – subreach 4

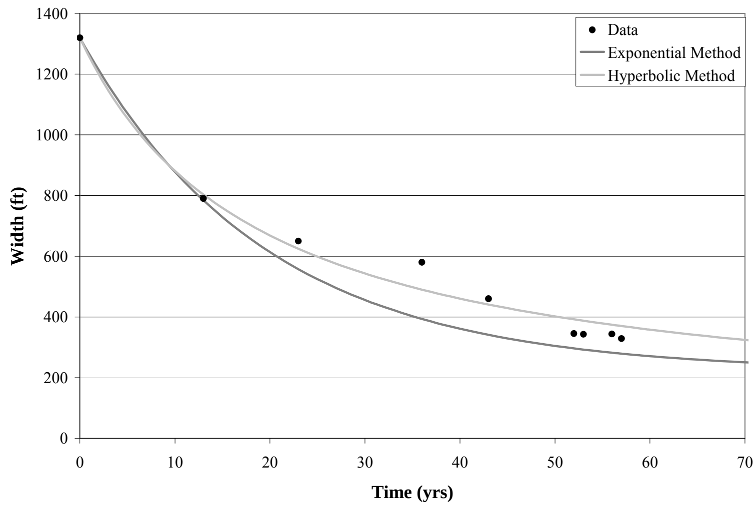

Figure 5.8 – Hyperbolic and exponential regressions – total reach

As shown in Figures 5.4 – 5.8, the hyperbolic and exponential regression equations produce very similar results. Overall, both regressions seem to follow a trend to the measured data which matches the regressions.

Table 5.7 shows the hyperbolic regressions for each subreach, along with the predicted width in 2020 and the predicted equilibrium width. There is no good agreement between the 2020 width and the predicted equilibrium widths for the San Acacia reach. This suggests that the channel is continuing to narrowing at a significantly faster rate and more data points could help with better prediction. The model is doing a good job at predicting the width for subreach 4 because the 2020 and equilibrium predicted widths are similar. The reason subreach 4 has a better prediction is because it is already a pretty narrow subreach. In addition, this is also associated with the fact that subreach 4 was narrower for the beginning (Table 3.9).

Table 5.7 – Hyperbolic regression equations and predicted widths

Subreach	R^2	Regression Equation	W_{2020} (ft)	W_e (ft)
1	0.95	$\frac{W_t}{W_i} = \frac{t}{-0.54t - 2.03} + 1$	141	29
2	0.77	$\frac{W_t}{W_i} = \frac{t}{-0.53t - 1.10} + 1$	203	102
3	0.83	$\frac{W_t}{W_i} = \frac{t}{-0.54t - 3.39} + 1$	445	-238
4	0.08	$\frac{W_t}{W_i} = \frac{t}{-0.58t - 0.09} + 1$	179	176
Overall	0.89	$\frac{W_t}{W_i} = \frac{t}{-0.54t - 2.42} + 1$	321	60

Table 5.8 shows the exponential regression equations and predicted equilibrium widths. All of the equations are able to produce reasonable equilibrium widths. The equilibrium widths predicted by the exponential regression seem to provide a more reasonable range of widths for the channel.

Table 5.8 – Exponential regression equations and predicted widths

Subreach	R^2	Regression Equation	W_e (ft)
1	0.53	$W(t) = 139 + 511e^{-0.089t}$	139
2	0.36	$W(t) = 158 + 1262e^{-0.14t}$	158
3	0.25	$W(t) = 138 + 1512e^{-0.026t}$	138
4	0.08	$W(t) = 163 + 487e^{-0.29t}$	163
Total	0.49	$W(t) = 220 + 1100e^{-0.05t}$	220

5.3. Sediment Transport

5.3.1. Methods

The equilibrium slope of the channel was estimated using sediment transport equations. Equilibrium is achieved when the incoming suspended sediment matches the sediment capacity of the reach. When supply and capacity are equal, the channel should not aggrade or degrade and a constant slope should be maintained as long as the width does not change. A river is dynamic and will always be changing but the idea of equilibrium is that where the channel is going back and forth with not drastic change.

The incoming sediment supply for each subreach was estimated using the Bureau of Reclamation Automated Modified Einstein Procedure(BORAMEP). Suspended sediment data was obtained from the USGS gauging station located at the San Acacia Diversion Dam. The bed material gradation was obtained for the Bureau of Reclamations field survey. In addition, flow conditions, and suspended sediment concentration were also obtained at the San Acacia gage for the dates of the suspended sediment and bed material samples. The channel slope was then varied in HEC-RAS until the calculated sediment transport capacity was within 20% of the incoming sediment supply. The channel hydraulic data was determined by running HEC-RAS for the desired flow rate. The input and output from BORAMEP can be found in the Appendix E. A combination of suspended sediment samples from the San Acacia gage and bed material samples from the range lines were used as inputs into

BORAMEP to determine the total sediment load at each location. The calculated total sediment load at each gage was plotted against the water discharge. A power regression is fitted to the data set and the total sediment load is determined at a discharge of 5,000 cfs.

HEC-RAS 3.1.3 calculates sediment transport capacity using several different methods including those developed by, Ackers & White, Engelund & Hansen, Laursen, Meyer-Peter & Muller, Toffaleti, and Yang (sand). All methods except Meyer-Peter & Muller provide estimates of total bed material load. Meyer-Peter & Muller estimates bed load only. For a complete listing of the limits of application for these methods as provided by HEC-RAS refer to the HEC-RAS manual.

The total sediment load minus the wash load was estimated from BORAMEP and compared directly with the HEC-RAS bed material load calculations. The 2002 geometry data was used for the HEC-RAS runs because the sediment data used in BORAMEP ranges from 1995 to 2005. The wash load was estimated as the portion of the total load that was smaller than the d_{10} of the bed material samples collected at the range lines.

The total load for a discharge of 5000 cfs was determined from the rating curves developed from BORAMEP. The bed load was then determined by multiplying the total load by the percent of material not considered to be suspended load. The slope of the channel was varied until a slope was reached that matched incoming sediment supply and transport capacity. The equilibrium slope was determined for each method in each subreach.

5.3.2. Results

The total load rating curve for the incoming sediment is shown in Figure 5.9. Table 5.9 shows the total sediment load at 5,000 cfs for each subreach. The average d_{10} is determined from the bed sediment sample taken at the range lines for each subreach. Than based on the d_{10} from the bed material the percent of suspended sediment at the San Acacia gage was determined. That percent of sediment is assumed to be wash load and is removed from the total sediment load calculation to determine the bed material load, which will be compared to the HEC-RAS sediment data.

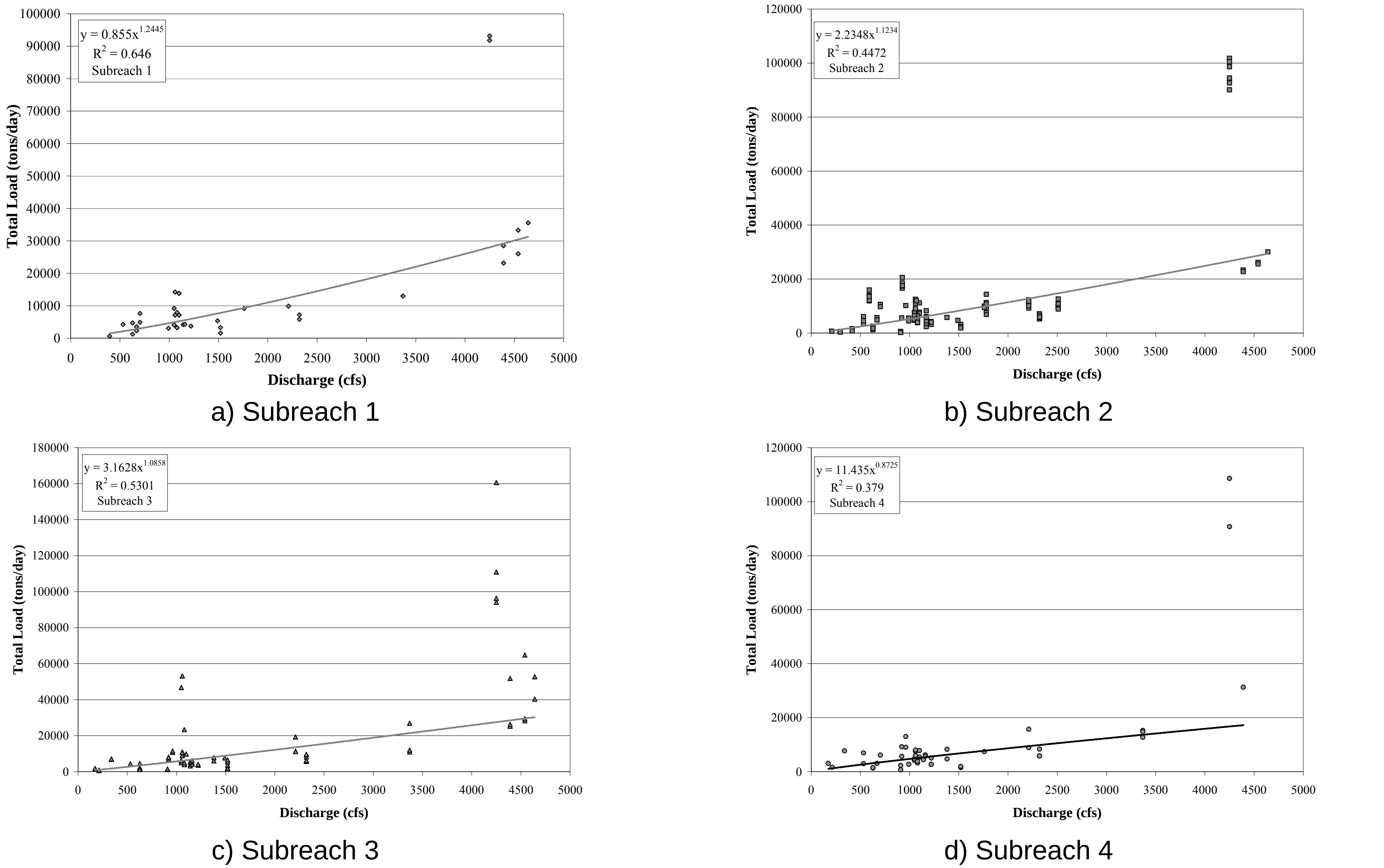

Figure 5.9 – Total load rating curves from BORAMEP analysis

Table 5.9 – Total load and bed load calculations

Subreach	Total Load (tons/day)	Bed material d_{10} (mm)	% smaller than d_{10} of bed	Bed Material Load (tons/day)
1	34,303	0.174	56.0	15,093
2	31,964	0.414	98.5	479
3	32,841	0.252	62.9	12,198
4	19,301	0.201	62.9	7,169

The existing condition load and channel slope are summarized in Table 5.10.

Table 5.10 – Existing Condition Load and Channel Slope

Parameter	Subreach 1	Subreach 2	Subreach 3	Subreach 4
Estimated Total Load (tons/day)	34303	31964	32841	19301
Estimated Bed Material Load (tons/day)	15093	479	12198	7169
Existing Channel Slope (from 1992)	0.000687	0.000692	0.000966	0.000620

The equilibrium sediment transport capacity and slope are shown for each reach and each method in Table 5.11. Some of the methods did not approach the target transport capacity within a reasonable range of slopes. These reaches do not show a specific equilibrium slope or transport capacity.

Table 5.11 – Equilibrium slope determined from transport capacity equations

Sediment Transport Equations	Subreach 1		Subreach 2		Subreach 3		Subreach 4	
	Transport Capacity (tons/day)	Slope	Transport Capacity (tons/day)	Slope	Transport Capacity (tons/day)	Slope	Transport Capacity (tons/day)	Slope
Ackers & White	15093	0.00020	-	<0.0002	12198	0.00038	-	<0.0002
Engelund & Hansen	15093	0.00035	-	<0.0002	12198	0.00049	-	<0.0002
Laursen	-	<0.0002	-	<0.0002	12198	0.00035	-	<0.0002
Toffaleti	15093	0.00029	-	<0.0002	12198	0.00051	-	<0.0002
Yang - Sand	15093	0.00044	-	<0.0002	12198	0.00061	7169	0.00038

Of the five methods tested, none of the transport methods was able to determine an equilibrium slope for subreach 2. This is due to the low amount of fines, thus giving a very low bed material load. The Yang equation was the only method able to predict an equilibrium slope for the other three subreaches, with an equilibrium slope ranging from 0.00038 to 0.00061. Based on the subscribed sediment transport methods the Laursen method results in the shallowest slope, while the Yang method results in the steepest slope.

Based on the equilibrium slope analysis all four subreaches require substantial changes to the channel slope. Table 5.12 shows the percent change that each subreach needs based on the transport equation. This suggests that the slope could reduce in the future as a result of upstream channel bed degradation or downstream aggradation.

Table 5.12 – Percent Change in Slope between Existing and Equilibrium Condition

Sediment Transport Equations	Subreach 1	Subreach 2	Subreach 3	Subreach 4
Ackers & White	70%	-	61%	-
Engelund & Hansen	49%	-	49%	-
Laursen	-	-	64%	-
Toffaleti	58%	-	47%	-
Yang - Sand	36%	-	37%	38%

Based on the results the slope for subreach 2, what not calculated. This occurs because subreach 2 is 1 to 2 orders of magnitude greater in bed material transport, due to the fact that there was significant wash load transported through this reach. Only the Yang sediment transport equation calculated a bed material load in subreach 4. This is most likely associated with the distance the reach is from the San Acacia gage where the suspended sediment samples were measured.

5.4. SAM

5.4.1. Methods

HEC-RAS 4.0 beta version stable channel design program, know as SAM, was used to determine the equilibrium slope and width for a series of suspended sediment inputs. SAM was developed for use as a preliminary design tool for flood control channels. The program assumes a trapezoidal channel and steady uniform flow in calculations. Given suspended sediment and water discharges, as well as a bed material gradation, SAM computes combinations of stable depth, width, and slope for the channel using Copeland’s flow resistance and sediment transport equations. The series of slope and width combinations can then be plotted. The minimum point on the resulting slope versus width graph is the point of minimum stream power for the input conditions.

The 2002 channel properties were used for the SAM analysis. Sediment sizes were the average of all four subreaches. The suspended sediment concentration is from the San Acacia Gage data. The inputs included a bank slope of 2H:1V, a bank roughness of n = 0.032, a discharge of 5000 cfs, and bed material gradation of d_{84} = 0.93 mm, d_{50} = 0.37 mm, d_{16} = 0.21 mm. A series of suspended sediment concentrations between 2,000 ppm to 3,000 ppm were input into SAM as well.

5.4.2. Results

Figure 5.10 shows the total reach slope versus width curves for each suspended sediment concentration. The width and slope of the channel for 2002 conditions are plotted for comparison. Based on the double mass curves the concentration should be

2,629 ppm at a flow rate of 5000 cfs. The width was determined from GIS planform measurements and the channel slope was determined from HEC-RAS. The point of minimum stream power on the graph predicts a width of about 150 ft regardless of the suspended sediment concentration. The predicted width is slightly less than the equilibrium width predicted by any other method shown in Tables 5.5, 5.7 and 5.8. Based on this analysis subreach 1 seems to be in equilibrium, while the other reaches are still in the process of changing based upon the SAM analysis.

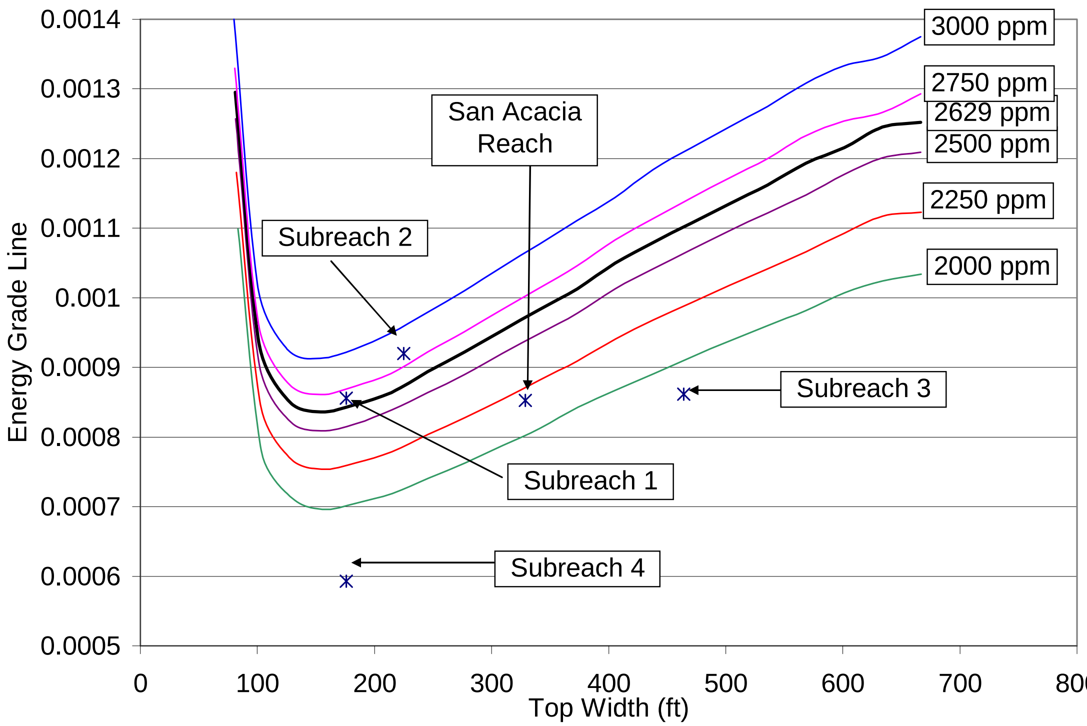

Figure 5.10 – Results from SAM for 2002 conditions at Q = 5000 cfs

Table 5.13 summarizes the width and slope for each subreach and the overall San Acacia reach based on the data available from 2002. In addition, the suspended sediment concentration determined from the double mass curve analysis on the San Acacia suspended sediment data are also included. The predicted width and slope calculated by SAM for those suspended sediment concentration is shown. While the equilibrium width is much lower than other methods predict (Tables 5.5, 5.7 and 5.8), the equilibrium slope (Table 5.11) is reasonable when compared with other methods.

Table 5.13 – Current conditions and equilibrium slope and width from SAM

Parameter		Subreach 1	Subreach 2	Subreach 3	Subreach 4	Total
2002	SS C (ppm)	2629	2629	2629	2629	2629
	Slope	0.0084	0.00069	0.00099	0.00065	0.00072
	Width (ft)	210	308	666	163	453
SAM	Slope	0.000839	0.000839	0.000839	0.000839	0.000839
	Width (ft)	157	157	157	157	157

6. Discussion

6.1. Historic Trends and Current Conditions

Channel pattern
Based on visual observations of the GIS non-vegetated active channel planforms, the channel planform has become much straighter since 1918 and the overall channel width has decreased significantly. This observation is confirmed by a steady decrease in sinuosity (refer to Table 3.3 and Figure 3.9). In subreaches 2 and 4 there is a drastic decrease in sinuosity from 1949 to 1962 due to levee construction and channelization. Based on the measured data the sinuosity in subreach 3 has not changed much since 1918. Overall since 1962 there has been little to no change in sinuosity for the San Acacia reach. The sinuosity suggests that the channel has been straightening, which is likely to have been caused by flood control and irrigation efforts implemented during the 1920's and 1930's.

The total channel has narrowed and deepened from 1918 to 2006 (see Figure 3.13). The decrease in top width is likely related to an increase in channel depth, because they are reflections of the same process. Subreaches 1 and 4 decrease in both channel width from 1962 until 1999, then increase from 1999 to 2005, while subreaches 2 and 3 decrease from 1962 to 1999, than increase from 1999 to 2002 and deceases again from 2002 to 2005. This is potentially occurring because the river is still trying to balance the amount of flow transported with the amount of available sediment.

Channel classification
The results of the channel classification methods indicated that the channel is primarily a straight and or braided channel. A comparison between the USBR study and this study is provided in Table 3.2. The comparison shows that there is some variability between the two studies. The Leopold and Wolman, Lane, and Schumm and Khan methods show similar results from the previous study. Both the Leopold and Wolman and Schumm and Khan methods indicate a straight planform. However the Lane methods indicates a transition planform between meandering and braiding. The methods that most closely estimated the actual channel planform were those that indicated a straight planform, as braiding is only seen in localized areas of the channel during low flows. Leopold and Wolman, and Schumm and Kahn indicated a straight channel planform. Rosgen's method also provides a good description of the channel planform and show some variability between the USBR 2003 study. Rosgen describes this sand bed reach as a slightly entrenched channel with a moderate width to depth ratio.

Vertical movement
In the San Acacia reach degradation is observed through changes in the mean bed elevation over time (see Figure 3.11 and Figure 3.12). The average degradation observed from 1962 to 2002 ranged from 4 to 9 feet for the San Acacia reach, with the most degradation observed in subreaches 1 and 2. From 1992 to 2002 there was a

slight aggradation observed in subreach 4, however since 1962 the subreach has degraded. The reason that the primary change in the San Acacia reach has been degradation is due to the reduction in sediment due to dam construction and the changes in the natural flow regime. However the construction of the levee along the western bank and the overall channelization (straightening) of the reach can also be contributing factors to the overall channel degradation because the river has a tendency to incise since it cannot widen.

An analysis was performed on the Escondida reach, to provide analysis on sediment continuity (Larsen et al. 2007) until 1995. In addition, Reclamation (Baird 2011) provided data regarding double mass curves for the Middle Rio Grande until 2005. The difference mass curve analysis was developed based on the suspended sediment data from the San Acacia and San Marcial USGS gages to show trends in aggradation and degradation. The data indicates that aggradation should have been observed from 1960 and 1985, followed by about 5 years of degradation, and then 5 years of aggradation. Finally, another cycle of degradation and aggradation is observed from 1992 to 2001 than from 2001 to 2005. Continuing to analyze the difference mass curve as more data becomes available may give an indication as to when the channel is approaching equilibrium.

It should be noted that for the San Acacia reach the mean bed elevation analysis and the difference mass curves analysis do not agree. On analysis indicates the reach is degrading while the other indicated the reach is aggrading. The reason is because the San Acacia reach is significantly closer to the input gage (San Acacia Diversion Dam) than the output gage (San Marcial). There has been a little aggradation observed in subreach 4 between 1992 to 2002 and this may suggest that more aggradation may be expected in the San Acacia reach until equilibrium is observed.

Channel geometry
Table 6.1 shows the magnitude of change for different channel geometric parameters. Decease in channel geometry is indicated by a red value in parenthesis. The magnitudes of the differences are summarized.

Table 6.1 – Channel geometry changes

Year	Subreach	Area	Top Width	Wetted Perimeter	Hydraulic Depth	Max Depth	W/D	Velocity	Fr
1962-1972	1	(240.00)	(230.00)	(220.00)	1.94	2.90	(20.00)	0.30	0.00
	2	(440.00)	(220.00)	(340.00)	0.65	1.50	(15.00)	3.50	(0.41)
	3	(290.00)	(320.00)	(320.00)	0.33	1.30	(110.00)	0.20	0.01
	4	(140.00)	(90.00)	(90.00)	1.15	0.60	(30.00)	0.60	(0.05)
	Total	(290.00)	(260.00)	(282.00)	0.46	1.40	(70.00)	1.00	(0.11)
1972-1992	1	(150.00)	(60.00)	(60.00)	0.79	(1.60)	(10.00)	0.30	0.02
	2	740.00	110.00	120.00	0.98	0.10	(30.00)	(3.90)	(0.01)
	3	210.00	0.00	0.00	0.27	(1.80)	(120.00)	0.30	(0.02)
	4	200.00	10.00	10.00	0.84	0.70	0.00	(0.20)	0.04
	Total	280.00	10.00	18.00	0.47	(1.00)	(50.00)	(0.70)	(0.01)
1992-1997	1	(100.00)	(30.00)	(30.00)	0.45	1.90	0.00	0.40	(0.02)
	2	(233.00)	(100.00)	(100.00)	0.77	1.70	0.00	0.20	0.01
	3	(360.00)	(290.00)	(290.00)	0.64	1.50	20.00	0.30	(0.03)
	4	(110.00)	(20.00)	(20.00)	0.03	0.50	0.00	0.60	0.04
	Total	(270.00)	(180.00)	(186.00)	0.74	1.50	10.00	0.40	0.01
1997-1999	1	30.00	0.00	(10.00)	0.17	0.40	13.00	(0.20)	0.14
	2	39.00	20.00	10.00	(0.22)	(0.50)	30.00	0.10	0.12
	3	184.00	60.00	70.00	0.01	(0.20)	173.00	(0.30)	0.04
	4	(70.00)	(10.00)	0.00	(0.08)	0.10	17.00	0.50	(0.04)
	Total	40.00	40.00	40.00	(0.27)	(0.20)	92.00	(0.10)	0.04
1999-2002	1	(139.58)	32.00	30.12	(1.66)	(3.89)	(43.00)	1.10	0.04
	2	(203.12)	35.00	22.04	(1.16)	(2.60)	(85.00)	0.80	0.04
	3	(127.24)	200.00	96.06	(0.96)	(2.12)	(373.00)	(0.20)	0.01
	4	313.75	89.00	73.85	(0.80)	(1.72)	(47.00)	(0.70)	(0.01)
	Total	(62.30)	106.00	48.61	(0.85)	(2.31)	(192.00)	0.20	0.01
2002-2005	1	(162.42)	(7.18)	(3.65)	(0.62)	1.15	0.00	0.40	(0.47)
	2	(151.12)	(52.78)	(45.22)	0.18	1.29	0.00	0.87	(0.47)
	3	(287.48)	(236.63)	(176.28)	0.37	2.55	0.00	0.90	(0.46)
	4	(162.27)	(5.09)	4.59	(0.59)	1.29	0.00	(0.04)	(0.41)
	Total	(249.16)	(169.67)	(129.70)	0.57	2.00	0.00	0.87	(0.46)

The data indicates that there is significant channel adjustment occurring and the river is still responding to the changes associated with channelization, dam construction and climate variation.

Bed material

Sand-sized particles are the primary bed material throughout the reach. Historically, the bed material has ranged from very find sand to medium sand. A slight coarsening of the bed material has been seen between 1972 and 2002 (See Figure 3.16). This may be due to the effects of the closure of Cochiti Dam. In addition, the coarsening may also be caused by new inputs of coarse material from tributaries and arroyos, a decreased supply of fine sediments, or increased transport capacity due to higher discharges.

Discharge
The daily discharge at both the San Acacia and San Marcial gages increased to about 4 times the previous daily discharge around 1979. The daily discharge decreased by about 3 times around 2000 (Larsen et al. 2007). These changes occurred due to the installation and operation of the Cochiti Dam, San Acacia Diversion Dam and the LFCC. In addition, decreased flows in resent years are associated with the fact that Elephant Butte Reservoir is at capacity.

Suspended sediment
The daily suspended sediment discharge recorded at both gages has changed little since early 1960's (Larsen et al. 2007). As a result, the suspended sediment concentration has varied inversely with discharge over time. The concentration decreased by about 5 times following the increase in discharge in 1979. The effects of the recent decrease in discharge are not known because suspended sediment data is unavailable after 1996.

Bedforms
The Simons and Richadson and van Rijn methods had a tendency to accurately predict dune formation 75%, antidune development 50% and ripples formation 25% of the time. The difficulty in calculating the expected bedforms stems from the high variability of the cross-sections in the reach. Two or more different types of bedforms were typically observed at a typical cross-section. In addition, it could be attributed to the fact that the methods were developed based on laboratory data and not field data. Dunes were the easier to predict because they occurred often.

6.2. Channel response models

6.2.1. Schumm's (1969) river metamorphosis model

Schumm (1969) developed a model to describe a channel's response to changes in water and sediment discharge. Schumm hypothesized that changes in water and sediment discharge would effect channel width, depth, width/depth ratio, channel slope, sinuosity and meander wavelength. The response of these parameters can be described by the following equations where a plus (+) exponent indicates an increase and a minus (-) exponent indicates a decrease.

Decreased bed material load:

$$Q_s^- \sim W^- D^+ P^+ L^- S^-$$

Increase bed material load:

$$Q_s^+ \sim W^+ D^- P^- L^+ S^+$$

Decreased water discharge:

$$Q^- \sim W^- D^- L^- S^+$$

Increased water discharge:

$$Q^+ \sim W^+ D^+ L^+ S^-$$

Decreased water discharge and bed material load:

$$Q^- Q_t^- \sim W^- D^\pm F^- L^- S^\pm P^+$$

Increased water discharge and bed material load:

$$Q^+ Q_t^+ \sim W^+ D^\pm F^+ L^+ S^\pm P^-$$

Where Q is water discharge, Q_s is bed material load, Q_t is the percent of the total load that is sand or bed material load, W is channel top width, D is flow depth, F is width/depth ratio, L is meander wavelength, P is sinuosity, and S is channel slope.

Table 6.2 shows Schumm's equations in tabular form.

Table 6.2 – Schumm's (1969) channel metamorphosis model

	W	D	S	F = W/D	P	L
Qs^-	-	+	-		+	-
Qs^+	+	-	+		-	+
Q^-	-	-	+			-
Q^+	+	+	-			+
Q^-Qt^-	-	+ -	+ -	-	+	-
Q^+Qt^+	+	+ -	+ -	+	-	+

Table 6.3 shows the observed changes in the San Acacia reach for each year and subreach and the metamorphosis model which matches the observations.

Table 6.3 – Observed channel changes at Q = 5000 cfs and the corresponding metamorphosis model (Schumm 1969)

Year	Subreach	W	D	S	F = W/D	P	Schumm's Model	
1962-1972	1	-	+	-	-	+	Q^-Qt^-	Decreased Water Discharge and Bed Material Load
	2	-	+	-	-	+	Q^-Qt^-	Decreased Water Discharge and Bed Material Load
	3	-	+	-	-	-	NA	
	4	-	+	+	-	+	Q^-Qt^-	Decreased Water Discharge and Bed Material Load
	Total	-	+	-	-	-	NA	
1972-1992	1	-	-	-	-	+	Q^-Qt^-	Decreased Water Discharge and Bed Material Load
	2	+	+	+	-	+	NA	
	3	=	-	-	-	+	Q^-Qt^-	Decreased Water Discharge and Bed Material Load
	4	+	+	-	=	+	Q^+	Increased Water Discharge
	Total	+	-	-	-	+	NA	
1992-2002	1	+	-	-	+	+	NA	
	2	-	-	-	=	-	NA	
	3	-	-	+	+	-	Q^-	Decreased Water Discharge
	4	+	-	-	+	-	Q^+Qt^+	Increased Water Discharge and Bed Material Load
	Total	-	-	-	+	-	NA	
1962-2002	1	-	-	-	-	+	Q^-Qt^-	Decreased Water Discharge and Bed Material Load
	2	-	+	-	-	-	NA	
	3	-	-	-	-	-	NA	
	4	-	+	+	-	+	Q^-Qt^-	Decreased Water Discharge and Bed Material Load
	Total	-	-	-	-	-	NA	

Based on the physical characteristics the Schumm river metamorphosis model suggest what the river reach is doing in regard to water discharge and bed material load. Only certain years and certain subreaches tend to follow the Schumm metamorphosis model, this is most likely associated with the fact that the river is changing. From 1962 to 1972 the observed changes indicate that there is a decrease in both the water discharge and the bed material load based on the Schumm model. The data from the USGS (Section 2, figure 2.5 and 2.6 and Escondida Reach Report) supports the Schumm metamorphosis model with a decrease in both discharge and sediment supply for this reach compared to previous years. Then from 1972 to 1992 in subreaches 1 and 3 there is a continued decrease in both the water discharge and the bed material load, however in subreach 4 there is an increase in the discharge based on the Schumm model. An analysis of the USGS data indicates the volume of water increases but there are less peak flows. Thus the Schumm model and USGS data follow subreach 4 and the sediment supply continues to decrease as suggested by subreach 1 and 3. From 1992 to 2002, subreach 3 shows a decrease in flow while subreach 4 shows and increase in discharge and bed material load. An analysis of the USGS data does not show an increase in discharge or a decrease in sediment and discharge. There seems to be a relatively constant flow and sediment discharge. An additional, comparison is provided from 1962 to 2002 but a trend in subreaches 2 and 3 and the overall reach could not be evaluated based on the Schumm metamorphosis model. In general based on all the data the results from 1962 to 2002 indicate that the reach is responding to a decrease in the overall peak discharge and sediment supply, which is associated with the regulation of the flow due to Cochiti Dam. The river has not reached equilibrium, thus the USGS data and the Schumm model do not always show agreement.

6.2.2. Lane's Balance (1955)

Lane's balance model is illustrated in Figure 6.1 (Lane 1955). The channel parameters examined by Lane were channel slope, discharge, median grain size, and sediment discharge. The model states that a change in any one of the four driving variables will result in a change of the other three variables such that the channel will tend toward a new equilibrium state.

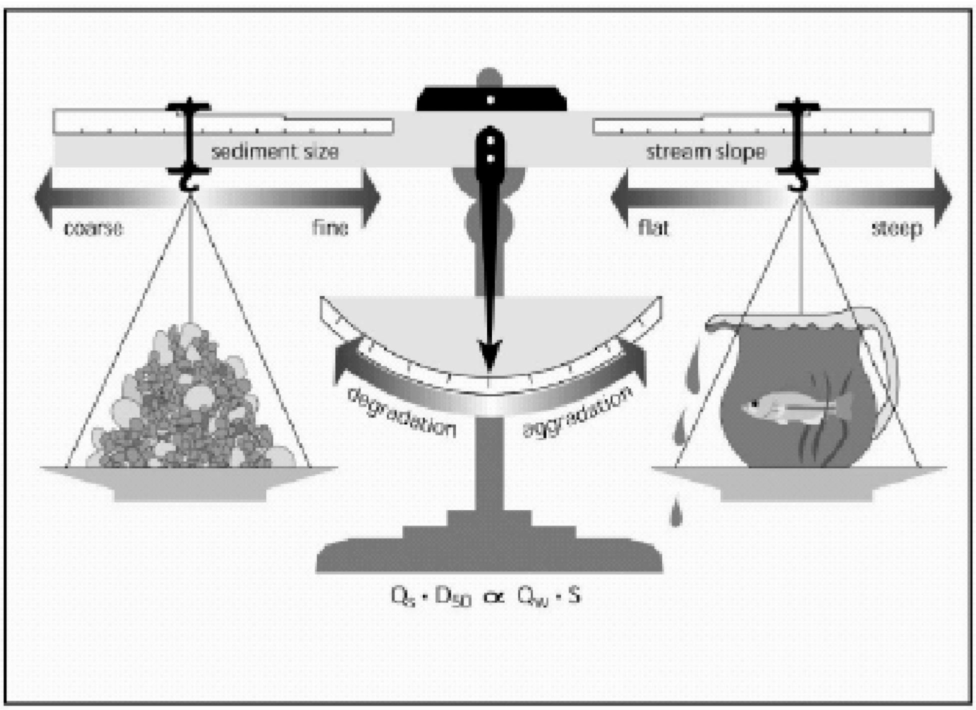

Figure 6.1 – Lane's Balance

Table 6.4 shows the observed channel changes from 1962 to 2002 as well as the variable to which the channel may be reacting. The variable initiating change was determined by selecting a variable as the initial point of change, and evaluating the changes in the other variables to determine if they followed the pattern outlined by Lane. If the changes balanced according to Lane, the variable could have been the trigger of channel change. Discharge and suspended sediment discharge were always considered first because the channel cannot change the amount or water or sediment entering the reach from upstream. If the slope of the channel increases, the discharge, sediment supply and particle size will have a tendency to decrease to balance the scale.

Table 6.4 – Change in channel characteristics for Lane's balance

Year	Subreach	Q	S	Qs	d_{50}	Trigger variable
1962-1972	1	-	-	-	-	None
	2	-	-	-	-	None
	3	-	-	-	-	None
	4	-	+	-	-	S
	Total	-	-	-	-	None
1972-1992	1	+	-	-	+	Q
	2	+	+	-	+	Qs
	3	+	-	-	+	Q
	4	+	-	-	+	Q
	Total	+	-	-	+	Q
1992-2002	1	-	-	-	+	d_{50}
	2	-	-	-	+	d_{50}
	3	-	+	-	+	Q or Qs
	4	-	-	-	+	d_{50}
	Total	-	-	-	+	d_{50}
1972-2002	1	-	-	-	+	d_{50}
	2	-	+	-	+	Q or Qs
	3	-	-	-	+	d_{50}
	4	-	-	-	+	d_{50}
	Total	-	-	-	+	d_{50}

In cases where the trigger variable states none, the Lane balance cannot be used to identify the trigger. Much of the triggers on the Middle Rio Grande are associated with the construction and operation of Cochiti Dam and the channelization on the Middle Rio Grande. According to Lane's balance from 1962 to 1972 Lane's balance cannot be used to predict the changes that were observed. This can be attributed to the closure of Cochiti Dam and operation of both Cochiti and San Acacia Diversion Dam. Between 1972 and 1992, discharge seemed to be the main triggering variable. This is primarily associated with the controlled release of flows down the channelized Middle Rio Grande. From 1992 to 2002 the particle size seems to be the primary trigger for the channel approaching equilibrium, which is also the case when looking at the data from 1972 to 2002. This is mostly associated with the degradation (Figure 3.13) caused by dam operation and channelization. In addition, it is likely that the channel is actually under the influence of multiple channel changes at any given time. However, this simplified approach gives some idea of what changes may be having the greatest influence on the channel morphology during a given period.

6.3. Future Dynamic Equilibrium Conditions

A stream classified as being in dynamic equilibrium does not have to be static. It will exhibit temporary morphological changes in response to the impacts of extreme events or even extended periods of low flow. It will take time (recovery time) for a moderate event to restore the stream; this is considered a river which is dynamically stable.

6.3.1. Equilibrium Width

Hydraulic Geometry

The hydraulic geometry equation developed by Blench (1957) over predicted the equilibrium widths for all subreaches ranging is width from 1200 to 2400 feet. This occurred because the Blench data was based on flume results. Simons and Albertson (1963), Nouh (1988), and Julien-Waradalam (1995) all predicted similar equilibrium widths between 250 ft and 350 ft. The consistent prediction by these three methods indicates that they may be the most effective in predicting a dynamic equilibrium width condition for this reach, but the river is still changing.

Hyperbolic and Exponential Models

The hyperbolic model developed by Williams and Wolman (1984) fit well with historic width data from the San Acacia reach. The widths predicted for 2020 by the hyperbolic model ranged from about 150 ft to 450 ft. When the model is extended to predict the equilibrium condition a negative equilibrium is reached for subreach 3. However, the values for the remaining reaches range from 30 ft to 175 ft. More data will improve the equilibrium prediction for this reach.

The exponential model developed by Richard et al. (2005) produced results very similar to those calculated by the hyperbolic model for the 2020 prediction. The model values range from 140 ft to 445 feet.

SAM

The final equilibrium width prediction method used was the HEC-RAS stable channel design program (SAM). Based on the incoming suspended sediment concentration determine from a combination of gage data and range line data), the equilibrium widths for the channel were all about 150 ft. This width is within the range of the other methods and provides a reasonable estimate of equilibrium channel width.

6.3.2. Equilibrium Slope

Hydraulic Geometry

Julien and Wargadalam (1995) predicted equilibrium slopes for the 2002 channel geometry between 0.00122 and 0.00156. These slopes are steeper than the majority of the reach, where the observed slopes range from 0.001 to 0.007 in the channel in 2002. This suggest that the channel may not be in equilibrium. The predicted slopes are, however, reasonable when compared to historic channel slopes.

SAM

The equilibrium slope was also estimated from the HEC- Ras stable channel design program. The program estimated the equilibrium slope to 0.000839 based on an incoming sediment supply of 2,629 ppm. The slope is approximately 40% less than what was predicted by the Julien-Wargadalam method.

Sediment Transport

The HEC- Ras sediment transport analysis was used to determine an equilibrium slope for the channel based on sediment transport. The equilibrium slope was estimated as the slope at which sediment supply equals sediment transport capacity. Yang's method was the only method able to provide reasonable slope predictions for all subreaches. These methods estimated the equilibrium slope to be between 0.0003 and 0.0009. This slope range is much less steep than the slopes estimated by Julien-Wargadalam. The slope predicted by SAM is within the range predicted by the sediment transport analysis in HEC-RAS. Improvements could be made to these slope estimates by having a accounting of incoming sediment from all sources, such as arroyos and other ungauged tributaries may improve the predictions provided by the sediment transport analysis..

7. Summary

This study is an update of the San Acacia reach analyzed by Reclamation which extends from 1918 to 2006. The reach covers 11.6 miles of the Middle Rio Grande in central New Mexico. The previous study looked at changes from 1918 to 1992. This study includes data from 1918 to 2006 and more quantitative estimates of channel hydraulic geometry, slope and sediment transport. Numerous techniques were used to perform the analysis. Changes in channel geometry and morphology, and water and sediment discharge were observed. In addition, historic bedform data were analyzed. Finally, the dynamic equilibrium conditions of the reach were estimated.

Spatial and temporal trends in channel geometry and morphology were identified using visual observations of aerial photographs and GIS active channel planforms, cross-section surveys, hydraulic modeling using HEC- Ras, and channel classification methods. Observations of the GIS active channel planforms and aerial photographs show that the channel has narrowed between 1918 and 2006. Analysis of channel geometry trends using HEC- Ras hydraulic modeling output shows a series of increases and decreases in most channel properties. The fluctuations in channel geometry may be the result of a complex response to past channel changes. Bed material samples obtained from cross-section surveys and at the USGS San Acacia gage between 1972 and 2002 show a slight coarsening of the bed from a mean diameter of 0.1 mm to 0.36 mm.

Historic bedform observations were compiled and compared to predicted bedforms at the survey locations. Simons and Richardson and van Rijn were used to calculate the expected bedforms at each survey locations. These predictions were compared with field observations of bedforms. The bedform predictor resulted in significant scatter. This scatter is likely due to the wide variability across individual cross-sections in the reach. When dunes were observed the two bedform predictor methods performed the best with a 75% prediction rating.

Trends in water and sediment discharge were analyzed using mass curves developed from USGS gage data (Larsen et al. 2007).

Estimates of potential equilibrium slope and width conditions were made using hydraulic geometry equations, hyperbolic and exponential regressions, stable channel geometry, and sediment transport relationships. An equilibrium width of ranging between 150 feet to 450 feet was estimated using several methods, indicating that the channel will continue to narrow. The equilibrium slope ranges from 0.0003 and 0.00156, depending on the subreach and the method used. There is significant variability; the predicted slopes suggest that the channel needs to reduce its slope by bed changes, channel lengthening (lateral migration), or both to reach the estimated dynamic equilibrium.

The main conclusions of this study are:

- The active channel has narrowed for the overall reach from approximately 800 feet to 340 feet aand the sinuosity decreased from 1.19 to 1.09 between 1918 and 2006. In addition, the mean bed material diameter increased from 0.1 mm to 0.36 mm between 1962 and 2002.

- Bedform prediction methods by van Rijn and Simons and Richardson produced a reasonable fit when the observed data was dunes. The wide scatter is likely caused by the high degree of bedform variability across a cross-section.

- Equilibrium width and slope predictors forecast a channel width of between 150 feet to 450 feet and a slope between 0.0003 and 0.00156. These estimates were confirmed by multiple methods and suggest that the channel is narrowing and has the potential to meander if sufficient area is provided.

The collective observations of the reach indicate that this is a very dynamic reach that has not yet reached a state of dynamic equilibrium. The channel will likely continue to narrow. Lateral movement, sinuosity changes and bed elevation changes are also likely as the channel attempts to reach an equilibrium slope. The constructed levee setback projects will create a new dynamic equilibrium condition for this reach and more studies will need to be performed to evaluate effects of these projects.

8. References

Ackers, P., and Charlton, F. G. (1982).

Bauer, T. R. (2000). "Morphology of the Middle Rio Grande from Bernalillo Bridge to the San Acacia Diversion Dam, New Mexico," Colorado State University, Fort Collins.

Blench, T. (1957). *Regime Behavior of Canals and Rivers.*, Butterworths Scientific Publications, London.

Bullard, K. L., and Lane, W. L. (1993). "Middle Rio Grande Peak Flow Frequency Study." U.S. Department of Interior, U.S. Bureau of Reclamation, Albuquerque, NM.

Chang, H. H. (1979). "Minimum Stream Power and River Channel Patterns." *Journal of Hydrology*, 41, 303-327.

Henderson, F. M. (1966). *Open Channel Flow*, MacMillan Publishing Co., Inc., New York.

Julien, P. Y. (1998). *Erosion and Sedimentation*, Cambridge University Press, New York.

Julien, P. Y., and Wargadalam, J. (1995). "Alluvial Channel Geometry: Theory and Applications " *Journal of Hydraulic Engineering*, 121(4), 312-325.

Klaassen, G. J., and Vermeer, K. (1988). "Channel Charcateristics of the Brading Jamuna River, Bangladesh." International Conference on River Regime, W. R. White, ed., Hydraulic Research Ltd., Wallingford, UK, 173-189.

Lane, E. W. (1955). "The importance of fluvial morphology in hydraulic engineering." *Proc. ASCE*, 81(745), 1-17.

Larsen, A., Shah-Fairbank, S. C., and Julien, P. (2007). "Escondida Reach. Escondida to San Antonio. Hydraulic Modeling Analysis 1962-2006." Colorado State University Fort Collins, CO.

Leopold, L. B., and Wolman, M. G. (1957). "River Channel Patterns: Braided, Meandering and Straight." *Professional Paper 282-B*, US Geological Survey.

Massong, T. M. (2005a). "Geomorphology Summary, Rio Grande-Bernalillo Bridge Reach. ." U.S. Department of the Interior, Bureau of Reclamation Technical Report, Albuquerque, New Mexico.

MRGCD. (2006). "Middle Rio Grande Conservancy District website."

Nanson, G. C., and Croke, J. C. (1992). "A genetic classification of floodplains." *Geomorphology*, 4, 459-486.

Nouh, M. (1988). "Regime Channels of an Extremely Arid Zone." International Conference of Regimr, W. R. White, ed., Hydraulic Research Ltd., Wallingford, UK, 55-66.

Novak, S. J. (2006). "Hydraulic modeling analysis of the Middle Rio Grande from Cochiti Dam to Galisteo Creek, New Mexico," Colorado State University, Fort Collins.

Parker, G. (1976). "On the Cause and Characteristic Scales of Meandering and Braiding in Rivers." *Journal of Fluid Mechanics*, 76(3), 457-480.

Raff, D. A., Bledsoe, B. P., and Flores, A. N. (2003). "GeoTool Version 3." Engineering Research Center, Colorado State Uuniversity, Fort Collins.

Richard, G., Julien, P. Y., and Baird, D. C. (2005). "Case Study: Modeling the Lateral Mobility of the Rio Grande below Cochiti Dam, New Mexico." *Journal of Hydraulic Engineering*, 131(11), 931-941.

Richards, G. (2001). "Quantification and Prediction of Lateral Channel Adjustments Downstream from Cochiti Dam, Rio Grande, NM," Colorado State Univeristy, Fort Collins.

Rosgen, D. (1996). *Applied River Morphology*, Wildland Hydrology, Pagosa Springs, CO.

Schumm, S. A. (1969). "River Metamorphosis." *Journal of Hydraulic Division, ASCE*, 95(1), 255-273.

Schumm, S. A., and Khan, H. R. (1972). "Experimental Study of Channel Patterns." *Geological Society of America Bulletin*, 83, 1755-1770.

Scurlock, D. (1998). "From the Rio to the Sierra: An Environmental History of the Middle Rio Grande Basin." *General Technical Rerport RMRS-GTR5*, United States Department of Agriculture, Forest Service, Rocky Mountain Research Station, Fort Collins.

Simons, D. B., and Albertson, M. L. (1963). "Uniform Water Conveyance Channels in Alluvial Material. Part 1." *Transactions of the American Society of Civil Engineers*, 12(3399), 65-107.

TetraTech. (2002). "Development of the Middle Rio Grande FLO-2D Flood Routing Model Cochiti Dam to Elephant Butte Reservoir." Tetra Tech, Inc.

USBR. (2003). "Geomorphologic Assesment of the Rio Grande San Acacia Reach. Final Report." U.S. Department of the Interior, Bureau of Reclamation, Albuquerque, NM.

USBR. (2007). "Middle Rio Grande Maintenance Plan Part 1 Perot.".S. Department of the Interior, Bureau of Reclamation, Albuquerque, New Mexico.

USFWS. (1997). "Final Determination of Critical Habitat for the Southwestern Willow Flycatcher." Federal Register, 39129-39147.

USFWS. (1999). "Final Designation of Critical Habitat for the Rio Grande Silvery Minnow." Federal Register, 36274-36290.

van den Berg, J. H. (1995). "Prediction of Alluvial Channel Pattern of Perennial Rivers." *Geomorphology* 12, 259-279.

van Rijn, L. C. (1984). "Sediment Transport, Part III: Bedforms and Alluvial Roughness." *Journal of the Hydraulic Division, ASCE*, 110(12), 1733-1754.

Wargadalam, J. (1993). "Hydraulic Geometry of Alluvial Channels," Colorado State Univeristy, Fort Collins.

Williams, G., and Wolman, G. (1984). "Downstream Effects of Dams on Alluvial Rivers." *Professional Paper 1286*, U.S. Geological Survey

Appendix A – Relocation Map of Low Flow Conveyance Channel

RM 111 – 2008

2008 aerial photography - BOR

RECLAMATION
Managing Water in the West

RM 2011 - 2010

2010 aerial photography - USACE

RECLAMATION
Managing Water in the West

0 500 1,000 2,000 Feet

RM 113/114 - 2008

Appendix B – Cross Section Comparison

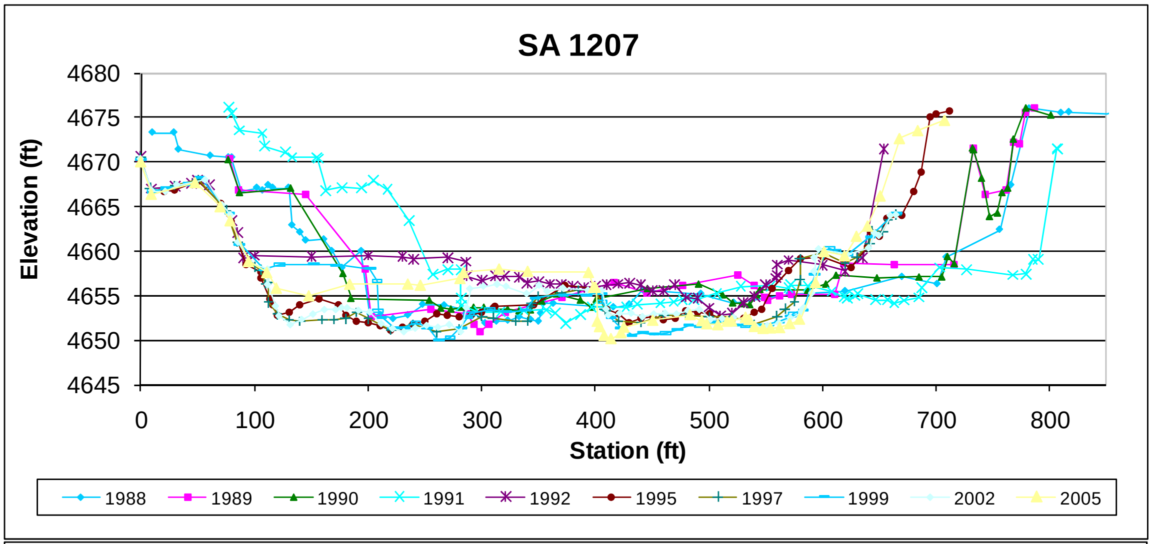
SA 1207
Elevation (ft)
4680
4675
4670
4665
4660
4655
4650
4645
0
100
200
300
400
500
600
700
800
Station (ft)
1988
1989
1990
1991
1992
1995
1997
1999
2002
2005

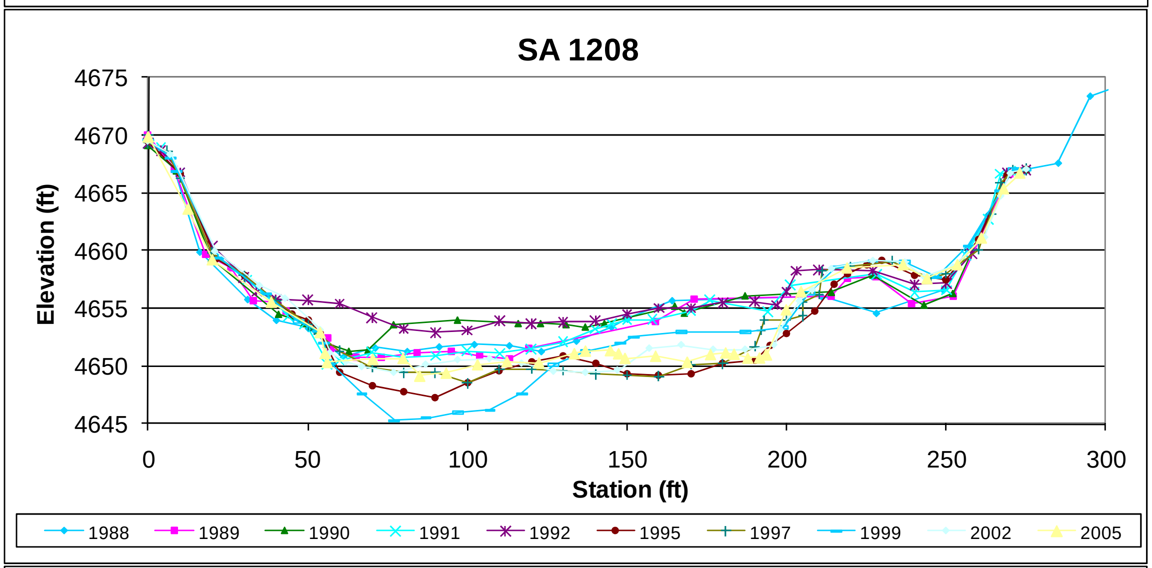
SA 1208
Elevation (ft)
4675
4670
4665
4660
4655
4650
4645
0
50
100
150
200
250
300
Station (ft)
1988
1989
1990
1991
1992
1995
1997
1999
2002
2005

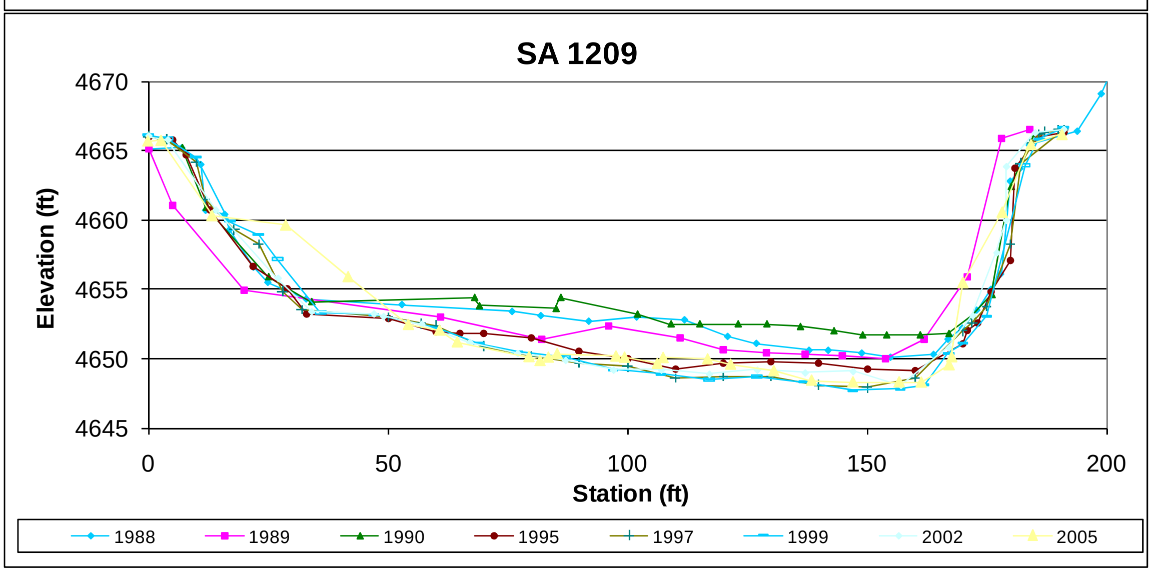
SA 1209
Elevation (ft)
4670
4665
4660
4655
4650
4645
0
50
100
150
200
Station (ft)
1988
1989
1990
1995
1997
1999
2002
2005

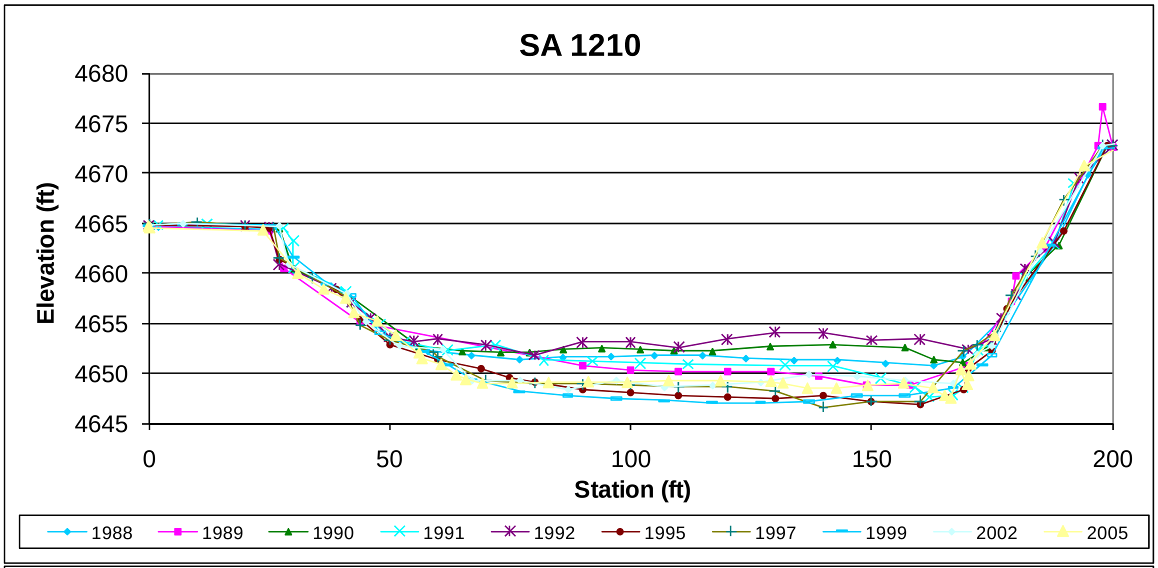
SA 1210
Elevation (ft)
4680
4675
4670
4665
4660
4655
4650
4645
0
50
100
150
200
Station (ft)
1988
1989
1990
1991
1992
1995
1997
1999
2002
2005

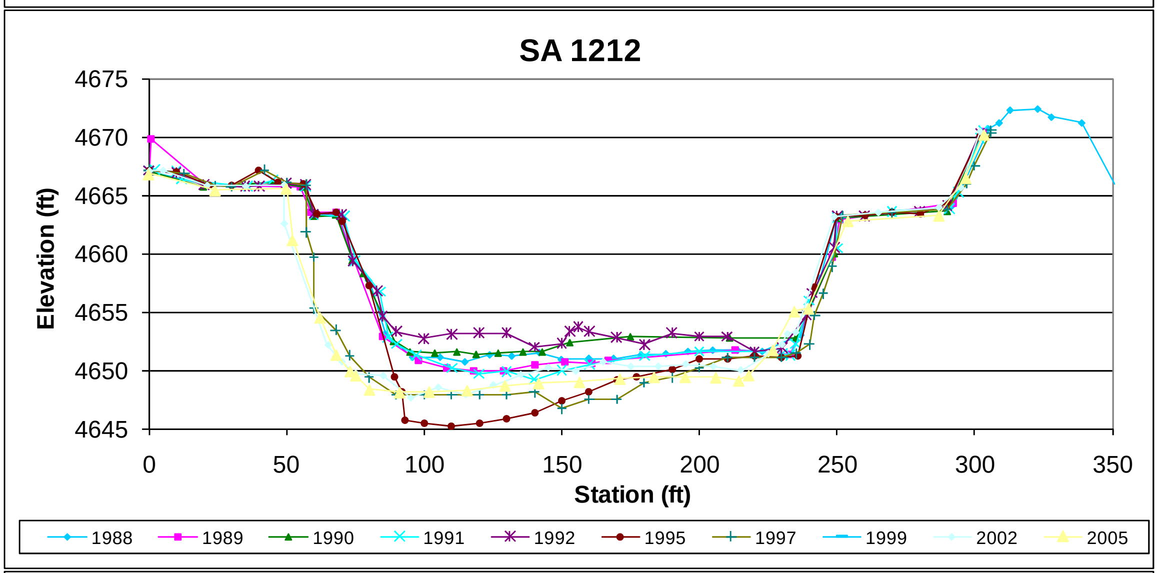
SA 1212
Elevation (ft)
4675
4670
4665
4660
4655
4650
4645
0
50
100
150
200
250
300
350
Station (ft)
1988
1989
1990
1991
1992
1995
1997
1999
2002
2005

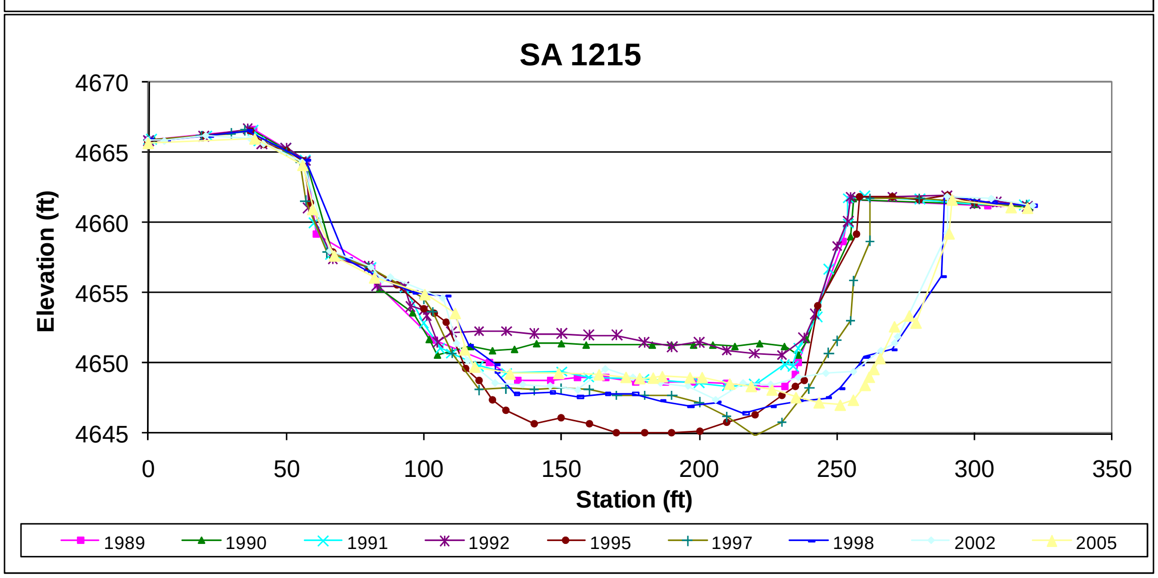
SA 1215
Elevation (ft)
4670
4665
4660
4655
4650
4645
0
50
100
150
200
250
300
350
Station (ft)
1989
1990
1991
1992
1995
1997
1998
2002
2005

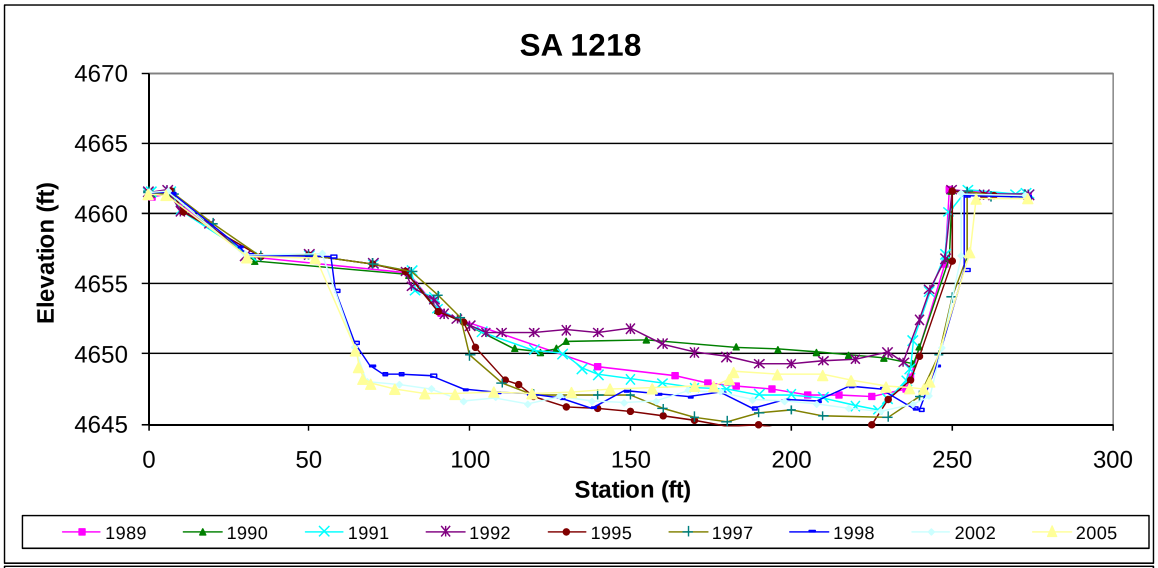
SA 1218
Elevation (ft)
Station (ft)
4670
4665
4660
4655
4650
4645
0
50
100
150
200
250
300
1989
1990
1991
1992
1995
1997
1998
2002
2005

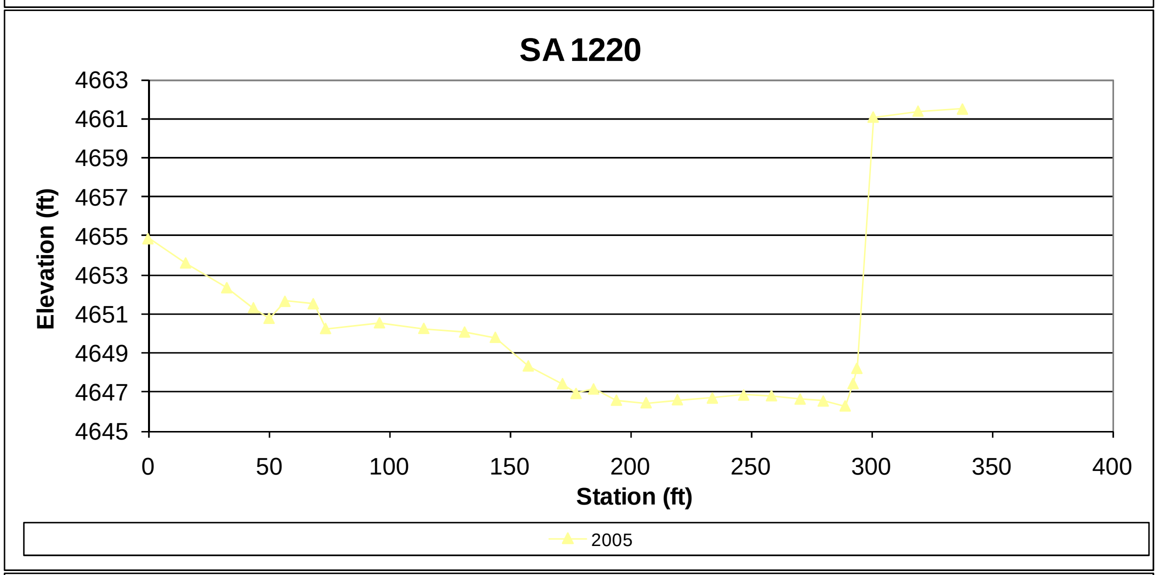
SA 1220
Elevation (ft)
Station (ft)
4663
4661
4659
4657
4655
4653
4651
4649
4647
4645
0
50
100
150
200
250
300
350
400
2005

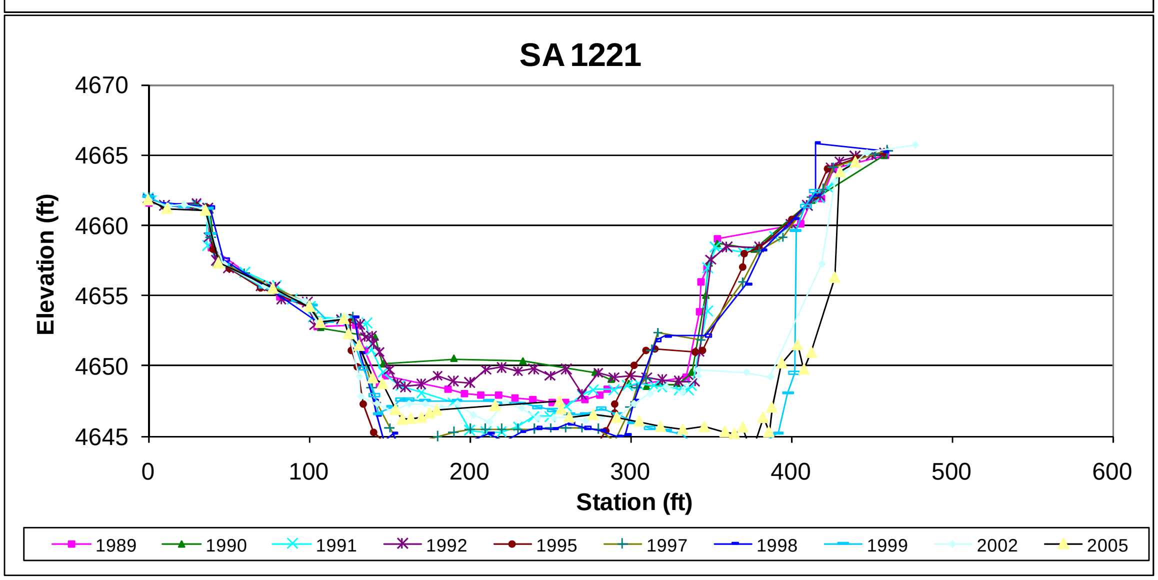
SA 1221
Elevation (ft)
Station (ft)
4670
4665
4660
4655
4650
4645
0
100
200
300
400
500
600
1989
1990
1991
1992
1995
1997
1998
1999
2002
2005

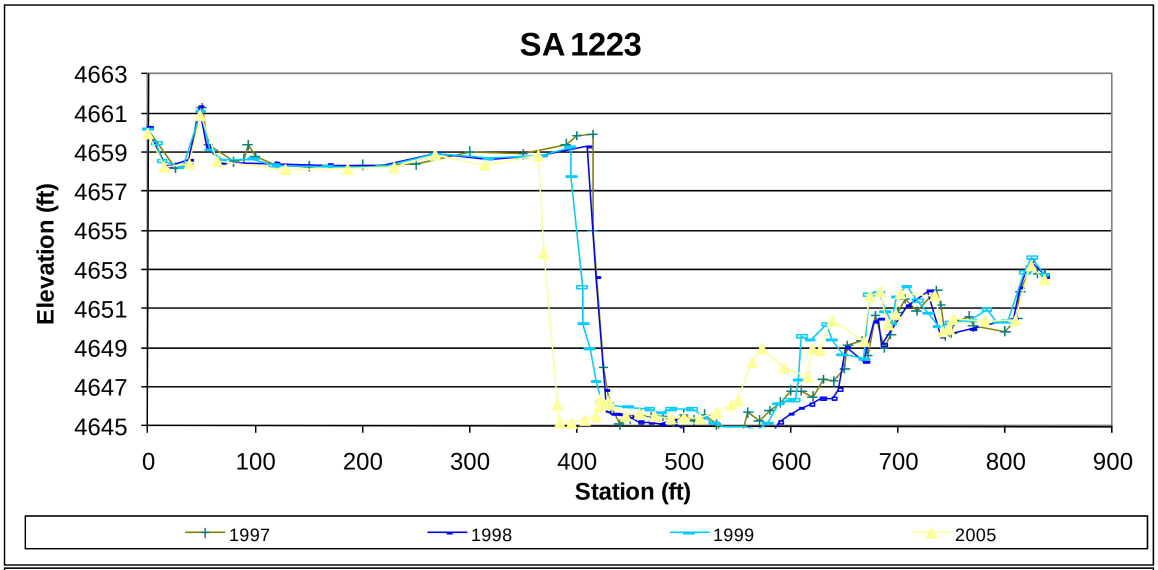
SA 1223
Elevation (ft)
4663
4661
4659
4657
4655
4653
4651
4649
4647
4645
0
100
200
300
400
500
600
700
800
900
Station (ft)
1997
1998
1999
2005

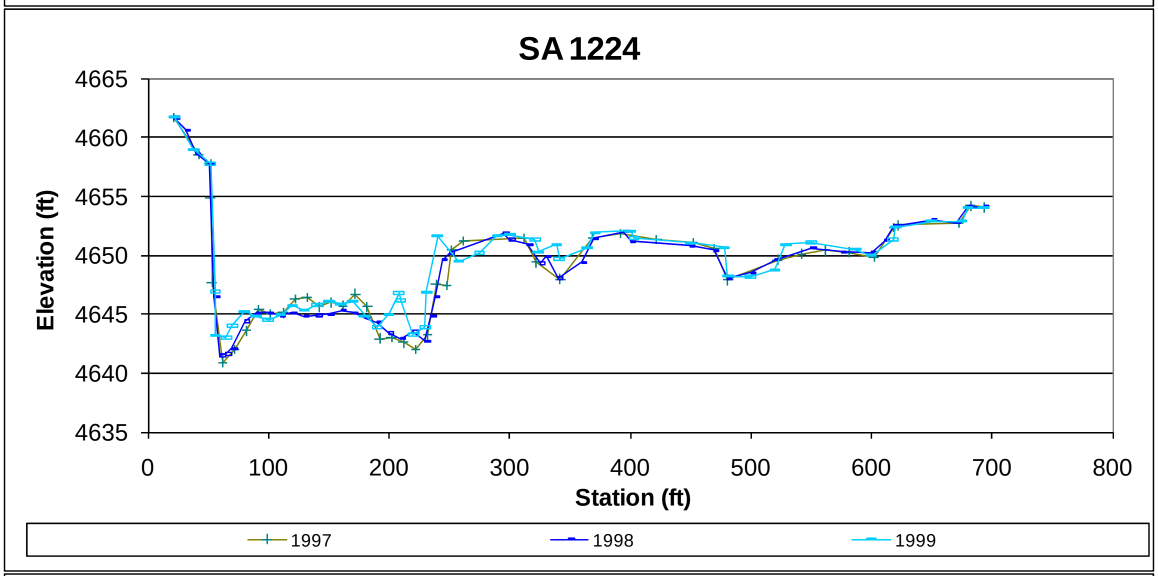
SA 1224
Elevation (ft)
4665
4660
4655
4650
4645
4640
4635
0
100
200
300
400
500
600
700
800
Station (ft)
1997
1998
1999

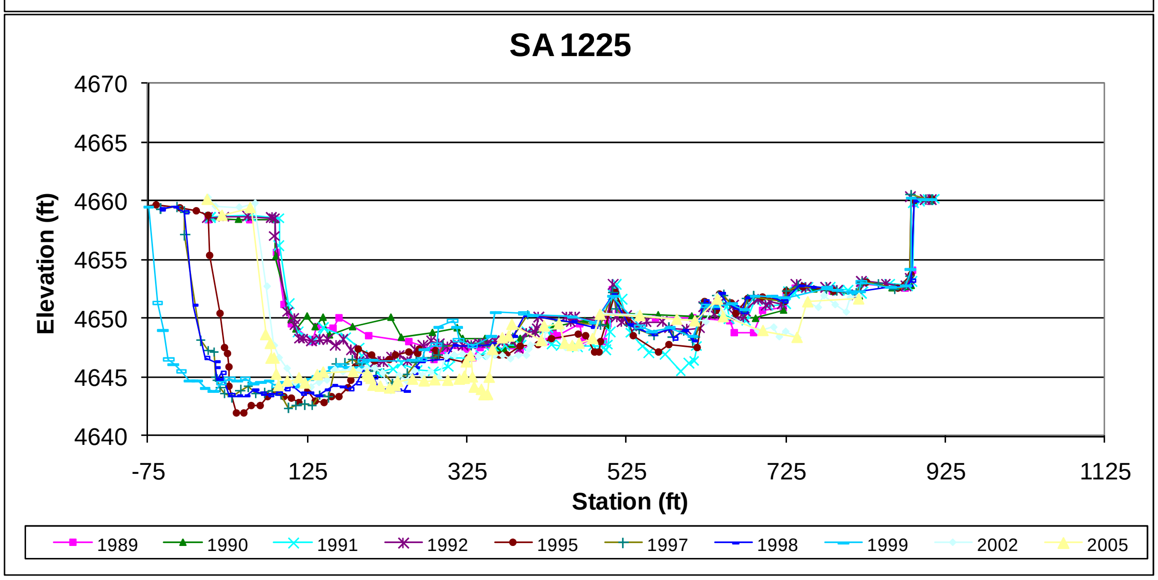
SA 1225
Elevation (ft)
4670
4665
4660
4655
4650
4645
4640
-75
125
325
525
725
925
1125
Station (ft)
1989
1990
1991
1992
1995
1997
1998
1999
2002
2005

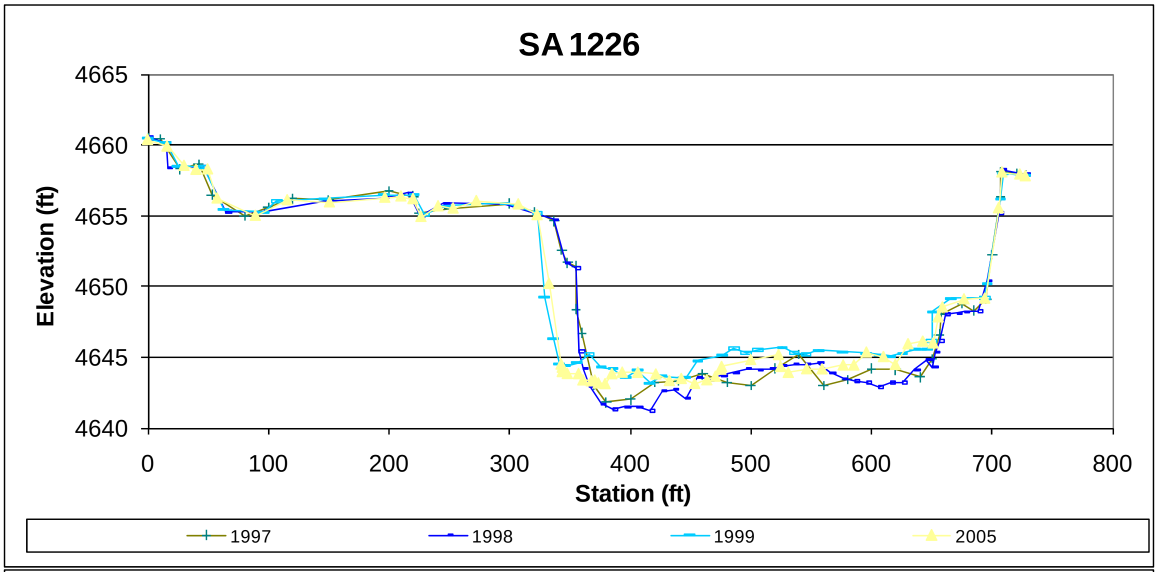
SA 1226
Elevation (ft)
4665
4660
4655
4650
4645
4640
0
100
200
300
400
500
600
700
800
Station (ft)
1997
1998
1999
2005

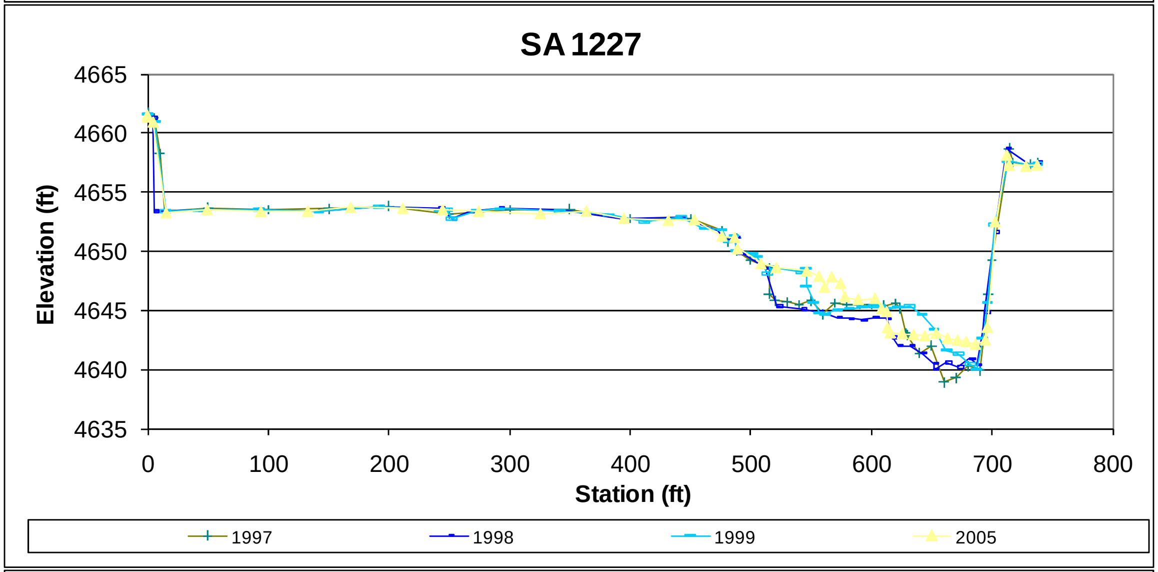
SA 1227
Elevation (ft)
4665
4660
4655
4650
4645
4640
4635
0
100
200
300
400
500
600
700
800
Station (ft)
1997
1998
1999
2005

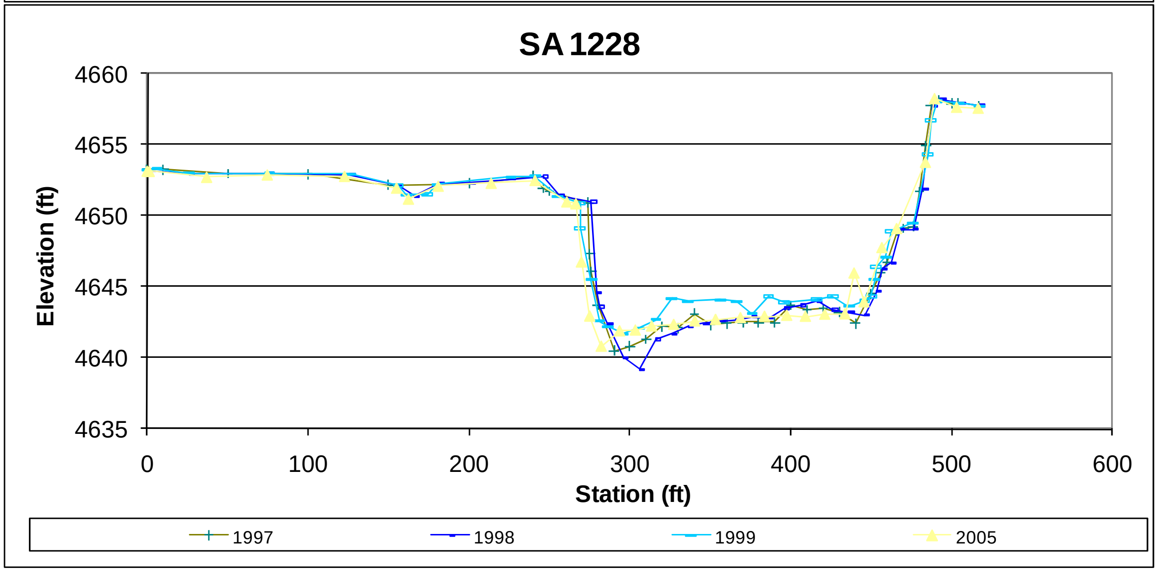
SA 1228
Elevation (ft)
4660
4655
4650
4645
4640
4635
0
100
200
300
400
500
600
Station (ft)
1997
1998
1999
2005

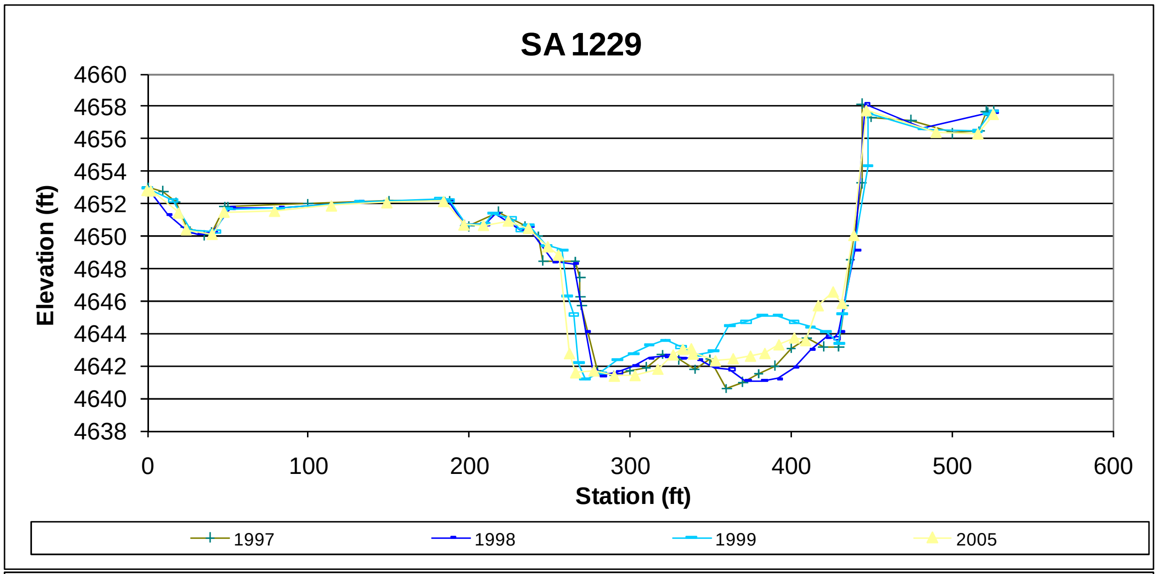

SA 1229
Elevation (ft)
4660
4658
4656
4654
4652
4650
4648
4646
4644
4642
4640
4638
0
100
200
300
400
500
600
Station (ft)
1997
1998
1999
2005

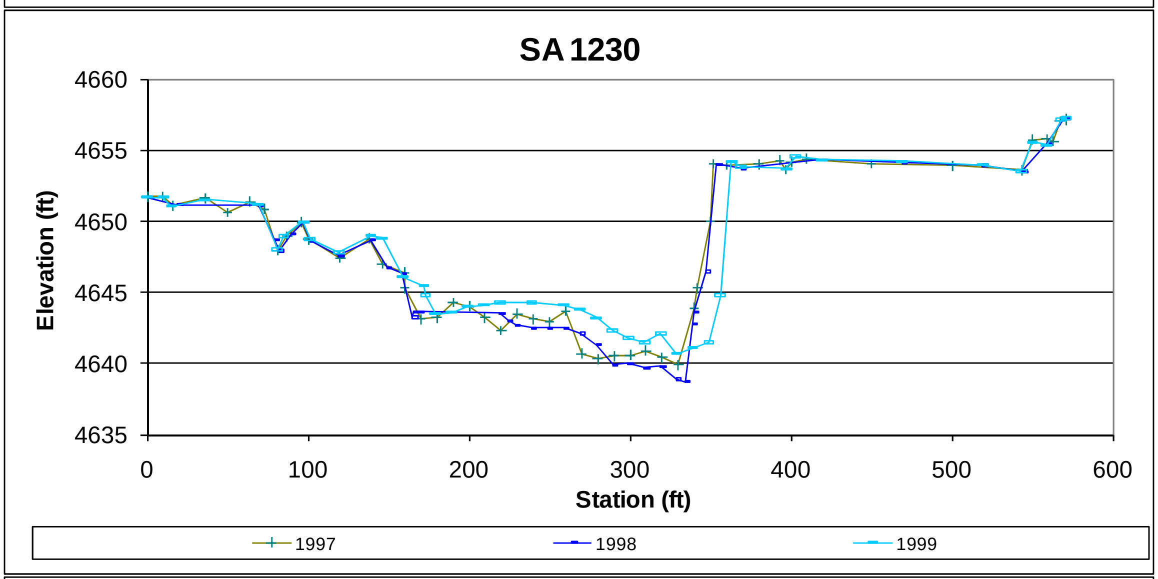

SA 1230
Elevation (ft)
4660
4655
4650
4645
4640
4635
0
100
200
300
400
500
600
Station (ft)
1997
1998
1999

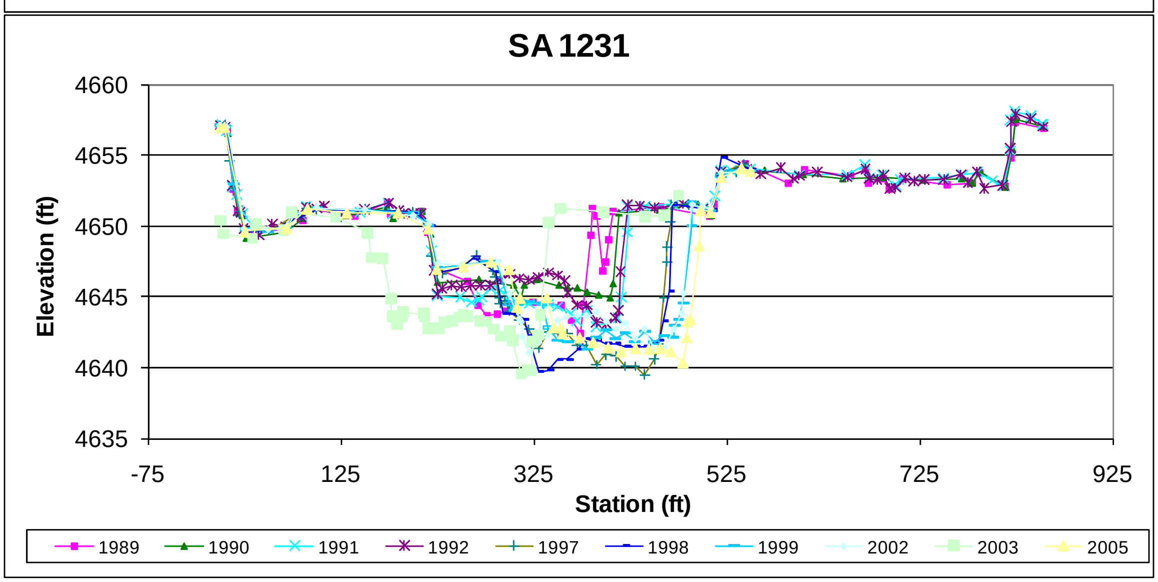

SA 1231
Elevation (ft)
4660
4655
4650
4645
4640
4635
-75
125
325
525
725
925
Station (ft)
1989
1990
1991
1992
1997
1998
1999
2002
2003
2005

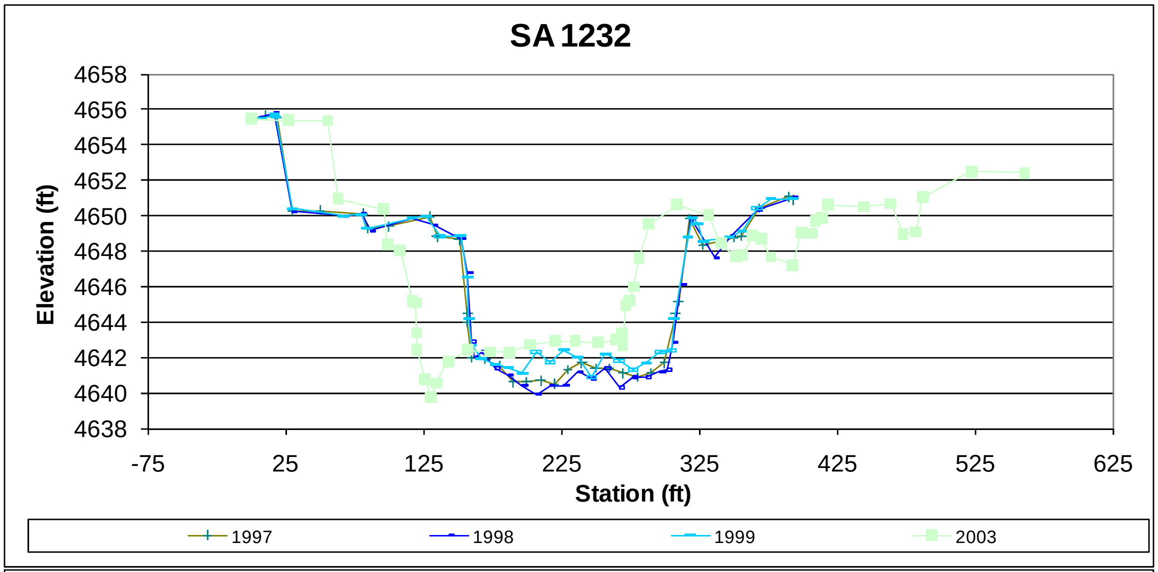
SA 1232
Elevation (ft)
4658
4656
4654
4652
4650
4648
4646
4644
4642
4640
4638
-75
25
125
225
325
425
525
625
Station (ft)
1997
1998
1999
2003

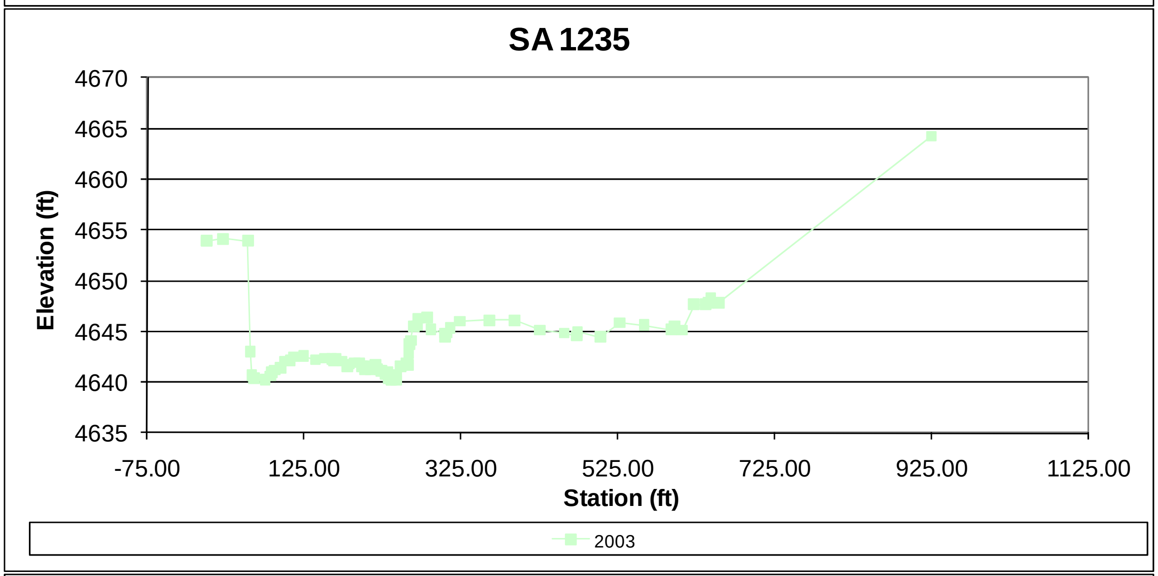
SA 1235
Elevation (ft)
4670
4665
4660
4655
4650
4645
4640
4635
-75.00
125.00
325.00
525.00
725.00
925.00
1125.00
Station (ft)
2003

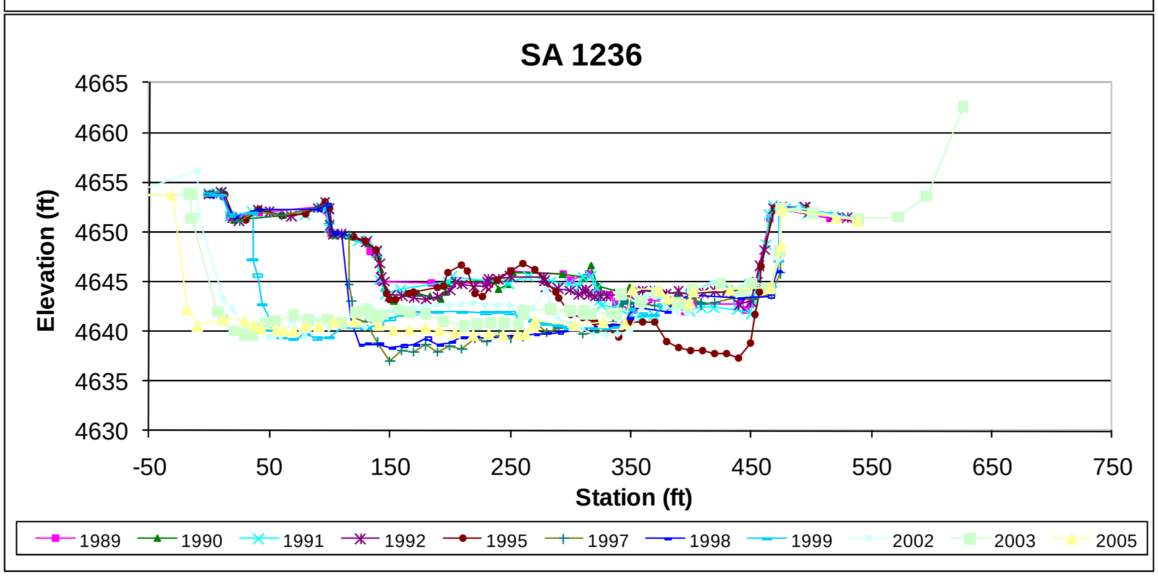
SA 1236
Elevation (ft)
4665
4660
4655
4650
4645
4640
4635
4630
-50
50
150
250
350
450
550
650
750
Station (ft)
1989
1990
1991
1992
1995
1997
1998
1999
2002
2003
2005

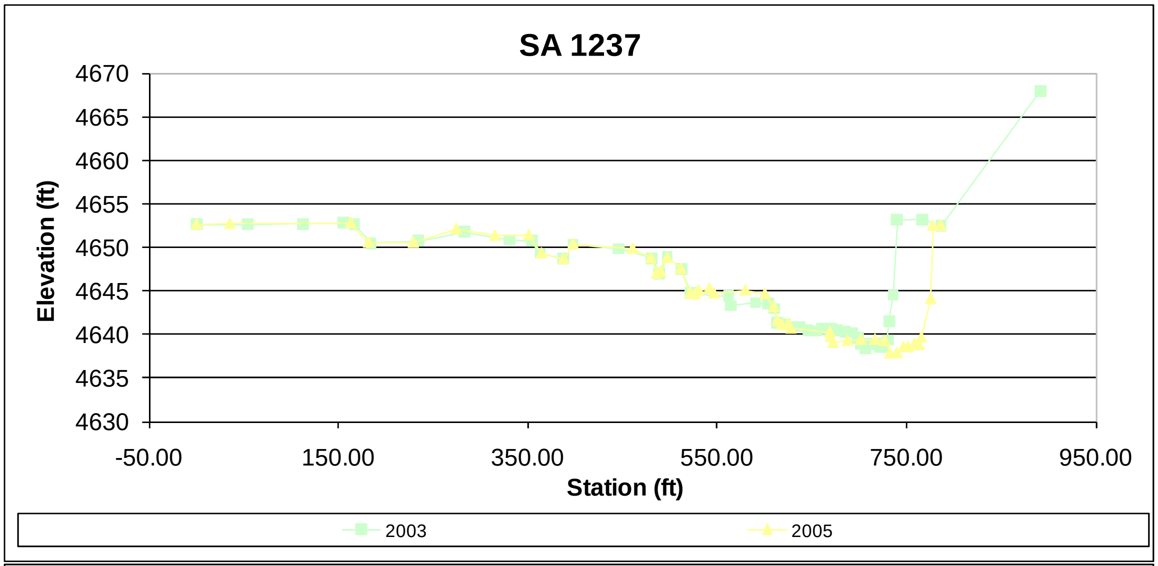
SA 1237
Elevation (ft)
4670
4665
4660
4655
4650
4645
4640
4635
4630
-50.00
150.00
350.00
550.00
750.00
950.00
Station (ft)
2003
2005

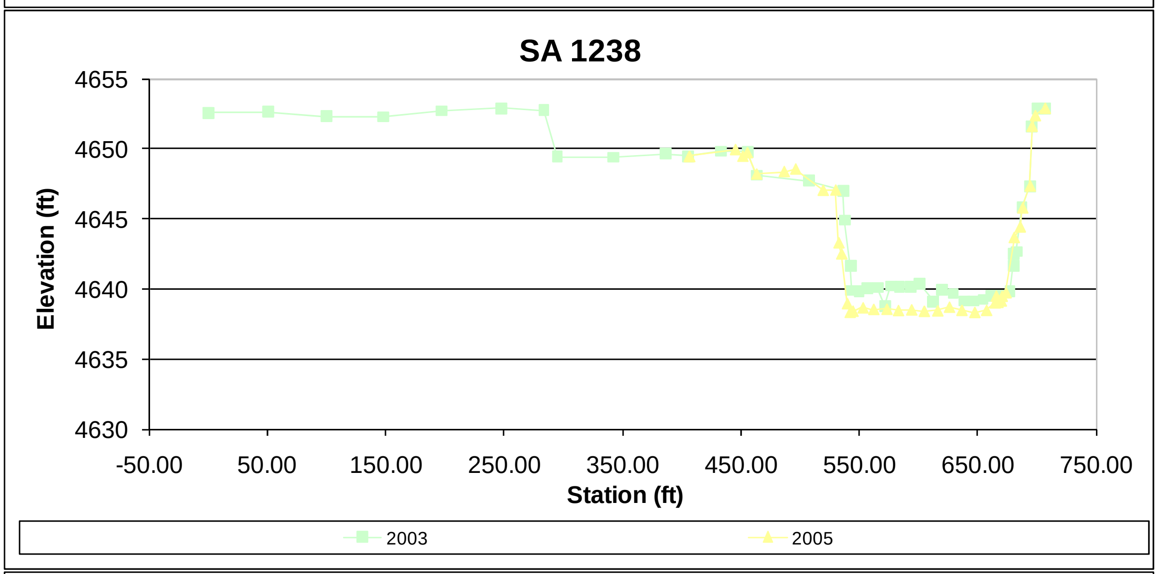
SA 1238
Elevation (ft)
4655
4650
4645
4640
4635
4630
-50.00
50.00
150.00
250.00
350.00
450.00
550.00
650.00
750.00
Station (ft)
2003
2005

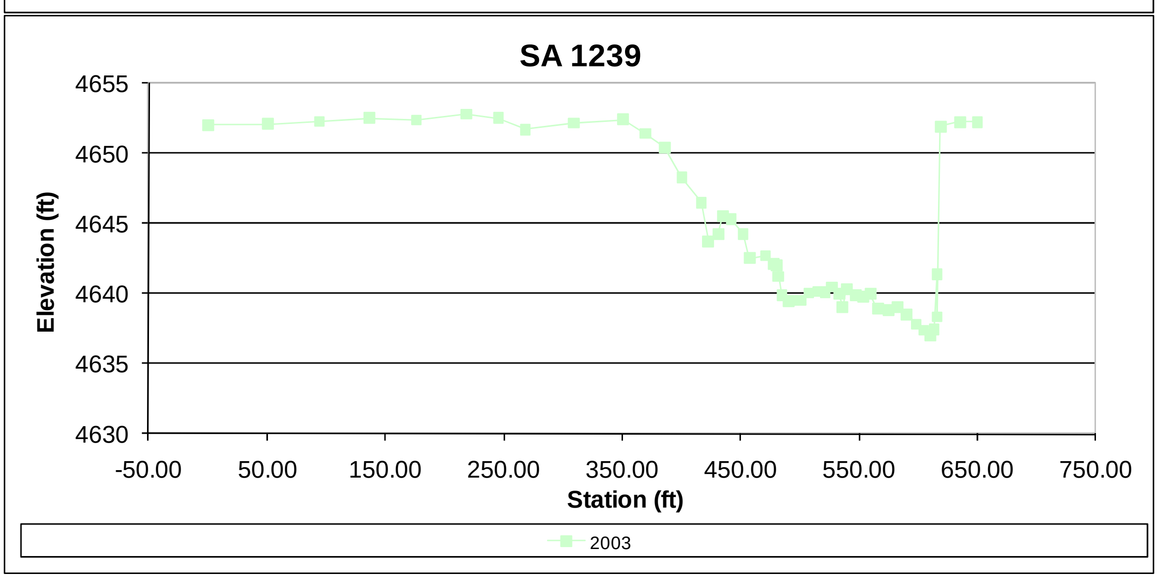
SA 1239
Elevation (ft)
4655
4650
4645
4640
4635
4630
-50.00
50.00
150.00
250.00
350.00
450.00
550.00
650.00
750.00
Station (ft)
2003

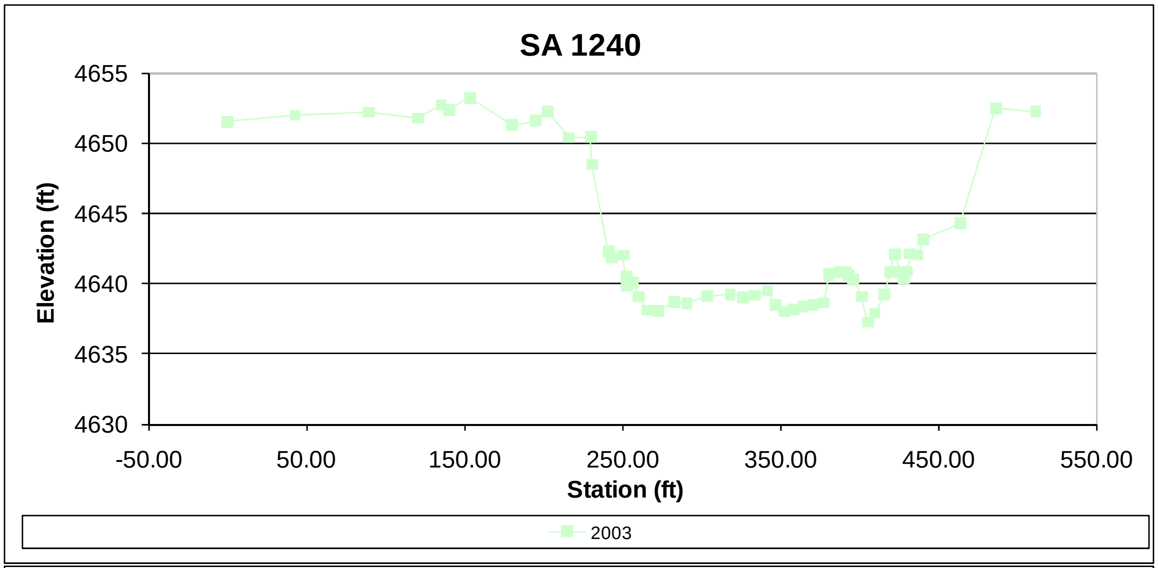
SA 1240
Elevation (ft)
Station (ft)
2003

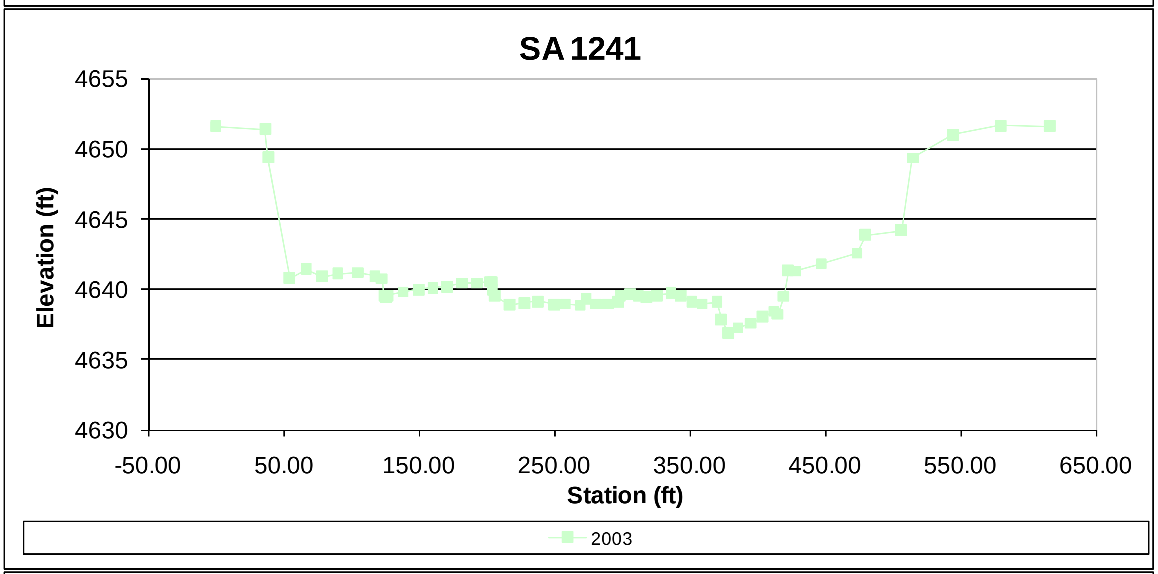
SA 1241
Elevation (ft)
Station (ft)
2003

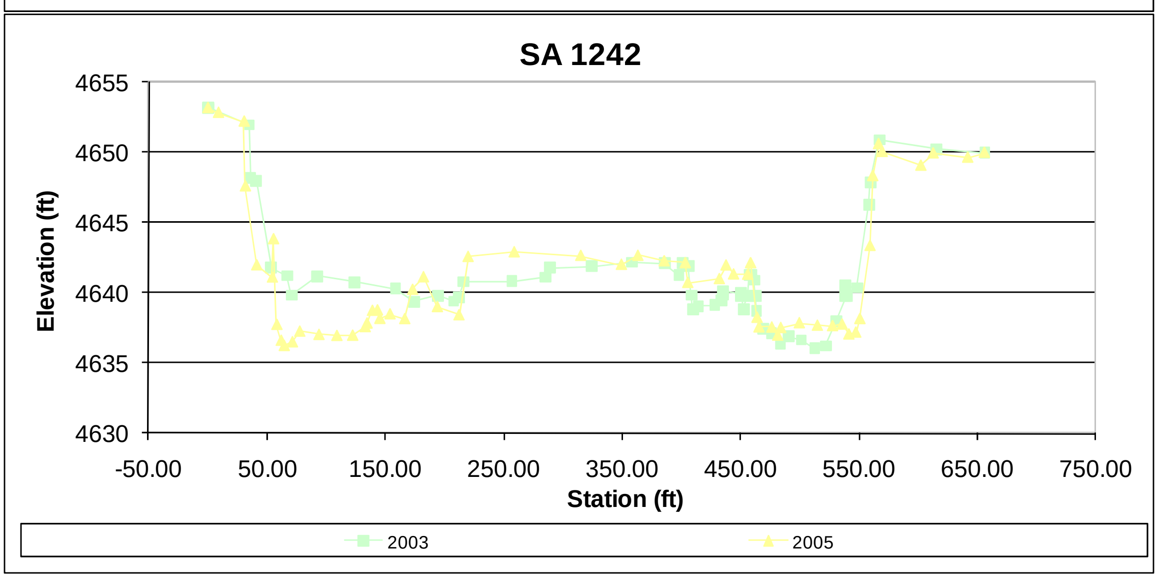
SA 1242
Elevation (ft)
Station (ft)
2003
2005

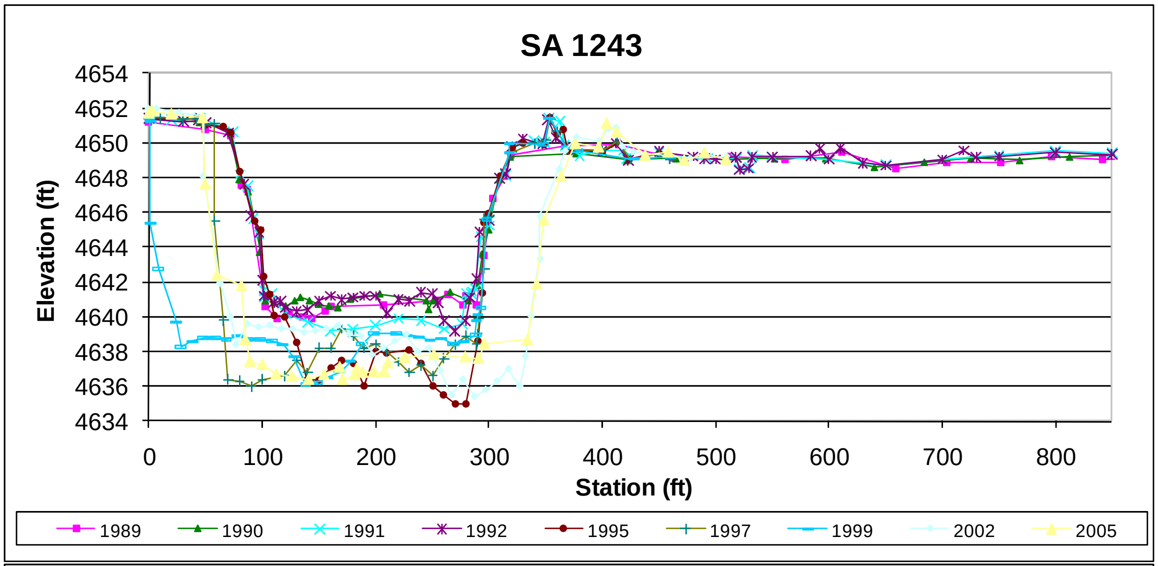

SA 1243
Elevation (ft)
Station (ft)
4654
4652
4650
4648
4646
4644
4642
4640
4638
4636
4634
0
100
200
300
400
500
600
700
800
1989
1990
1991
1992
1995
1997
1999
2002
2005

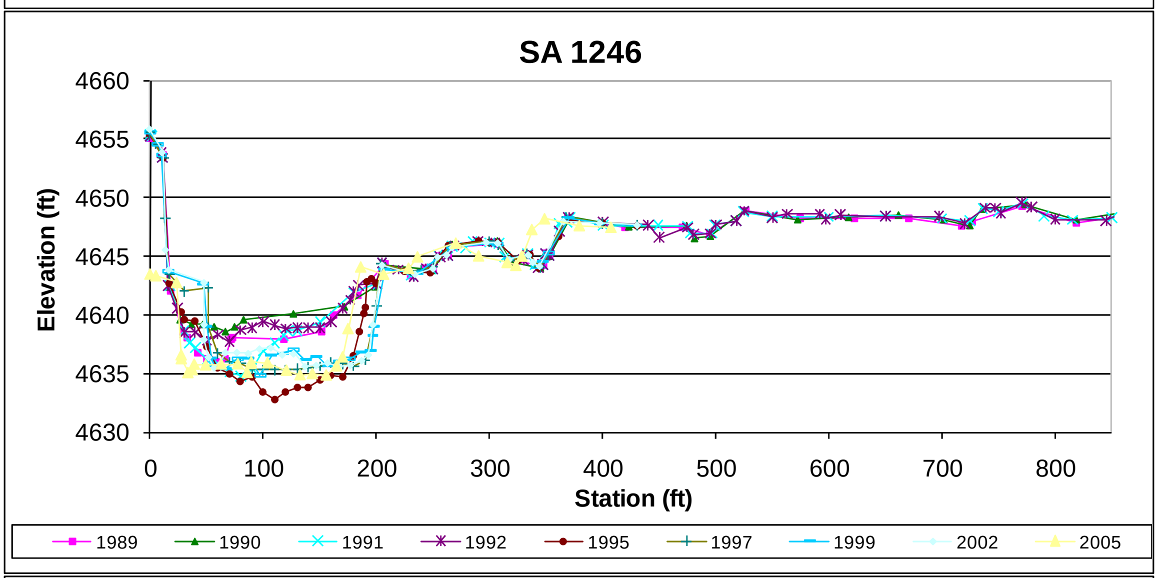

SA 1246
Elevation (ft)
Station (ft)
4660
4655
4650
4645
4640
4635
4630
0
100
200
300
400
500
600
700
800
1989
1990
1991
1992
1995
1997
1999
2002
2005

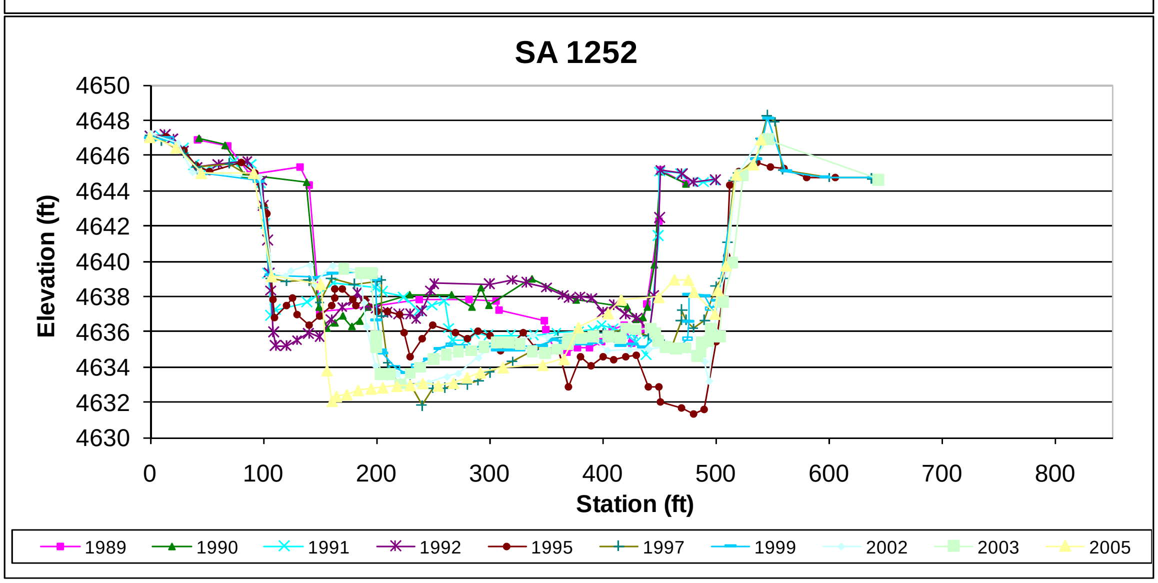

SA 1252
Elevation (ft)
Station (ft)
4650
4648
4646
4644
4642
4640
4638
4636
4634
4632
4630
0
100
200
300
400
500
600
700
800
1989
1990
1991
1992
1995
1997
1999
2002
2003
2005

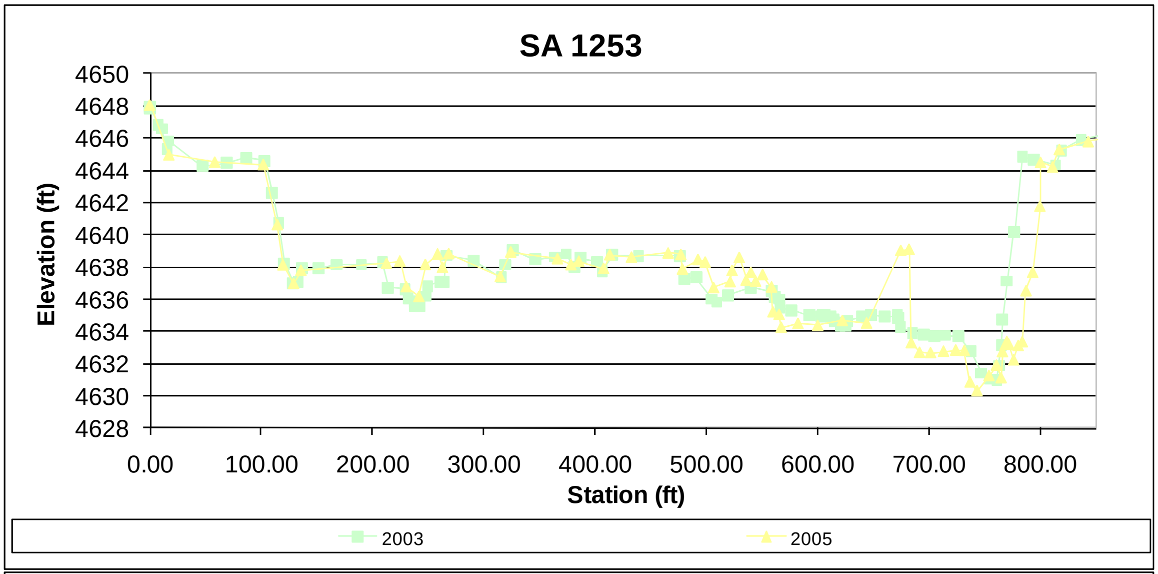

SA 1253
Elevation (ft)
4650
4648
4646
4644
4642
4640
4638
4636
4634
4632
4630
4628
0.00
100.00
200.00
300.00
400.00
500.00
600.00
700.00
800.00
Station (ft)
2003
2005

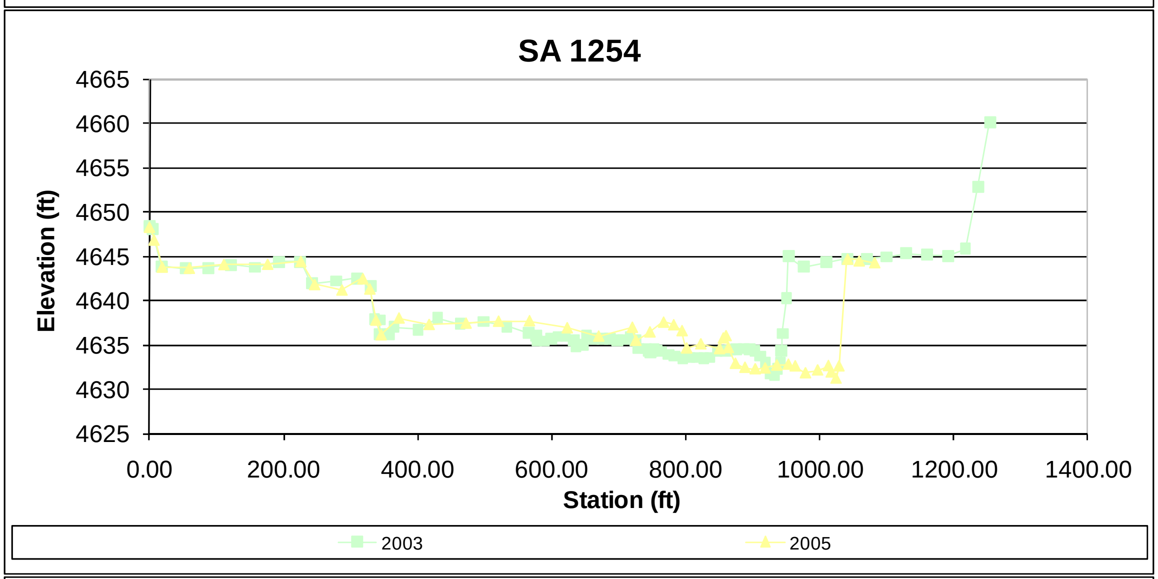

SA 1254
Elevation (ft)
4665
4660
4655
4650
4645
4640
4635
4630
4625
0.00
200.00
400.00
600.00
800.00
1000.00
1200.00
1400.00
Station (ft)
2003
2005

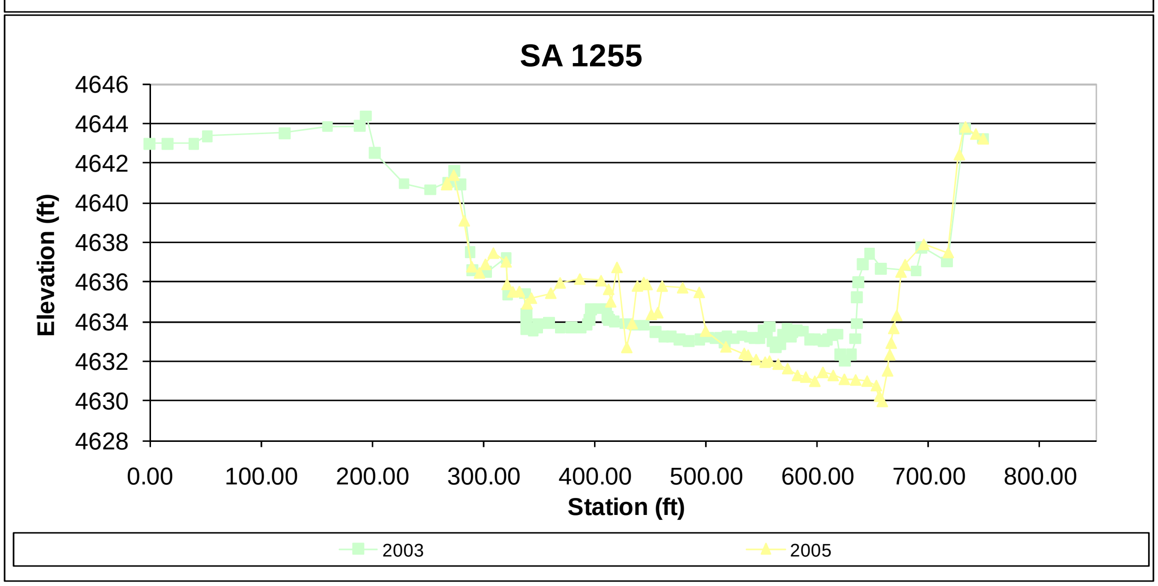

SA 1255
Elevation (ft)
4646
4644
4642
4640
4638
4636
4634
4632
4630
4628
0.00
100.00
200.00
300.00
400.00
500.00
600.00
700.00
800.00
Station (ft)
2003
2005

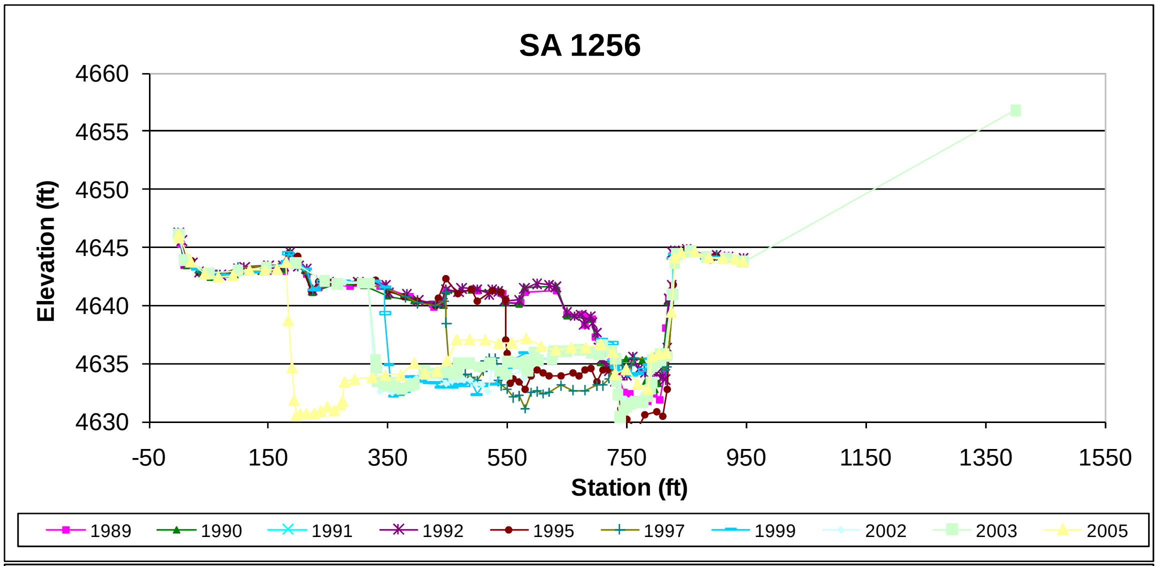
SA 1256
Elevation (ft)
4660
4655
4650
4645
4640
4635
4630
-50
150
350
550
750
950
1150
1350
1550
Station (ft)
1989
1990
1991
1992
1995
1997
1999
2002
2003
2005

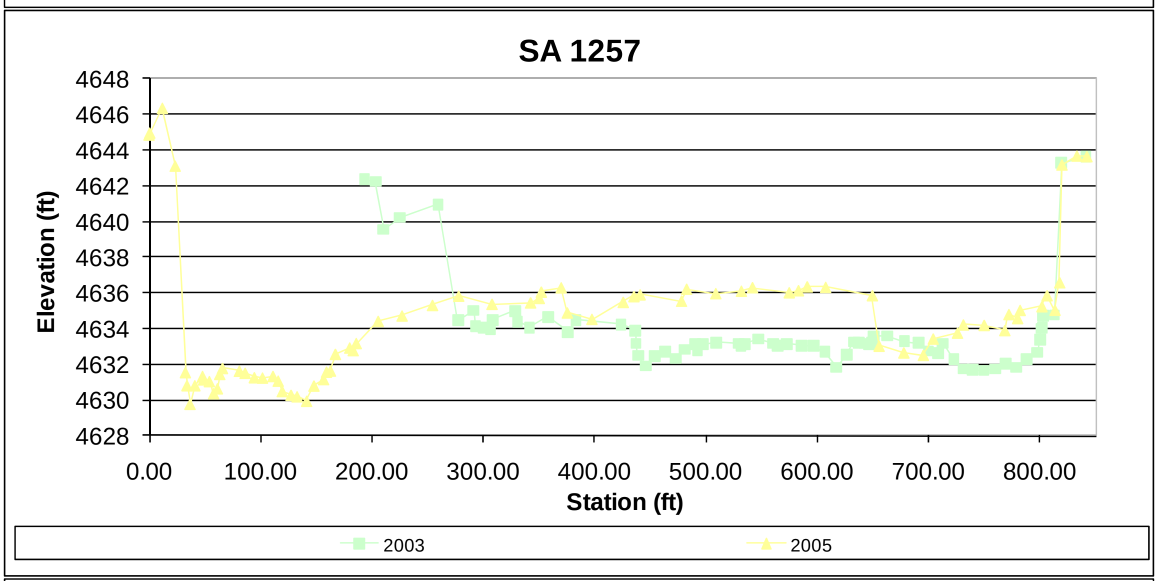
SA 1257
Elevation (ft)
4648
4646
4644
4642
4640
4638
4636
4634
4632
4630
4628
0.00
100.00
200.00
300.00
400.00
500.00
600.00
700.00
800.00
Station (ft)
2003
2005

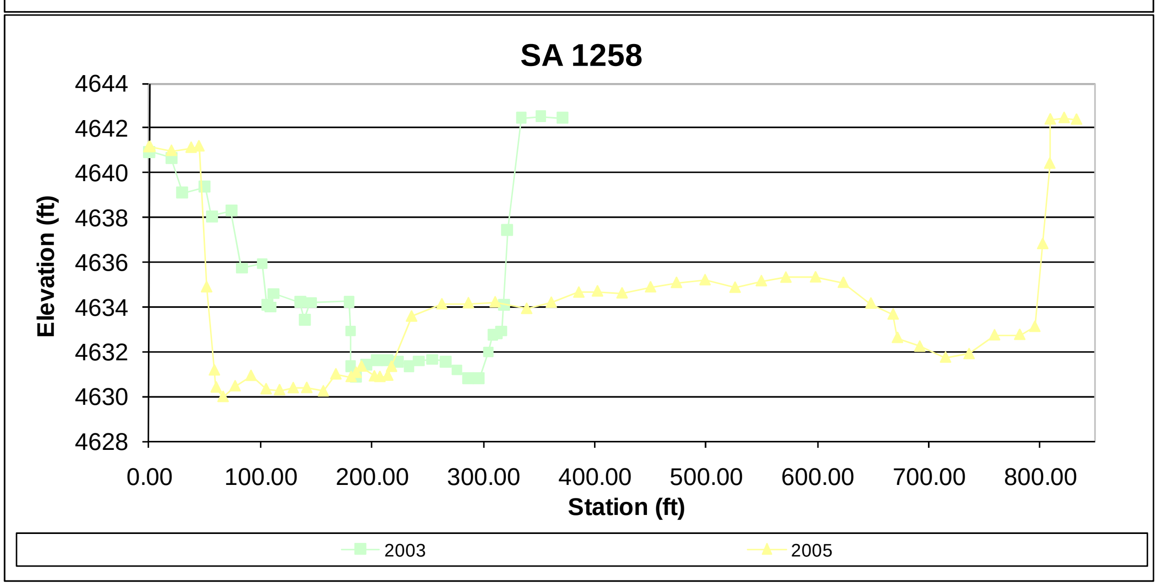
SA 1258
Elevation (ft)
4644
4642
4640
4638
4636
4634
4632
4630
4628
0.00
100.00
200.00
300.00
400.00
500.00
600.00
700.00
800.00
Station (ft)
2003
2005

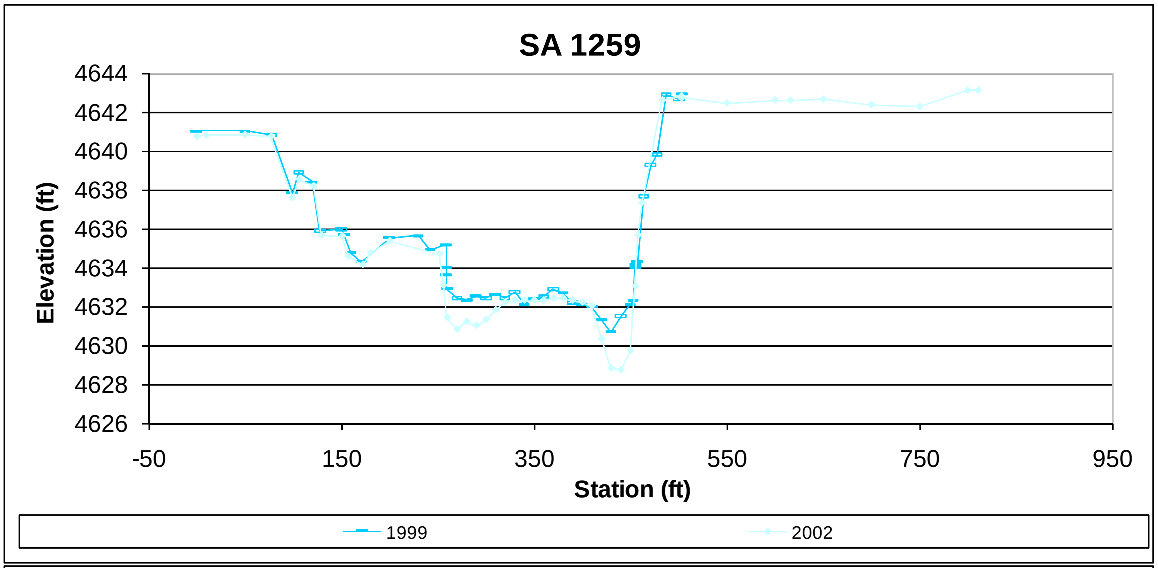
SA 1259
Elevation (ft)
4644
4642
4640
4638
4636
4634
4632
4630
4628
4626
-50
150
350
550
750
950
Station (ft)
1999
2002

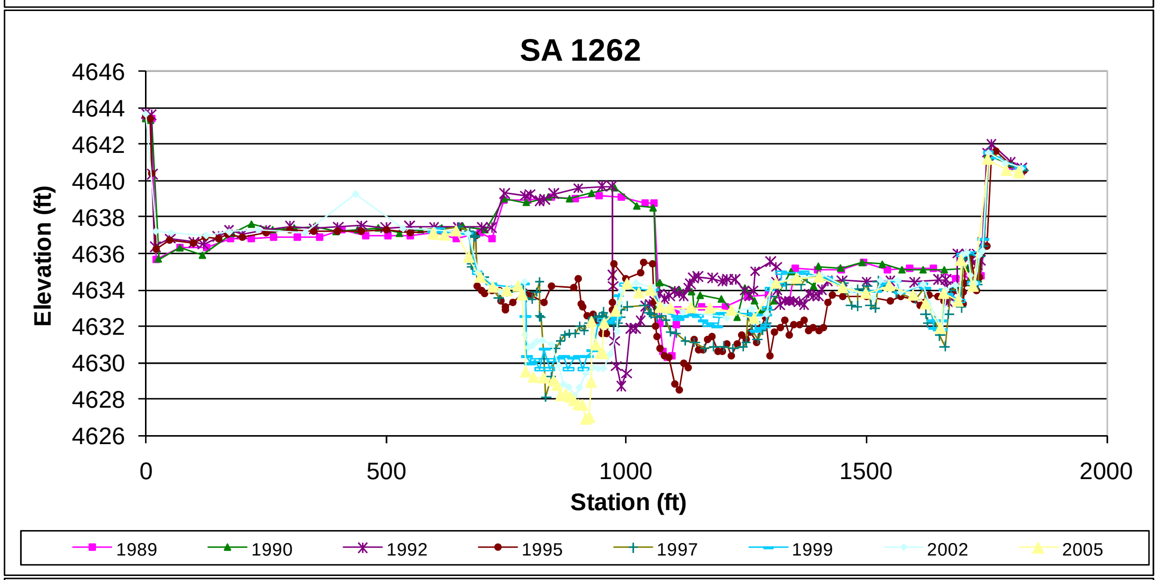
SA 1262
Elevation (ft)
4646
4644
4642
4640
4638
4636
4634
4632
4630
4628
4626
0
500
1000
1500
2000
Station (ft)
1989
1990
1992
1995
1997
1999
2002
2005

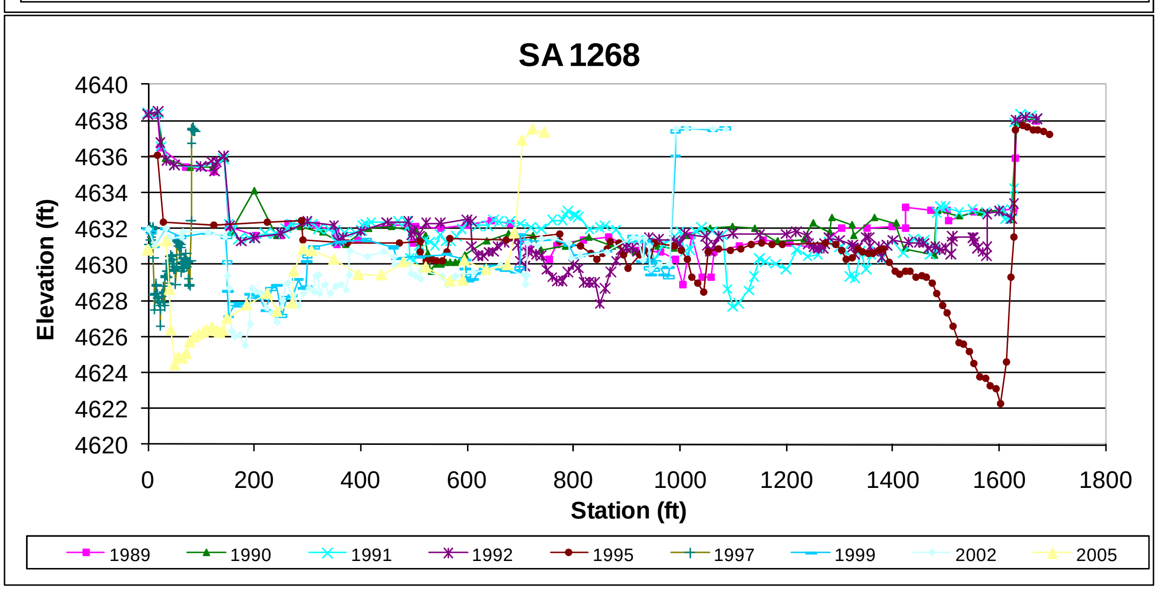
SA 1268
Elevation (ft)
4640
4638
4636
4634
4632
4630
4628
4626
4624
4622
4620
0
200
400
600
800
1000
1200
1400
1600
1800
Station (ft)
1989
1990
1991
1992
1995
1997
1999
2002
2005

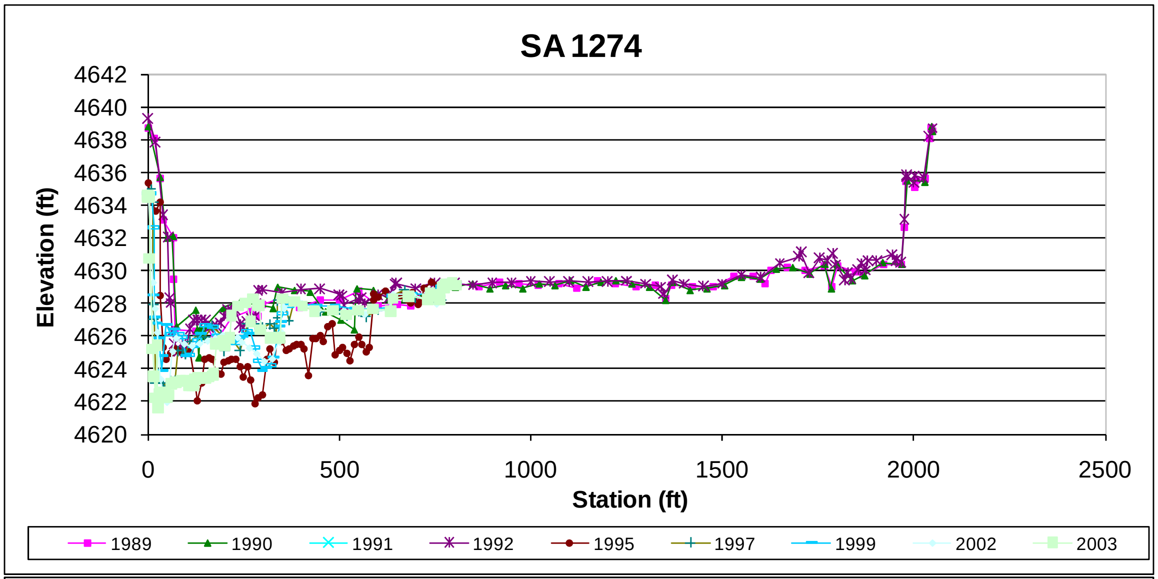
SA 1274
Elevation (ft)
Station (ft)
1989
1990
1991
1992
1995
1997
1999
2002
2003

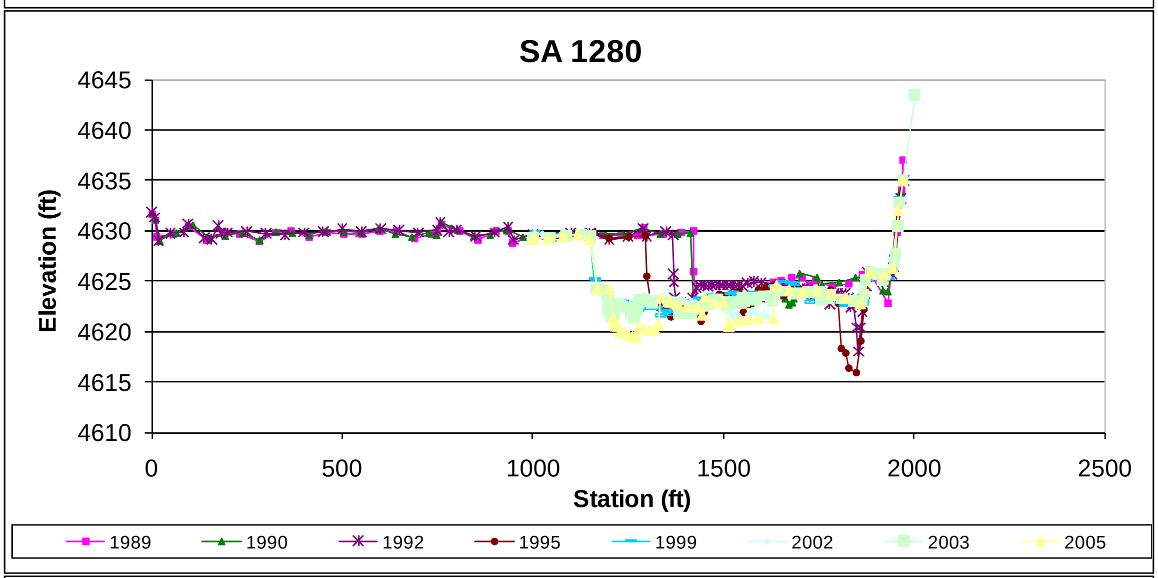
SA 1280
Elevation (ft)
Station (ft)
1989
1990
1992
1995
1999
2002
2003
2005

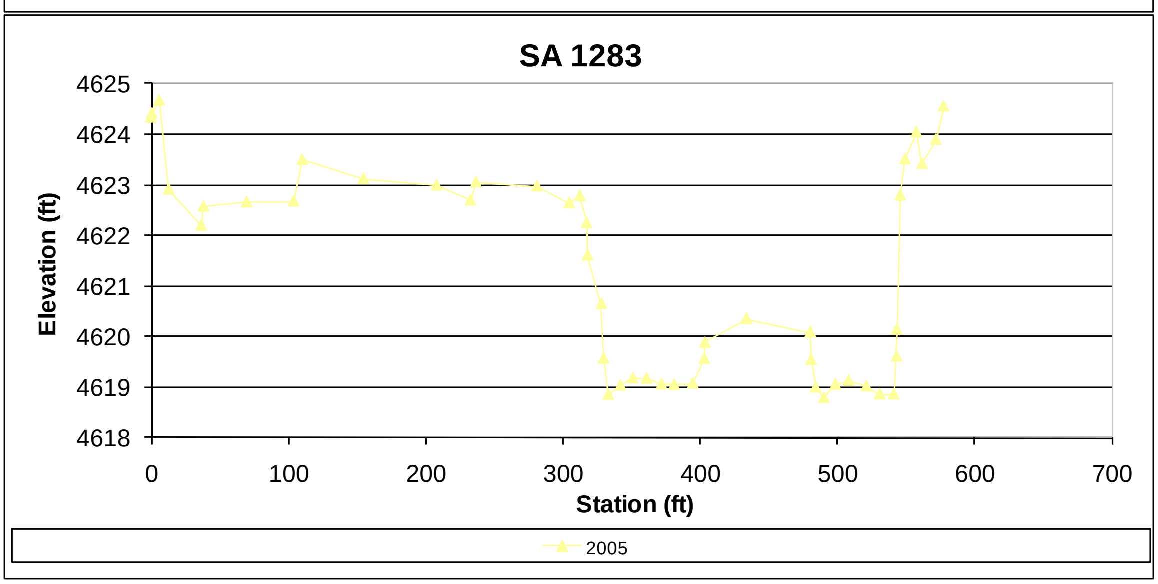
SA 1283
Elevation (ft)
Station (ft)
2005

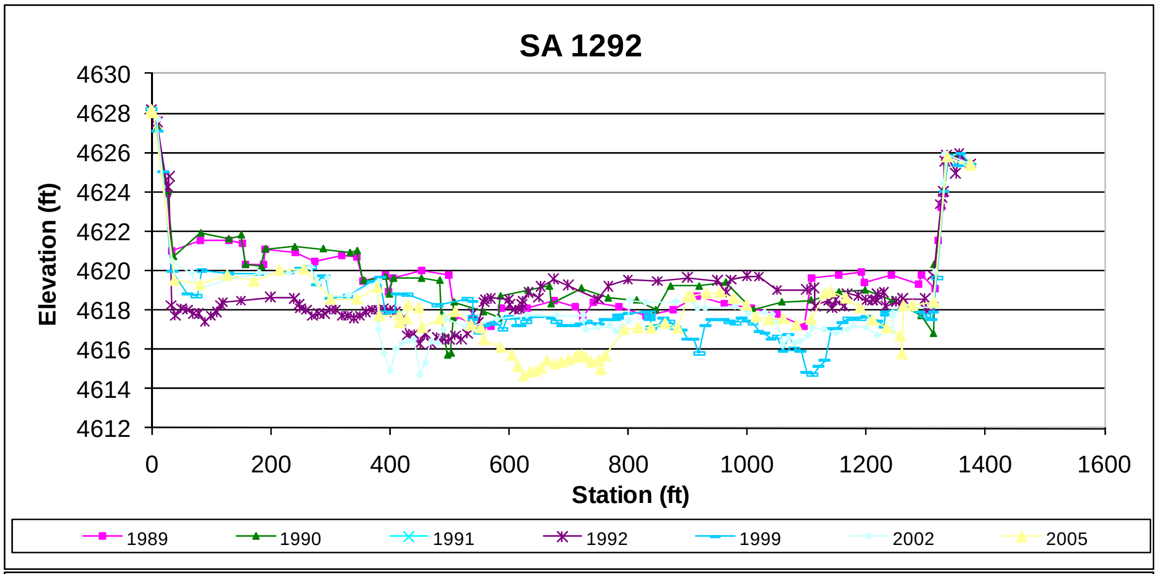
SA 1292
Elevation (ft)
4630
4628
4626
4624
4622
4620
4618
4616
4614
4612
0
200
400
600
800
1000
1200
1400
1600
Station (ft)
1989
1990
1991
1992
1999
2002
2005

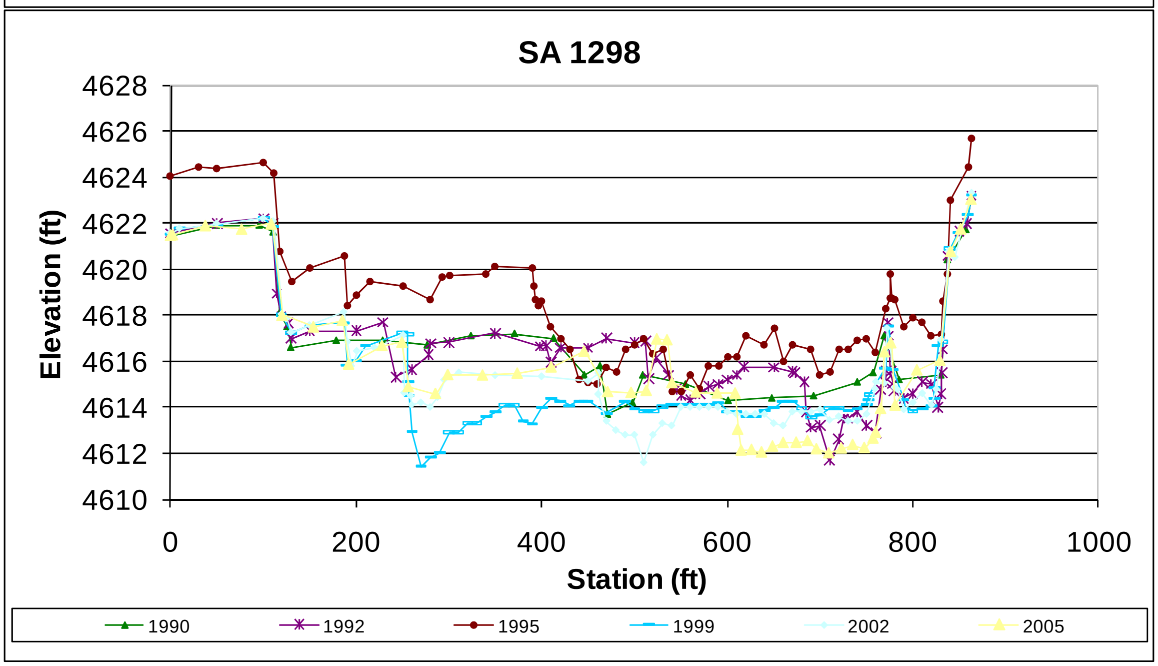
SA 1298
Elevation (ft)
4628
4626
4624
4622
4620
4618
4616
4614
4612
4610
0
200
400
600
800
1000
Station (ft)
1990
1992
1995
1999
2002
2005

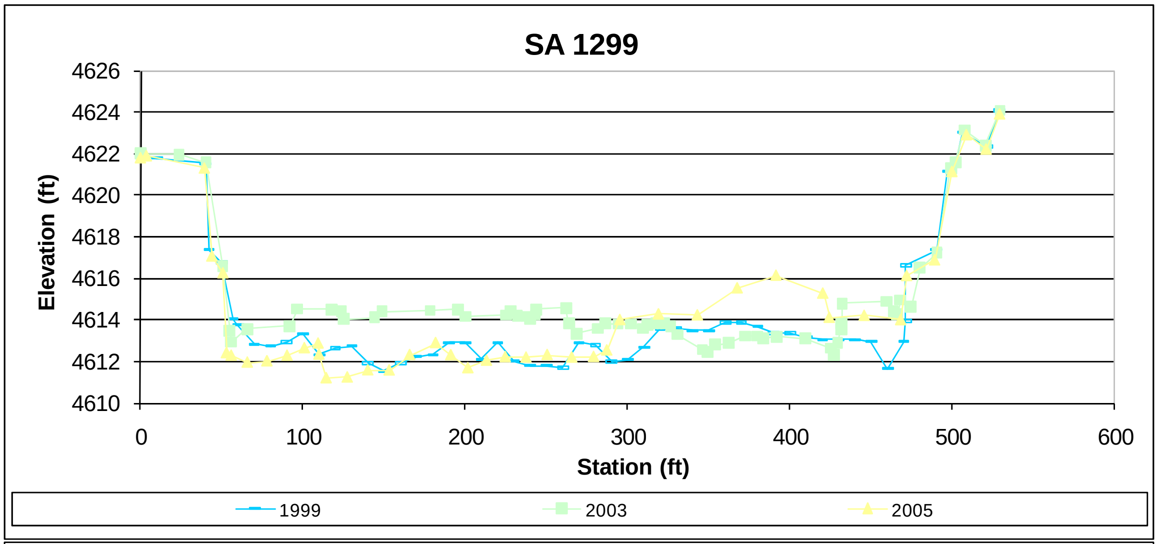
SA 1299
Elevation (ft)
4626
4624
4622
4620
4618
4616
4614
4612
4610
0
100
200
300
400
500
600
Station (ft)
1999
2003
2005

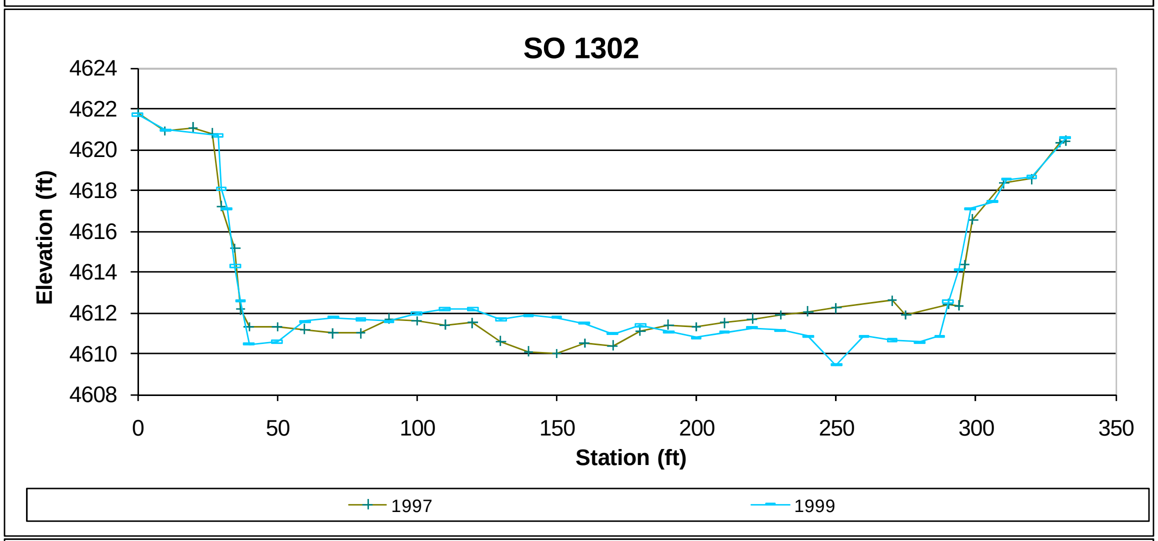
SO 1302
Elevation (ft)
4624
4622
4620
4618
4616
4614
4612
4610
4608
0
50
100
150
200
250
300
350
Station (ft)
1997
1999

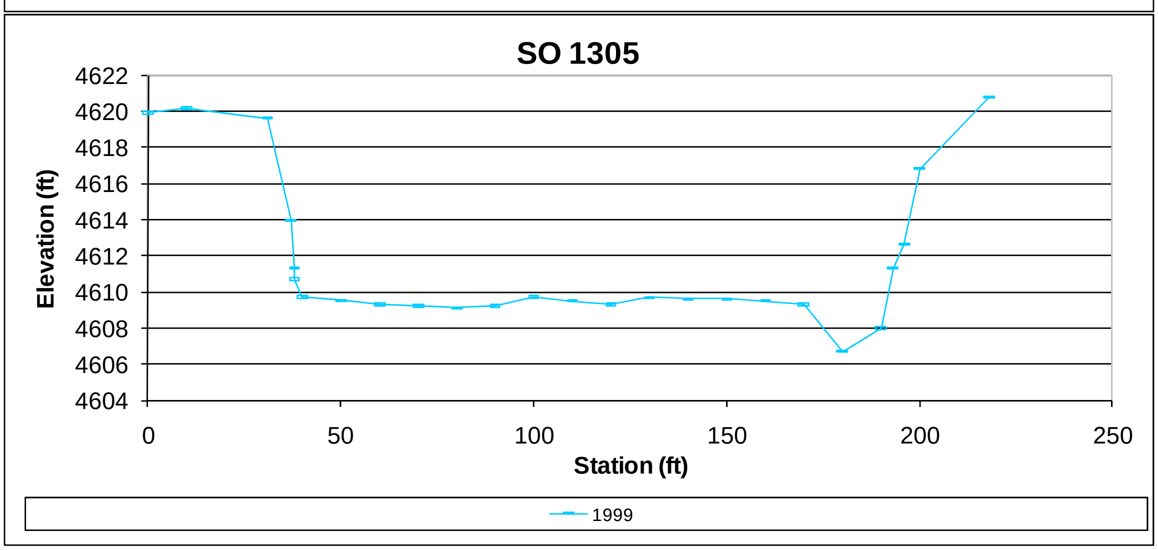
SO 1305
Elevation (ft)
4622
4620
4618
4616
4614
4612
4610
4608
4606
4604
0
50
100
150
200
250
Station (ft)
1999

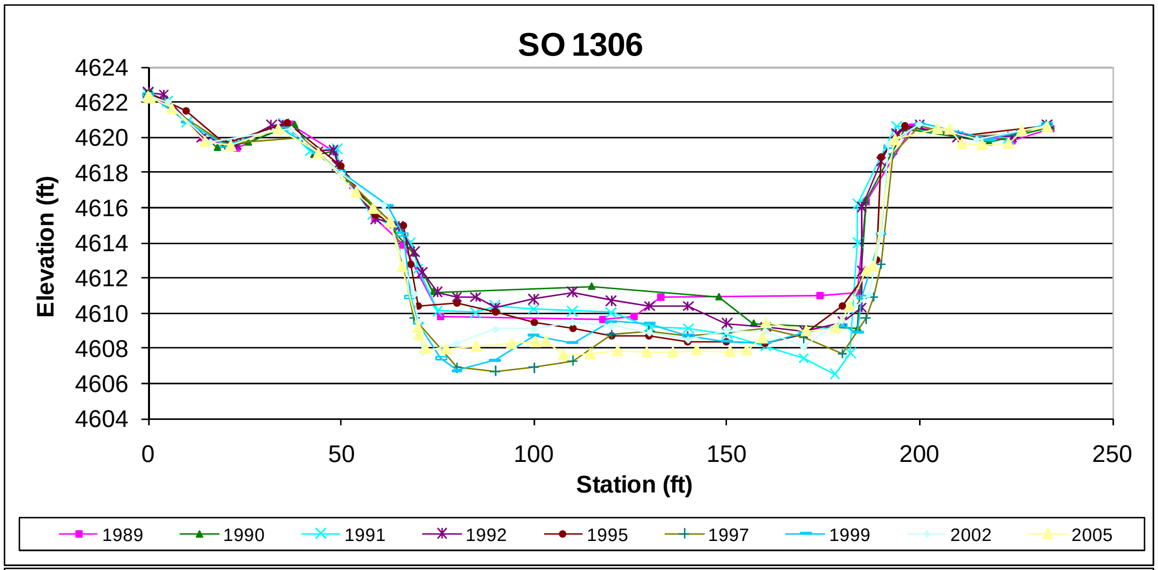
SO 1306
Elevation (ft)
4624
4622
4620
4618
4616
4614
4612
4610
4608
4606
4604
0
50
100
150
200
250
Station (ft)
1989
1990
1991
1992
1995
1997
1999
2002
2005

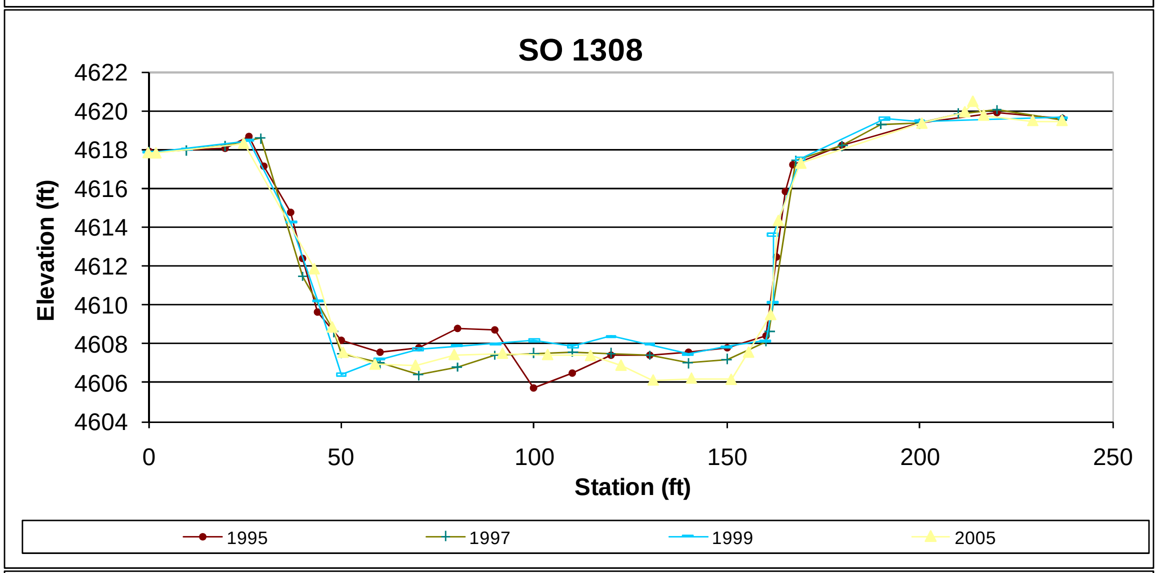
SO 1308
Elevation (ft)
4622
4620
4618
4616
4614
4612
4610
4608
4606
4604
0
50
100
150
200
250
Station (ft)
1995
1997
1999
2005

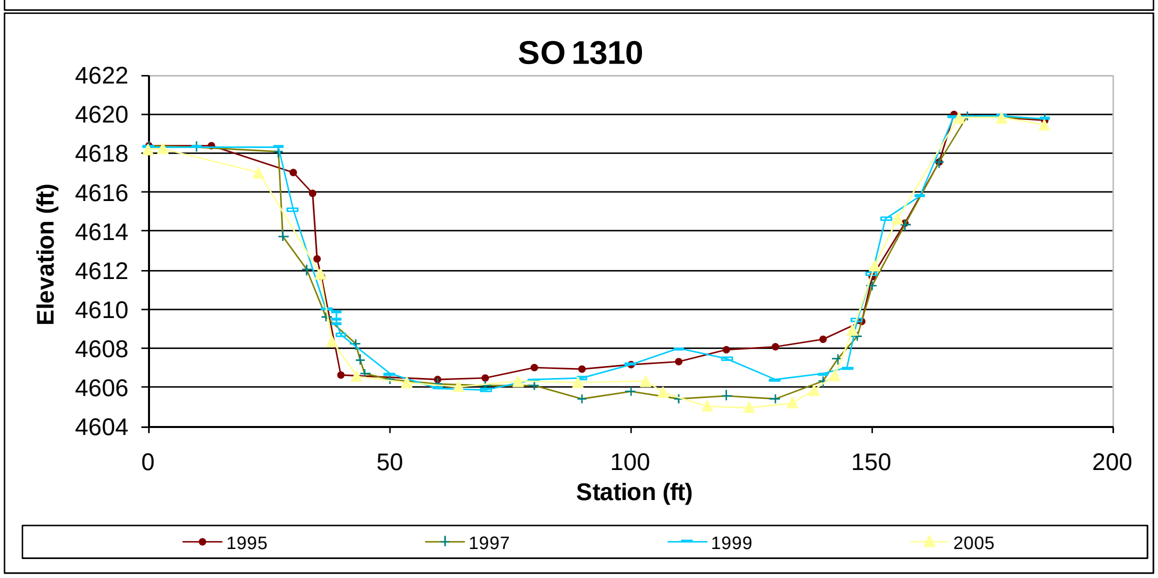
SO 1310
Elevation (ft)
4622
4620
4618
4616
4614
4612
4610
4608
4606
4604
0
50
100
150
200
Station (ft)
1995
1997
1999
2005

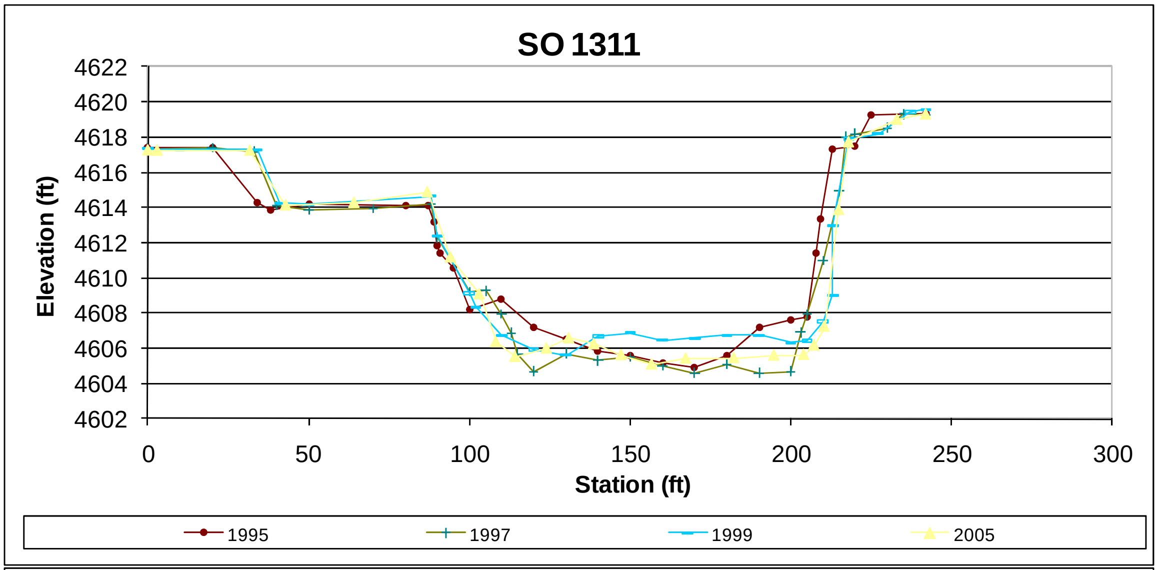
SO 1311
Elevation (ft)
4622
4620
4618
4616
4614
4612
4610
4608
4606
4604
4602
0
50
100
150
200
250
300
Station (ft)
1995
1997
1999
2005

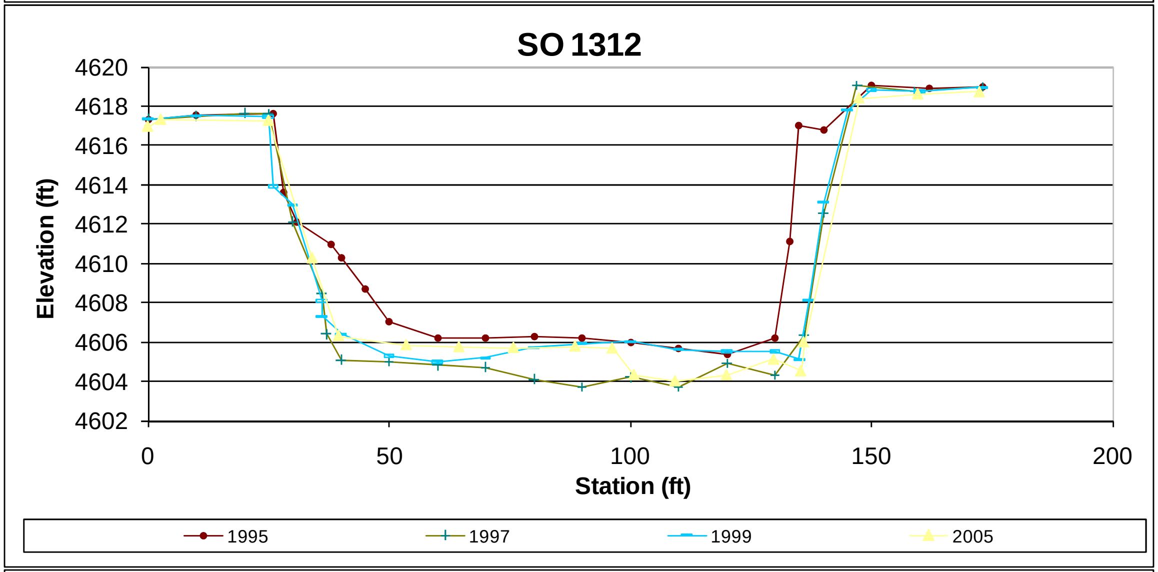
SO 1312
Elevation (ft)
4620
4618
4616
4614
4612
4610
4608
4606
4604
4602
0
50
100
150
200
Station (ft)
1995
1997
1999
2005

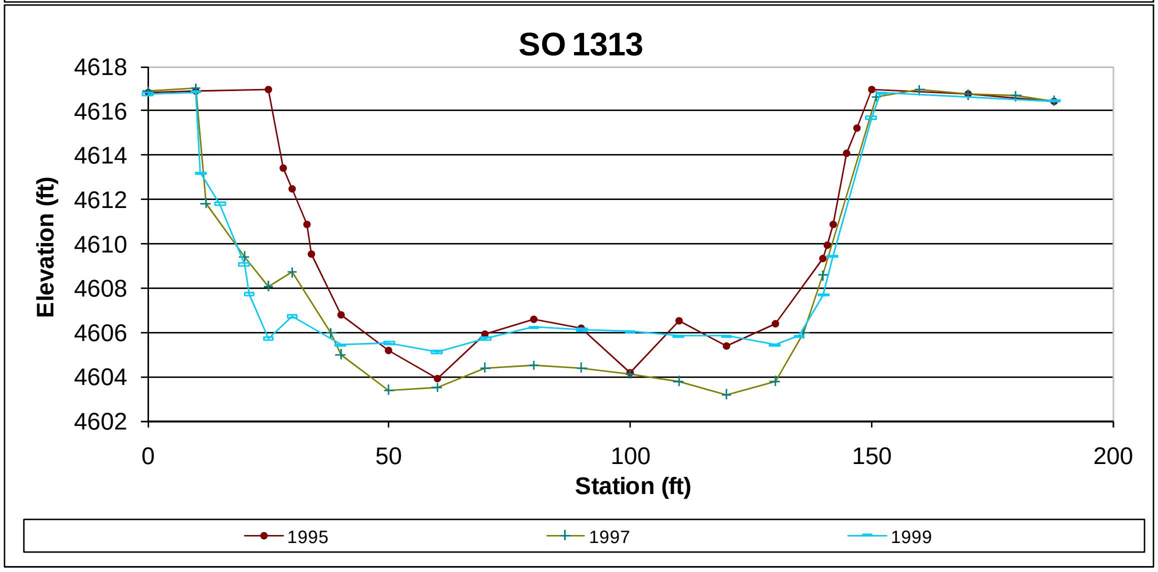
SO 1313
Elevation (ft)
4618
4616
4614
4612
4610
4608
4606
4604
4602
0
50
100
150
200
Station (ft)
1995
1997
1999

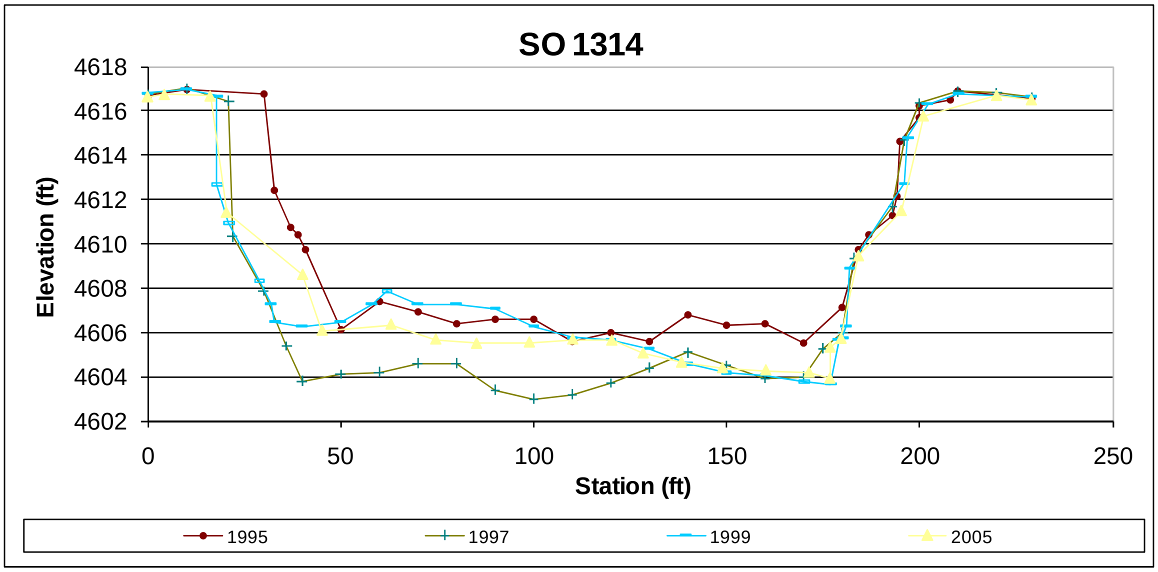
SO 1314
Elevation (ft)
4618
4616
4614
4612
4610
4608
4606
4604
4602
0
50
100
150
200
250
Station (ft)
1995
1997
1999
2005

Appendix C – Aerial Photo Information and Site Photographs

Date	San Acacia Mean Daily Discharge (cfs)	Scale	Notes 1918-2002 (from Novak 2006) 2005: from ArcGIS metadata
1918	No Data	1:12,000	Hand-drafted linens (39 sheets). USBR Albuquerque Area Office. Surveyed in 1918. Published in 1922.
1935	No Data	1:8,00	Black and white photography. USBR Albuquerque Area Office. Flown in 1935. Published in 1936.
1949	No Data	1:5,000	Photo-mosaic. J-Ammann Photogrammetric Engineers, San Antonio, TX. USBR Albuquerque Area Office.
March 1962	25 cfs	1:4,800	Photo-mosaic. Abram Aerial Survey Corp, Lansing, MI. USBR Albuquerque Area Office.
April 1972	4 cfs	1:4,800	Photo-mosaic. Limbaugh Engineers, Inc., Albuquerque, NM. USBR Albuquerque Area Office.
March 1985	1900 cfs	1:4,800	Orthophoto. M&I Consulting Engineers, Fort Collins, CO. Aero-Metric Engineering, Sheboygan, MN. USBR Albuquerque Area Office.
February 1992	1020 cfs	1:4,800	Ratio-rectified photo-mosaic. Koogle and Poules Engineering, Albuquerque, NM. USBR Albuquerque Area Office.
February 2001	770 cfs	1:4,800	Ratio-rectified photo-mosaic. Pacific Western Technologies, Ltd., Albuquerque, NM. USBR Albuquerque Area Office.
March 2002	310 cfs	1:4,800	Digital ortho-imagery. Pacific Western Technologies, Ltd., Albuquerque, NM. USBR Albuquerque Area Office.
April 2005	2270 cfs	1:4,800	Digital ortho-rectified imagery. Aero-Metric, Inc., Fort Collins, Co. USBR Albuquerque Area Office.
January 2006		1:4,800	Digital ortho-rectified imagery. Aero-Metric, Inc., Fort Collins, Co. USBR Albuquerque Area Office.

Upstream of San Acacia Diversion Dam, with antidune formation

Downstream of San Acacia Diversion Dam

Bank Erosion along San Acacia Reach

Riprap to protect bank Erosion

Looking downstream at Escondida Bridge

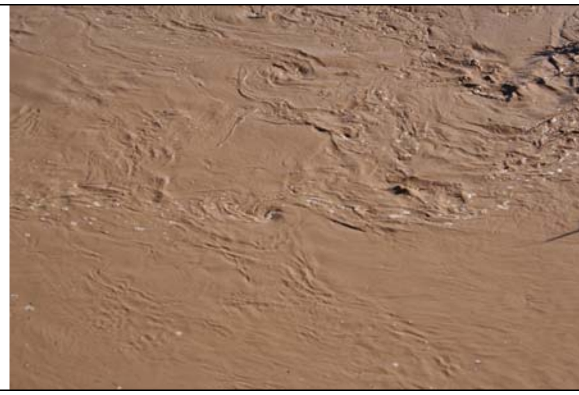

Dune formation near Escondida Bridge

Appendix D – HEC-RAS Hydraulic Model Output

2002 Agg/Deg Lines
2002 Range Lines
2005 Range Lines

2002 Agg/Deg Analysis at 5000 cfs

Subreach	River Sta	Agg & Deg #	Min Ch El	W.S. Elev	Crit W.S.	E.G. Elev	E.G. Slope	Vel Chnl	Flow Area	Top Width	Froude #
			(ft)	(ft)	(ft)	(ft)	(ft/ft)	(ft/s)	(sq ft)	(ft)	
Reach 1	585	1207	4652.25	4658.32		4658.38	0.00009	2.02	2474	501.47	0.16
	584	1208	4652.43	4657.73		4658.25	0.000761	5.77	866.38	181.78	0.47
	583	1209	4650.82	4657.46		4657.91	0.000516	5.42	922.18	153.77	0.39
	582	1210	4651.05	4656.85		4657.51	0.000854	6.56	761.97	141	0.5
	581	1211	4650.7	4655.75	4654.65	4656.86	0.001704	8.47	590.17	125.44	0.69
	580	1212	4650.14	4655.73	4653.23	4656.17	0.00056	5.29	944.62	176.78	0.4
	579	1213	4649.66	4655.64	4652.5	4655.88	0.0003	3.95	1267.26	231.69	0.3
	578	1214	4650.28	4654.93	4653.52	4655.67	0.001197	6.89	725.63	162.05	0.57
	577	1215	4648.41	4655.01	4651.57	4655.32	0.000354	4.49	1112.53	188.94	0.33
	576	1216	4648.03	4654.58	4651.67	4655.07	0.000671	5.62	889.55	172.61	0.44
	575	1217	4648.7	4654.29	4651.85	4654.72	0.000673	5.27	949.18	206.38	0.43
	574	1218	4648.62	4654.04	4651.51	4654.43	0.000515	5.01	998.57	190.57	0.39
	573	1219	4649.04	4652.67	4652.22	4653.85	0.002631	8.73	573.81	194.96	0.82
	572	1220	4647.56	4653.05	4649.89	4653.25	0.000269	3.56	1404.13	276.47	0.28
	571	1221	4647.1	4652.92	4649.65	4653.11	0.000264	3.51	1426.35	281.93	0.27
Reach 2	570	1222	4648.63	4652.47	4651.14	4652.88	0.000962	5.1	986.84	313.04	0.49
	569	1223	4647.47	4652.22	4650.08	4652.5	0.000531	4.26	1280.28	374.53	0.38
	568	1224	4647.71	4650.7	4650.69	4651.87	0.004303	8.81	686.01	342.92	0.99
	567	1225	4647.04	4651.04		4651.15	0.000323	2.64	1903.72	712.5	0.28
	566	1226	4646.84	4650.72	4648.81	4650.96	0.000486	3.93	1270.9	340.16	0.36
	565	1227	4644.67	4650.32	4647.96	4650.69	0.000585	4.87	1026.3	225.98	0.4
	564	1228	4645.54	4649.61	4648.45	4650.24	0.001282	6.36	786.16	211.13	0.58
	563	1229	4644.67	4649.03	4647.63	4649.66	0.001163	6.37	784.68	194.25	0.56
	562	1230	4644	4648.87	4646.79	4649.16	0.000518	4.34	1150.77	277.45	0.38
	561	1231	4643.42	4648.63	4646.52	4648.92	0.000507	4.34	1150.97	272.48	0.37
	560	1232	4642.82	4647.98	4646.07	4648.57	0.000857	6.18	809.16	165.92	0.49
	559	1233	4642.03	4647.62	4645.46	4648.14	0.000755	5.77	866.26	178.18	0.46
	558	1234	4641.88	4647.42	4644.89	4647.68	0.000751	4.05	1235.09	434.43	0.42
Subreach	River Sta	Agg & Deg #	Min Ch El	W.S. Elev	Crit W.S.	E.G. Elev	E.G. Slope	Vel Chnl	Flow Area	Top Width	Froude #
			(ft)	(ft)	(ft)	(ft)	(ft/ft)	(ft/s)	(sq ft)	(ft)	

	557	1235	4642.53	4647.24	4645.3	4647.38	0.000382	2.99	1681.59	592.64	0.31
	556	1236	4641.74	4647.2		4647.27	0.000099	2.13	2352.14	478.64	0.17
	555	1237	4641.3	4646.67		4647.12	0.000851	5.37	930.64	233.76	0.47
	554	1238	4640.82	4646.04		4646.67	0.000882	6.35	787.08	156.6	0.5
Reach 2	553	1239	4641.1	4644.81	4644.48	4645.86	0.002868	8.24	607.11	200.43	0.83
	552	1240	4639.79	4644.67		4645.08	0.000634	5.13	975.68	214.06	0.42
	551	1241	4640.05	4644.75		4644.85	0.000167	2.52	1987.93	466.13	0.21
	550	1242	4638.94	4644.7	4641.24	4644.78	0.000115	2.17	2304.29	505.58	0.18
	549	1243	4639.6	4644.47		4644.68	0.000312	3.66	1366.52	291.03	0.3
	548	1245	4638.12	4644.34		4644.52	0.000296	3.43	1456.17	326.28	0.29
	547	1246	4638.41	4643.69		4644.26	0.000858	6.06	824.74	173.14	0.49
	546	1247	4637.8	4641.82	4641.82	4643.4	0.004065	10.09	506.98	178.27	1
	545	1248	4635.47	4641.14		4641.62	0.000748	5.57	896.91	191.01	0.45
	544	1249	4635.92	4640.91	4639.21	4641.18	0.000797	4.23	1181.03	408.57	0.44
	543	1250	4636.13	4640.26	4639.51	4640.64	0.001545	4.95	1010.22	454.74	0.59
	542	1251	4635.13	4639.76	4638.73	4640.03	0.000976	4.14	1208.46	500.66	0.47
	541	1252	4636.04	4639.04	4638.07	4639.46	0.001579	5.2	961.92	409.49	0.6
	540	1253	4635.16	4638.42	4637.29	4638.73	0.001378	4.43	1127.73	550.06	0.55
	539	1254	4634.58	4638.12	4636.47	4638.28	0.000532	3.18	1570.03	614.38	0.35
Reach 3	538	1255	4634.68	4637.39	4636.74	4637.82	0.001792	5.27	948.28	435.38	0.63
	537	1256	4632.74	4637.27	4635.13	4637.41	0.000328	2.99	1670.14	496.62	0.29
	536	1257	4633.46	4637.16	4634.96	4637.26	0.000221	2.58	1941.03	541.95	0.24
	535	1258	4631.78	4636.45	4635.16	4636.99	0.001204	5.89	848.51	242.52	0.56
	534	1259	4632.25	4635.79	4634.99	4636.28	0.001552	5.62	890.15	333.02	0.61
	533	1260	4631.52	4635.58	4633.7	4635.74	0.000568	3.17	1578.07	655.13	0.36
	532	1261	4630.98	4635.33	4633.02	4635.45	0.000607	2.81	1782.01	932.28	0.36
	531	1262	4631.12	4634.53	4633.98	4634.96	0.00196	5.31	1047.76	748.58	0.65
	530	1263	4630.92	4634.19	4633.07	4634.37	0.000689	3.4	1592.69	879.31	0.39
	529	1264	4630.69	4633.61	4632.85	4633.88	0.001799	4.18	1195.84	778.81	0.59
Subreach	**River Sta**	**Agg & Deg #**	**Min Ch El**	**W.S. Elev**	**Crit W.S.**	**E.G. Elev**	**E.G. Slope**	**Vel Chnl**	**Flow Area**	**Top Width**	**Froude #**
			(ft)	**(ft)**	**(ft)**	**(ft)**	**(ft/ft)**	**(ft/s)**	**(sq ft)**	**(ft)**	
	528	1265	4630.17	4633.13	4632.36	4633.27	0.000904	2.97	1685.27	1098.48	0.42
	527	1266	4630.3	4632.57		4632.75	0.00142	3.39	1474.82	1102.78	0.52
	526	1267	4628.65	4632.33	4630.28	4632.42	0.000379	2.33	2158	1077.8	0.29

	525	1268	4629.56	4631.78	4631.18	4632.01	0.001464	3.82	1344.4	927.05	0.54
	524	1269	4628.13	4631.23	4630.14	4631.4	0.000704	3.38	1996.58	1628.65	0.4
	523	1270	4628.73	4630.36	4630.05	4630.74	0.002555	5.02	1227.36	1055.34	0.71
	522	1271	4627.04	4630.1	4628.46	4630.25	0.000397	3.04	1869.55	959.13	0.31
	521	1272	4627.53	4629.76	4628.8	4629.96	0.000818	3.61	1453.65	814.95	0.43
	520	1273	4627.09	4629.44	4628.32	4629.57	0.000614	2.89	1731.57	881.45	0.36
	519	1274	4625.31	4629.02	4627.29	4629.2	0.000876	3.45	1447.67	737.95	0.43
	518	1275	4625.39	4628.64	4627.26	4628.78	0.0007	3.01	1712.5	1063.42	0.38
	517	1276	4625	4627.62	4627.37	4628.07	0.002612	5.62	1430.9	1344.03	0.74
	516	1277	4624.53	4627.08	4626.03	4627.3	0.000817	3.84	1617.12	1163.01	0.43
	515	1278	4624.18	4626.5	4625.84	4626.73	0.001511	3.82	1309.37	870.03	0.55
	514	1279	4623.2	4625.92	4625.05	4626.08	0.000955	3.2	1564.67	950.56	0.44
Reach 3	513	1280	4622.85	4625.59	4624.31	4625.73	0.000521	2.92	1712.4	755.82	0.34
	512	1281	4622.46	4625.17	4624	4625.41	0.000825	3.87	1301.28	597.93	0.44
	511	1282	4621.84	4624.56	4623.79	4624.83	0.001476	4.21	1187.49	659.85	0.55
	510	1283	4620.5	4623.94	4623.04	4624.2	0.001068	4.13	1217.12	659.59	0.49
	509	1284	4620.9	4622.81	4622.64	4623.25	0.003491	5.32	939.75	703.16	0.81
	508	1285	4619.58	4622.55	4621.12	4622.66	0.000426	2.61	1912.38	855.16	0.31
	507	1286	4617.7	4622.48	4619.14	4622.54	0.000127	1.87	2672.63	792.05	0.18
	506	1287	4619.45	4622.1	4621.39	4622.36	0.001307	4.08	1226.88	652.93	0.52
	505	1288	4618.88	4621.26	4620.67	4621.55	0.001864	4.32	1158.55	738.61	0.61
	504	1289	4618.6	4620.29	4619.79	4620.53	0.0018	3.96	1266.68	901.73	0.59
	503	1290	4617.49	4620.01	4618.73	4620.11	0.000431	2.44	2052.13	1041.46	0.3
	502	1291	4617.69	4619.75	4618.84	4619.86	0.000602	2.71	1856.1	1038.36	0.35
	501	1292	4617.24	4619.47	4618.42	4619.58	0.000523	2.57	1957.69	1101.94	0.33
	500	1293	4616.29	4619.23	4617.94	4619.35	0.000459	2.78	1972.3	1175.95	0.32
Subreach	**River Sta**	**Agg & Deg #**	**Min Ch El**	**W.S. Elev**	**Crit W.S.**	**E.G. Elev**	**E.G. Slope**	**Vel Chnl**	**Flow Area**	**Top Width**	**Froude #**
			(ft)	**(ft)**	**(ft)**	**(ft)**	**(ft/ft)**	**(ft/s)**	**(sq ft)**	**(ft)**	
	499	1294	4616.14	4618.99	4617.49	4619.11	0.000431	2.76	1809.55	751.24	0.31
	498	1295	4615.55	4618.61	4617.5	4618.82	0.000817	3.66	1367.63	602.28	0.43
Reach 3	497	1296	4615.01	4618.58	4616.53	4618.63	0.000156	1.94	2582.8	854.42	0.2
	496	1297	4615	4618.48	4616.6	4618.55	0.000195	2.1	2385.94	827.78	0.22
	495	1298	4613.46	4618.42	4615.38	4618.47	0.000114	1.87	2669.63	731.18	0.17
	494	1299	4613.81	4618.3	4615.44	4618.4	0.000167	2.57	1948.49	444.65	0.22

Reach 4	493	1300	4613.33	4618.16	4615.26	4618.31	0.000217	3.06	1631.93	345	0.25
	492	1301	4611.44	4618.14	4613.47	4618.23	0.000088	2.39	2088.52	321.95	0.17
	491	1302	4611.11	4618.07	4613.31	4618.18	0.000098	2.58	1941.03	295.56	0.18
	490	1303	4612.83	4617.85	4615.11	4618.08	0.000327	3.84	1304.17	273.84	0.31
	489	1304	4611.31	4617.73	4613.96	4617.92	0.000244	3.49	1432.27	271.02	0.27
	488	1305	4611.65	4617.24	4614.86	4617.71	0.000618	5.51	906.91	172.91	0.42
	487	1306	4609.98	4616.92	4613.76	4617.43	0.000525	5.7	877.49	136.61	0.4
	486	1307	4610.74	4616.58	4614.29	4617.11	0.000806	5.81	860.17	184.69	0.47
	485	1308	4609.69	4616.4	4613.09	4616.79	0.000405	4.98	1004.52	159.53	0.35
	484	1309	4609.7	4615.92	4613.37	4616.5	0.000657	6.09	820.72	138.55	0.44
	483	1310	4608.35	4615.66	4612.41	4616.18	0.000519	5.77	867.06	132.31	0.4
	482	1311	4608.82	4615.31	4612.69	4615.84	0.000822	5.83	857.7	185.75	0.48
	481	1312	4608.27	4614.28	4612.4	4615.18	0.001102	7.59	658.41	116.45	0.56
	480	1313	4607.93	4613.99	4611.53	4614.57	0.000687	6.11	817.92	140.71	0.45
	479	1314	4608.96	4613.15	4612.13	4613.97	0.001559	7.25	689.58	175.69	0.64
	478	1315	4607.18	4612.79	4610.61	4613.38	0.000775	6.18	809.06	152.32	0.47
	477	1316	4607.64	4611.67	4611.02	4612.77	0.002198	8.4	595.15	157.09	0.76
	476	1317	4606.5	4609.77	4609.77	4611.35	0.004041	10.11	494.79	154.91	1

2002 Range Line Analysis at 5000 cfs

Subreach	River Sta	Agg & Deg #	Min Ch El (ft)	W.S. Elev (ft)	Crit W.S. (ft)	E.G. Elev (ft)	E.G. Slope (ft/ft)	Vel Chnl (ft/s)	Flow Area (sq ft)	Top Width (ft)	Froude #
Reach 1	585	1207	4650.9	4657.14		4657.25	0.000234	2.74	1823.32	480.53	0.25
	584	1208	4649.5	4656.57		4657.05	0.000629	5.59	894.58	169.81	0.43
	583	1209	4648.1	4656.14		4656.71	0.000704	6.08	822.74	149.24	0.46
	582	1210	4648.4	4655.55		4656.25	0.000855	6.72	744.54	133.51	0.5
	580	1212	4647.6	4654.78		4655.34	0.000781	5.98	843.01	176.26	0.48
	577	1215	4647.4	4653.13		4653.98	0.001553	7.42	674.07	165.6	0.65
	574	1218	4645.9	4652.16		4652.58	0.000551	5.16	969.23	187.17	0.4
	571	1221	4646	4650.86		4651.37	0.001245	5.75	869.84	265.64	0.56
Reach 2	567	1225	4643.9	4649.65		4649.86	0.000494	3.67	1407.96	483.31	0.35
	561	1231	4641	4646.9		4647.59	0.001309	6.64	753.02	191.64	0.59
	556	1236	4639.5	4644.64		4644.91	0.0008	4.16	1201.32	427.79	0.44
	549	1243	4635.4	4642.28		4642.59	0.000568	4.45	1124.39	280.34	0.39
	547	1246	4635.5	4640.78		4641.68	0.001531	7.59	658.86	151.55	0.64
	541	1252	4632.98	4638.27		4638.59	0.000715	4.55	1100.11	315.23	0.43
	537	1256	4631.7	4637.15		4637.34	0.00054	3.49	1431.45	492.46	0.36
Reach 3	534	1259	4628.7	4635.68		4636.12	0.001195	5.35	934.85	329.17	0.54
	531	1262	4628.19	4634.18		4634.47	0.001059	4.36	1231.66	667.18	0.49
	525	1268	4625.5	4631.49		4631.66	0.000868	3.27	1532.35	852.46	0.43
	524	1269	4626.6	4630.96		4631.16	0.00079	3.54	1410.67	635.04	0.42
	519	1274	4621.94	4628.35		4628.61	0.00128	4.04	1238.62	660	0.52
	513	1280	4621	4625.04		4625.24	0.000899	3.54	1413.34	703.27	0.44
	501	1292	4614.7	4619.01		4619.18	0.001089	3.27	1526.95	984.67	0.46
	495	1298	4611.6	4617.98		4618.05	0.00019	2.22	2253.65	700.83	0.22
Reach 4	487	1306	4607.8	4616.45		4616.91	0.000432	5.45	916.74	131.6	0.36
	373	1320	4601.9	4607.71	4607.71	4609.54	0.003995	10.86	460.44	126.38	1

2005 Range Line Analysis at 5000 cfs

Subreach	River Sta	Agg & Deg #	Min Ch El (ft)	W.S. Elev (ft)	Crit W.S. (ft)	E.G. Elev (ft)	E.G. Slope (ft/ft)	Vel Chnl (ft/s)	Flow Area (sq ft)	Top Width (ft)	Froude #

	585	1207	4652.53	4659.48		4659.75	0.000692	4.22	1183.56	368.44	0.42
	584	1208	4651.55	4658.9		4659.42	0.000613	5.8	896.31	171.11	0.43
	583	1209	4650.69	4658.28		4659.02	0.00091	6.91	723.58	128.79	0.51
	582	1210	4649.9	4657.79		4658.48	0.000833	6.66	750.83	130.92	0.49
Reach 1	580	1212	4650.5	4657.3	4654.58	4657.73	0.000513	5.23	956.24	172.39	0.39
	577	1215	4649.44	4656.2		4656.84	0.000908	6.4	787.78	170.99	0.51
	574	1218	4649.55	4655.1		4655.58	0.000696	5.51	908.16	189.7	0.44
	572	1220	4648.68	4653.62	4653.01	4654.41	0.002088	7.16	698.67	234.58	0.72
	571	1221	4646.47	4653.47	4651.17	4653.76	0.000447	4.3	1172.79	276.46	0.35
	569	1223	4647.56	4652.41	4651.03	4652.99	0.001065	6.15	903.42	286.39	0.54
	567	1225	4645.89	4652.12	4649.43	4652.31	0.000317	3.58	1506.18	498.48	0.3
	566	1226	4645.53	4651.98		4652.12	0.000183	3	1694.36	361.14	0.23
	565	1227	4644.51	4650.37	4649.93	4651.74	0.002941	9.42	531.05	144.78	0.87
	564	1228	4643.2	4650.48		4650.9	0.000577	5.19	963.09	190.07	0.41
	563	1229	4643.78	4649.92		4650.53	0.000864	6.29	815.25	177.53	0.5
Reach 2	561	1231	4642.75	4648.28		4649.26	0.001792	7.96	659.27	188.93	0.69
	556	1236	4642.05	4647.83		4647.94	0.000164	2.72	1986.01	489.6	0.22
	555	1237	4640.25	4647.1		4647.68	0.000841	6.15	819.31	181.08	0.49
	554	1238	4640.73	4646.68		4647.29	0.000747	6.24	805.24	152.97	0.47
	550	1242	4638.65	4644.44		4645.1	0.001494	6.96	1090.97	330.53	0.62
	549	1243	4638.79	4644.21		4644.52	0.000528	4.48	1115.91	260.92	0.38
	547	1246	4637.23	4642.87		4643.58	0.001077	6.81	734.43	153.67	0.55
	541	1252	4634.48	4641.01		4641.26	0.000448	3.99	1272.72	332.36	0.35
	540	1253	4632.71	4640.36	4638.57	4640.82	0.000838	5.45	933.52	361.2	0.47
Reach 3	539	1254	4633.59	4639.94		4640.19	0.001058	4.02	1242.87	574.93	0.48
	538	1255	4632.38	4639.27	4637.16	4639.72	0.000651	5.46	1133.19	369.74	0.43
	537	1256	4632.92	4638.9		4639.22	0.001202	4.53	1103.37	469.24	0.52
Subreach	**River Sta**	**Agg & Deg #**	**Min Ch El (ft)**	**W.S. Elev (ft)**	**Crit W.S. (ft)**	**E.G. Elev (ft)**	**E.G. Slope (ft/ft)**	**Vel Chnl (ft/s)**	**Flow Area (sq ft)**	**Top Width (ft)**	**Froude #**
	536	1257	4632.19	4638.36		4638.6	0.001072	3.95	1264.62	605.79	0.48
	535	1258	4632.37	4637.99		4638.13	0.000521	2.93	1705.95	748.82	0.34
	531	1262	4629.28	4636.04	4634.36	4636.65	0.000966	6.31	823.36	524.92	0.52
	524	1269	4626.84	4633.38	4631.7	4633.75	0.000753	4.93	1415.26	661.56	0.45

	519	1274	4624.05	4629.61		4630.28	0.001908	6.6	795.31	269.99	0.68
Reach 3	513	1280	4621.87	4627.31		4627.48	0.00043	3.4	1723.98	712.66	0.33
	512	1281	4620.77	4626.91		4627.19	0.000729	4.31	1289.64	498.94	0.43
	510	1283	4621.19	4625.7	4624.42	4626.23	0.001104	5.83	913.96	512.7	0.54
	501	1292	4617.08	4621.47	4620.43	4621.69	0.0008	3.8	1686.48	1025.16	0.43
	495	1298	4614.39	4619.55		4619.71	0.000559	3.17	1575.27	644.74	0.36
	494	1299	4613.6	4619.34		4619.5	0.00035	3.2	1564.07	444.29	0.3
	487	1306	4610	4616.96		4617.66	0.00079	6.69	747.19	125.84	0.48
	485	1308	4608.52	4616.34		4616.94	0.000621	6.21	805.53	126.06	0.43
Reach 4	483	1310	4607.38	4615.68		4616.28	0.000591	6.23	801.94	120.5	0.43
	482	1311	4607.48	4615.37		4615.96	0.000598	6.19	807.73	123.64	0.43
	481	1312	4606.41	4614.76		4615.49	0.000749	6.89	726.12	110.48	0.47
	479	1314	4606.3	4614.28		4614.68	0.000486	5.09	983.16	175.71	0.38
	473	1320	4604.01	4609.47	4609.47	4611.34	0.003932	10.97	455.9	122.19	1

Appendix E – Total Load Calculations using BORAMEP

Location	Date	Discharge (cfs)	Concentration (ppm)	Suspended Sample (tons/day)	Load (tons/day)		Concentration (mg/L)	
					Total	Sand	Total	Sand
1208-1	1/8/1999	1050	1109	3145	9157	7810	25961	22142
1208-2	2/11/1999	1080	786	2291	7908	6751	23059	19687
1208-5	5/21/1999	2320	787	4927	7198	2824	45090	17693
1208-6	6/30/1999	1520	233	956	3256	2335	13361	9581
1208-8	8/27/1999	1100	1938	5755	13817	10573	41035	31403
1208-9	9/13/1999	628	669	1134	4704	3947	7976	6693
1208-10	12/1/1999	1060	2067	5917	14195	13255	40625	37937
1210-1	1/19/1995	1140	707	2175	4141	3502	12747	10778
1210-2	2/1/1995	1160	938	2939	4262	1945	13349	6091
1210-3	5/16/1995	3370	950	8648	12958	6310	117907	57418
1210-4	6/8/1995	4390	1848	21903	28509	12604	337923	149391
1210-5	7/20/1995	4540	1988	24363	33258	15613	407678	191385
1210-7	10/17/1995	395	121	129	603	164	643	175
1210-9	1/16/1997	668	1409	2541	3542	2784	6388	5022
1210-10	2/11/1997	992	714	1912	3042	1309	8149	3506
1210-11	3/18/1997	703	2785	5287	7593	3843	14413	7295
1210-12	5/20/1997	4250	7376	84639	93169	33377	1069118	383002
1210-15	8/19/1997	532	1768	2540	4229	3787	6074	5440
1210-17	10/22/1997	2210	1269	7572	9867	6257	58876	37336
1210-18	11/18/1997	1760	1069	5081	9134	7827	43404	37193
1210-19	12/16/1997	1220	560	1844	3700	3097	12188	10202
1215-4	6/8/1995	4390	1848	21903	23135	7746	274220	91813
1215-5	7/20/1995	4540	1988	24363	26006	9133	318776	111950
1215-9	1/16/1997	668	1409	2541	2305	1573	4158	2838
1215-11	3/18/1997	703	2785	5287	4890	1577	9282	2994
1215-12	5/20/1997	4250	7376	84639	91804	29792	1053454	341858
1215-20	1/8/1999	1050	1109	3145	4092	3127	11601	8866
1215-21	2/11/1999	1080	786	2291	3196	2448	9320	7137
1215-24	5/21/1999	2320	787	4927	5776	1600	36181	10020
1215-25	6/30/1999	1520	233	956	1551	728	6366	2988
1215-27	8/27/1999	1100	1938	5755	7130	4410	21175	13099
1215-28	9/13/1999	628	669	1134	1224	568	2075	964
1215-29	12/1/1999	1060	2067	5917	7128	6328	20400	18111
1215-31	2/28/2005	1490	1059	4262	5349	1817	21518	7309
1215-32	4/26/2005	4640	2067	25900	35554	27587	445419	345605
1221-4	6/8/1995	4390	1848	21903	23354	7962	276811	94369
1221-5	7/20/1995	4540	1988	24363	26195	9322	321102	114271
1221-17	10/22/1997	2210	1269	7572	9251	5145	55202	30698
1221-21	2/23/1998	1170	703	2220	2421	1970	7648	6223
1221-23	5/18/1998	2510	1259	8532	9394	3258	63664	22081
1221-28	11/3/1998	1780	1279	6147	6861	5172	32974	24859
1221-34	5/21/1999	2320	787	4927	5235	1180	32790	7393
1223-4	5/20/1997	4250	7376	84639	101736	37550	1167416	430883
1223-9	10/22/1997	2210	1269	7572	12290	6958	73332	41515
1223-13	2/23/1998	1170	703	2220	3578	3126	11302	9875

Location	Date	Discharge (cfs)	Concentration (ppm)	Suspended Sample (tons/day)	Load (tons/day)		Concentration (mg/L)	
					Total	Sand	Total	Sand
1223-15	5/18/1998	2510	1259	8532	9966	3826	67541	25929
1223-19	10/5/1998	592	7237	11568	11909	4305	19035	6882
1223-20	11/3/1998	1780	1279	6147	8290	6568	39842	31565
1223-21	12/17/1998	926	6097	15243	16591	5331	41480	13328
1223-22	1/8/1999	1050	1109	3145	5156	4246	14616	12037
1223-23	2/11/1999	1080	786	2291	4341	3657	12658	10662
1223-26	5/21/1999	2320	787	4927	6030	1908	37775	11949
1223-27	6/30/1999	1520	233	956	2745	1913	11266	7849
1223-29	8/27/1999	1100	1938	5755	7726	5367	22946	15939
1223-31	12/1/1999	1060	2067	5917	6608	5831	18912	16689
1225-1	1/10/1996	1220	506	1666	3169	2448	10437	8062
1225-2	2/22/1996	1380	836	3113	5770	4974	21498	18534
1225-3	3/20/1996	910	75	184	599	325	1472	799
1225-10	11/13/1996	961	3074	7976	10178	6773	26408	17575
1225-11	12/17/1996	920	1818	4516	5617	4202	13952	10438
1225-15	5/20/1997	4250	7376	84639	94472	33415	1084066	383441
1225-18	8/19/1997	532	1768	2540	3329	2848	4782	4091
1225-20	10/22/1997	2210	1269	7572	10890	6597	64980	39366
1225-24	2/23/1998	1170	703	2220	4561	4087	14408	12912
1225-26	5/18/1998	2510	1259	8532	9804	3652	66442	24749
1225-30	10/5/1998	592	7237	11568	12145	4579	19413	7318
1225-31	11/3/1998	1780	1279	6147	9133	7385	43895	35494
1225-32	12/17/1998	926	6097	15243	17387	6092	43471	15231
1225-33	1/8/1999	1050	1109	3145	4726	3814	13398	10814
1225-34	2/11/1999	1080	786	2291	3851	3158	11229	9207
1225-37	5/21/1999	2320	787	4927	5673	1566	35533	9813
1225-38	6/30/1999	1520	233	956	2117	1302	8687	5345
1225-40	8/27/1999	1100	1938	5755	7298	4901	21676	14556
1225-41	9/13/1999	628	669	1134	1251	602	2121	1021
1225-42	12/1/1999	1060	2067	5917	7272	6497	20812	18595
1228-1	1/16/1997	668	1409	2541	5732	4325	10338	7800
1228-2	2/11/1997	992	714	1912	5498	2059	14725	5515
1228-3	3/18/1997	703	2785	5287	10631	4287	20178	8137
1228-4	5/20/1997	4250	7376	84639	98585	37345	1131264	428539
1228-7	8/19/1997	532	1768	2540	6074	5391	8724	7744
1228-9	10/22/1997	2210	1269	7572	11758	7853	70161	46858
1228-10	11/18/1997	1760	1069	5081	9991	7770	47478	36922
1228-11	12/16/1997	1220	560	1844	4318	3367	14224	11091
1228-13	2/23/1998	1170	703	2220	8273	7629	26134	24099
1228-15	5/18/1998	2510	1259	8532	12612	6300	85468	42697
1228-16	7/21/1998	295	240	191	678	443	540	353
1228-19	10/5/1998	592	7237	11568	15952	8204	25498	13113
1228-20	11/3/1998	1780	1279	6147	14360	12167	69013	58472
1228-21	12/17/1998	926	6097	15243	20607	9093	51522	22735
1228-22	1/8/1999	1050	1109	3145	7613	6550	21583	18569
1228-23	2/11/1999	1080	786	2291	6361	5523	18548	16105

Location	Date	Discharge (cfs)	Concentration (ppm)	Suspended Sample (tons/day)	Load (tons/day)		Concentration (mg/L)	
					Total	Sand	Total	Sand
1228-25	4/7/1999	418	100	113	1618	1205	1826	1360
1228-26	5/21/1999	2320	787	4927	7157	2921	44832	18298
1228-27	6/30/1999	1520	233	956	3242	2402	13307	9857
1228-29	8/27/1999	1100	1938	5755	11202	8502	33271	25250
1228-30	9/13/1999	628	669	1134	2539	1863	4305	3160
1228-31	12/1/1999	1060	2067	5917	12508	11646	35799	33331
1230-1	1/16/1997	668	1409	2541	4834	3742	8718	6749
1230-2	2/11/1997	992	714	1912	4455	1679	11932	4497
1230-3	3/18/1997	703	2785	5287	9794	4091	18590	7765
1230-4	5/20/1997	4250	7376	84639	92617	32469	1062776	372580
1230-7	8/19/1997	532	1768	2540	4578	4071	6576	5848
1230-9	10/22/1997	2210	1269	7572	10076	6210	60125	37056
1230-10	11/18/1997	1760	1069	5081	9488	7792	45086	37028
1230-11	12/16/1997	1220	560	1844	4050	3163	13340	10419
1230-13	2/23/1998	1170	703	2220	6055	5457	19127	17239
1230-15	5/18/1998	2510	1259	8532	10881	4652	73739	31524
1230-16	7/21/1998	295	240	191	381	173	303	138
1230-19	10/5/1998	592	7237	11568	13954	6318	22304	10099
1230-20	11/3/1998	1780	1279	6147	11354	9334	54568	44861
1230-21	12/17/1998	926	6097	15243	18531	7159	46330	17899
1230-22	1/8/1999	1050	1109	3145	6443	5107	18267	14479
1230-23	2/11/1999	1080	786	2291	5262	4096	15345	11944
1230-26	5/21/1999	2320	787	4927	6533	2120	40924	13282
1230-27	6/30/1999	1520	233	956	2403	1488	9863	6105
1230-30	9/13/1999	628	669	1134	2170	1468	3679	2489
1230-31	12/1/1999	1060	2067	5917	11039	10067	31595	28813
1232-4	5/20/1997	4250	7376	84639	100513	34032	1153386	390521
1232-12	1/20/1998	1070	1968	5684	11967	11348	34571	32784
1232-13	2/23/1998	1170	703	2220	5836	5354	18435	16913
1232-15	5/18/1998	2510	1259	8532	10846	4715	73504	31954
1232-16	7/21/1998	295	240	191	378	184	301	147
1232-18	9/15/1998	209	512	289	680	487	384	275
1232-19	10/5/1998	592	7237	11568	13561	5969	21676	9540
1232-20	11/3/1998	1780	1279	6147	10775	8995	51785	43231
1232-21	12/17/1998	926	6097	15243	17543	6409	43861	16024
1232-22	1/8/1999	1050	1109	3145	5012	3991	14210	11315
1232-23	2/11/1999	1080	786	2291	3936	3139	11479	9153
1232-25	4/7/1999	418	100	113	786	434	887	490
1232-26	5/21/1999	2320	787	4927	5962	1790	37348	11213
1232-27	6/30/1999	1520	233	956	1922	1130	7887	4636
1232-30	9/13/1999	628	669	1134	1753	1085	2972	1839
1232-31	12/1/1999	1060	2067	5917	9002	8139	25763	23294
1236-4	6/8/1995	4390	1848	21903	22782	7359	270032	87221
1236-5	7/20/1995	4540	1988	24363	25552	8641	313217	105917
1236-11	3/20/1996	910	75	184	212	48	520	118
1236-23	5/20/1997	4250	7376	84639	90091	27904	1033799	320196

Location	Date	Discharge (cfs)	Concentration (ppm)	Suspended Sample (tons/day)	Load (tons/day)		Concentration (mg/L)	
					Total	Sand	Total	Sand
1236-34	5/18/1998	2510	1259	8532	8908	2785	60370	18876
1236-52	2/28/2005	1490	1059	4262	4714	1423	18963	5724
1236-53	4/26/2005	4640	2067	25900	30085	22419	376901	280871
1243-1	1/19/1995	1140	707	2175	4105	3457	12636	10641
1243-2	2/1/1995	1160	938	2939	4756	2421	14895	7584
1243-3	5/16/1995	3370	950	8648	10981	4752	99916	43234
1243-4	6/8/1995	4390	1848	21903	25279	9669	299634	114606
1243-5	7/20/1995	4540	1988	24363	28326	11170	347216	136920
1243-12	5/20/1997	4250	7376	84639	94092	32682	1079706	375027
1243-17	10/22/1997	2210	1269	7572	11348	6632	67711	39575
1243-20	1/8/1999	1050	1109	3145	6077	5039	17227	14286
1243-21	2/11/1999	1080	786	2291	4847	4033	14133	11759
1243-24	5/21/1999	2320	787	4927	5728	1594	35881	9987
1243-25	6/30/1999	1520	233	956	1932	1140	7929	4677
1243-27	8/27/1999	1100	1938	5755	9770	7055	29018	20954
1243-28	9/13/1999	628	669	1134	4518	3841	7661	6512
1243-29	12/1/1999	1060	2067	5917	10958	10113	31362	28942
1246-1	1/19/1995	1140	707	2175	3245	2566	9990	7899
1246-2	2/1/1995	1160	938	2939	4198	1811	13149	5673
1246-3	5/16/1995	3370	950	8648	12000	5623	109187	51167
1246-4	6/8/1995	4390	1848	21903	26285	10219	311557	121123
1246-5	7/20/1995	4540	1988	24363	29434	11336	360798	138960
1246-9	1/10/1996	1220	506	1666	3601	2663	11861	8773
1246-10	2/22/1996	1380	836	3113	6040	4946	22505	18428
1246-11	3/20/1996	910	75	184	1278	494	3140	1214
1246-13	6/19/1996	214	213	123	668	106	386	61
1246-14	7/18/1996	340	6930	6362	6897	1314	6332	1206
1246-16	9/4/1996	174	2546	1196	1692	142	795	67
1246-18	11/13/1996	961	3074	7976	10714	6970	27799	18085
1246-19	12/17/1996	920	1818	4516	7128	5510	17706	13687
1246-23	5/20/1997	4250	7376	84639	96239	34266	1104339	393201
1246-26	8/19/1997	532	1768	2540	4312	3606	6194	5180
1246-28	10/22/1997	2210	1269	7572	11214	6491	66914	38735
1246-31	1/8/1999	1050	1109	3145	5017	3963	14222	11234
1246-32	2/11/1999	1080	786	2291	3940	3105	11490	9053
1246-35	5/21/1999	2320	787	4927	6053	1842	37914	11538
1246-36	6/30/1999	1520	233	956	1952	1145	8010	4699
1246-39	9/13/1999	628	669	1134	1686	1016	2859	1722
1246-40	12/1/1999	1060	2067	5917	8991	8117	25731	23230
1246-42	2/28/2005	1490	1059	4262	7671	3216	30862	12939
1246-43	4/26/2005	4640	2067	25900	40318	32127	505108	402492
1262-1	1/19/1995	1140	707	2175	5503	4608	16939	14183
1262-2	2/1/1995	1160	938	2939	6143	3197	19240	10014
1262-3	5/16/1995	3370	950	8648	26906	15630	244816	142220
1262-4	6/8/1995	4390	1848	21903	51789	30986	613860	367279
1262-5	7/20/1995	4540	1988	24363	64847	36808	794890	451193

Location	Date	Discharge (cfs)	Concentration (ppm)	Suspended Sample (tons/day)	Load (tons/day)		Concentration (mg/L)	
					Total	Sand	Total	Sand
1262-9	1/10/1996	1220	506	1666	4166	3227	13722	10631
1262-10	2/22/1996	1380	836	3113	7815	6648	29117	24769
1262-11	3/20/1996	910	75	184	1510	727	3711	1786
1262-13	6/19/1996	214	213	123	822	176	475	102
1262-14	7/18/1996	340	6930	6362	7125	1544	6541	1417
1262-16	9/4/1996	174	2546	1196	1801	265	846	124
1262-18	11/13/1996	961	3074	7976	11558	7809	29991	20262
1262-19	12/17/1996	920	1818	4516	8044	6414	19981	15932
1262-23	5/20/1997	4250	7376	84639	160617	58981	1843082	676811
1262-31	1/8/1999	1050	1109	3145	6124	4868	17362	13800
1262-32	2/11/1999	1080	786	2291	4969	3898	14491	11367
1262-35	5/21/1999	2320	787	4927	8205	3458	51398	21662
1262-36	6/30/1999	1520	233	956	3532	2559	14494	10504
1262-39	9/13/1999	628	669	1134	2134	1439	3618	2439
1262-40	12/1/1999	1060	2067	5917	10692	9734	30600	27858
1262-47	1/8/1999	1050	1109	3145	46739	39019	132505	110618
1262-48	2/11/1999	1080	786	2291	23371	18748	68150	54670
1262-51	5/21/1999	2320	787	4927	9565	4390	59915	27498
1262-52	6/30/1999	1520	233	956	5442	4144	22335	17006
1262-56	12/1/1999	1060	2067	5917	53215	50751	152300	145250
1283-3	4/26/2005	4640	2067	25900	52730	41652	660603	521814
1292-4	5/20/1997	4250	7376	84639	110886	43048	1272417	493981
1292-9	10/22/1997	2210	1269	7572	19312	11057	115233	65974
1292-16	5/21/1999	2320	787	4927	9616	3701	60237	23186
1292-17	6/30/1999	1520	233	956	6521	3013	26761	12365
1292-37	5/21/1999	2320	787	4927	6214	1575	38923	9866
1292-38	6/30/1999	1520	233	956	1722	686	7067	2817
1292-41	9/13/1999	628	669	1134	1225	569	2077	965
1306-3	5/16/1995	3370	950	8648	12698	5164	115541	46990
1306-9	1/10/1996	1220	506	1666	2681	1865	8831	6143
1306-10	2/22/1996	1380	836	3113	4681	3733	17442	13911
1306-11	3/20/1996	910	75	184	693	217	1702	533
1306-18	11/13/1996	961	3074	7976	9049	5564	23479	14438
1306-19	12/17/1996	920	1818	4516	5683	4183	14116	10391
1306-20	1/16/1997	668	1409	2541	3060	2308	5518	4162
1306-21	2/11/1997	992	714	1912	2707	952	7251	2551
1306-22	3/18/1997	703	2785	5287	6135	2632	11645	4996
1306-23	5/20/1997	4250	7376	84639	90751	30952	1041371	355170
1306-26	8/19/1997	532	1768	2540	2994	2568	4301	3688
1306-28	10/22/1997	2210	1269	7572	8929	5330	53278	31804
1306-29	11/18/1997	1760	1069	5081	7424	6114	35278	29053
1306-30	12/16/1997	1220	560	1844	2708	2115	8919	6968
1306-31	1/8/1999	1050	1109	3145	4170	3118	11821	8839
1306-32	2/11/1999	1080	786	2291	3218	2369	9384	6909
1306-35	5/21/1999	2320	787	4927	5812	1591	36409	9965
1306-36	6/30/1999	1520	233	956	1568	758	6437	3110

Location	Date	Discharge (cfs)	Concentration (ppm)	Suspended Sample (tons/day)	Load (tons/day)		Concentration (mg/L)	
					Total	Sand	Total	Sand
1306-39	9/13/1999	628	669	1134	1353	690	2295	1171
1306-40	12/1/1999	1060	2067	5917	7591	6731	21726	19264
1308-1	1/8/1999	1050	1109	3145	4753	3789	13474	10743
1308-2	2/11/1999	1080	786	2291	3817	3080	11132	8982
1308-5	5/21/1999	2320	787	4927	5821	1701	36461	10654
1308-6	6/30/1999	1520	233	956	1800	996	7388	4086
1308-8	8/27/1999	1100	1938	5755	7842	5359	23290	15915
1308-9	9/13/1999	628	669	1134	1412	752	2394	1276
1308-10	12/1/1999	1060	2067	5917	8035	7232	22996	20698
1311-2	2/1/1995	1160	938	2939	6188	2036	19382	6377
1311-3	5/16/1995	3370	950	8648	15285	5936	139082	54011
1313-5	5/21/1999	2320	787	4927	8388	1961	52543	12287
1313-6	6/30/1999	1520	233	956	1929	783	7915	3214
1313-8	8/27/1999	1100	1938	5755	5407	2064	16058	6131
1313-9	9/13/1999	628	669	1134	1511	716	2562	1213
1313-10	12/1/1999	1060	2067	5917	5965	4896	17071	14011
1316-1	1/19/1995	1140	707	2175	4436	3348	13654	10305
1316-2	2/1/1995	1160	938	2939	5688	2508	17815	7855
1316-3	5/16/1995	3370	950	8648	14775	7561	134439	68793
1316-4	6/8/1995	4390	1848	21903	31275	12240	370698	145082
1316-9	1/10/1996	1220	506	1666	5093	4020	16778	13243
1316-10	2/22/1996	1380	836	3113	8267	7008	30801	26110
1316-11	3/20/1996	910	75	184	2303	1022	5657	2511
1316-13	6/19/1996	214	213	123	1618	317	935	183
1316-14	7/18/1996	340	6930	6362	7750	2004	7114	1840
1316-16	9/4/1996	174	2546	1196	3085	527	1449	248
1316-18	11/13/1996	961	3074	7976	13026	8997	33798	23344
1316-19	12/17/1996	920	1818	4516	9203	7454	22861	18517
1316-23	5/20/1997	4250	7376	84639	108577	43906	1245922	503819
1316-26	8/19/1997	532	1768	2540	6966	5947	10005	8542
1316-28	10/22/1997	2210	1269	7572	15706	9822	93716	58610